301

Copy
RM A54B18a

CASE FILE COPY

NACA

RESEARCH MEMORANDUM

INVESTIGATION OF A THREE-BLADE PROPELLER IN COMBINATION

WITH TWO DIFFERENT SPINNERS AND AN NACA D-TYPE

COWL AT MACH NUMBERS UP TO 0.80

By George C. Kenyon and Robert M. Reynolds

Ames Aeronautical Laboratory
Moffett Field, Calif.

CLASSIFICATION CHANGED TO UNCLASSIFIED

AUTHORITY: NACA RESEARCH ABSTRACT NO. 97

DATE: FEBRUARY 24, 1956   WHL

NATIONAL ADVISORY COMMITTEE
FOR AERONAUTICS
WASHINGTON
April 21, 1954

NATIONAL ADVISORY COMMITTEE FOR AERONAUTICS

RESEARCH MEMORANDUM

INVESTIGATION OF A THREE-BLADE PROPELLER IN COMBINATION

WITH TWO DIFFERENT SPINNERS AND AN NACA D-TYPE

COWL AT MACH NUMBERS UP TO 0.80

By George C. Kenyon and Robert M. Reynolds

SUMMARY

An investigation has been made to determine the aerodynamic characteristics of a three-blade propeller designed to operate ahead of a D-type cowl. The propeller (designated NACA 3.638-(675)(057)-0572) in combination with two different spinner shapes and an NACA 1-62.8-070 D-type cowl was investigated at Mach numbers up to 0.80. The characteristics of the isolated propeller-spinner combination operating at positive thrust, negative thrust, and at near static conditions were also determined. Included are results of air-stream surveys of the local velocities in the plane of the propeller. All tests were made with the model at an angle of attack of $0°$ and at a Reynolds number of 1,000,000 per foot, based on free-stream conditions.

The efficiency of the propeller in the presence of the cowl was higher at all Mach numbers than that of the isolated propeller-spinner combination. At design cruise conditions (M = 0.60, $\beta = 53°$), the efficiency of the propeller with the 1-series spinner and cowl was 80 percent, as compared with 72 percent for the isolated propeller-spinner combination. The onset of marked compressibility losses was delayed from a Mach number of 0.50 to a Mach number of 0.60 by the addition of the cowl.

The effects of inlet velocity ratio and spinner shape on the propeller characteristics were not large except at the higher Mach numbers (0.70 and 0.80).

INTRODUCTION

Considerable research has been conducted on propeller-spinner-cowling combinations suitable for use with large turbine engines (refs. 1 to 5). To augment this research, an investigation was conducted in the Ames

12-foot pressure wind tunnel to determine the characteristics of a three-blade propeller and a D-type cowl with both an NACA 1-series spinner and a more nearly conical spinner. The pressure-recovery characteristics of these propeller-spinner-cowling combinations have been reported in reference 6. Reference 7 has presented some preliminary results for the propeller with the cowl and spinners.

Presented herein are results of force tests, obtained concurrently with the data presented in reference 6, for the propeller operating in the presence of the cowl with the two different spinners. Also presented are force-test results for the isolated propeller-spinner combination operating at positive thrust, negative thrust, and at near static conditions. The velocity distributions in the plane of the propeller are included.

The tests were conducted for a range of blade angles from $-20°$ to $63°$ and at Mach numbers up to 0.80. All tests were made with the model at an angle of attack of $0°$ and at a Reynolds number of 1,000,000 per foot, based on free-stream conditions.

NOTATION

a   speed of sound

b   blade width

C_P power coefficient, $\dfrac{P}{\rho n^3 D^5}$

C_T thrust coefficient, $\dfrac{T}{\rho n^2 D^4}$

c_{l_d} blade-section design lift coefficient

D   propeller diameter

HP   horsepower

h   maximum thickness of blade section

J   advance ratio, $\dfrac{V_0}{nD}$

M   Mach number, $\dfrac{V}{a}$

M_t tip Mach number, $M\sqrt{1 + \left(\dfrac{\pi}{J}\right)^2}$

n   propeller rotational speed

P   power

R   propeller-tip radius

r   blade-section radius

S   propeller disc area

T   thrust

T_c thrust coefficient, $\dfrac{T}{\rho V^2 D^2}$

U   local velocity in the plane of the propeller

V   air-stream velocity

V_o equivalent free-air velocity

$\dfrac{V_1}{V}$ inlet velocity ratio

β propeller blade angle at 0.75 R

β_d design propeller-section blade angle

η efficiency, $\dfrac{C_T}{C_P} J$

ρ air density

<center>Subscripts</center>

1   location of rake in cowl inlet

a   apparent (applied to propeller characteristics when operating
            ahead of the cowl)

<center>MODEL AND APPARATUS</center>

This investigation was conducted in the Ames 12-foot pressure wind
tunnel with the model mounted on the 1000-horsepower dynamometer (described
in ref. 8). A photograph of the model is presented in figure 1 and a
sketch of the general model arrangement is given in figure 2. The propel-
ler used was a three-blade type designed by Hamilton Standard Division and

it corresponded to the designation NACA 3.638-(675)(057)-0572. Blade-form curves for the propeller are shown in figure 3. Additional details of the model and its instrumentation as well as information on the full-scale design conditions can be found in reference 6.

Figure 4 is a photograph of the survey rake used to determine the velocity distribution in the plane of the propeller. The rake consisted of 24 static pressure tubes located at the radial stations listed in table I.

TESTS AND REDUCTION OF DATA

Thrust, torque, and rotational speed were measured (as described in refs. 2 and 8) for the propeller-spinner-cowl combinations and the isolated propeller-spinner combination (1-series spinner) for a range of blade angles from 33° to 63° at Mach numbers from 0.20 to 0.80. Data for the isolated propeller-spinner combination were obtained at negative thrust conditions at the same Mach numbers and blade angles and, in addition, data were obtained for this combination at a Mach number of 0.15 for blade angles from -20° to 25°. The characteristics of the isolated propeller-spinner combination were also measured at near static conditions for a blade-angle range from 10° to 25°.

Surveys of the air-stream velocity in the plane of the propeller were made at Mach numbers from 0.15 to 0.80. With the cowl installed, the effect of inlet velocity ratio on the local velocity in the propeller plane was also determined.

The Mach number used in this report was the average Mach number over the disc area as determined by velocity surveys reported in reference 8. For the tests made with the cowl installed, this Mach number (and the corresponding dynamic pressure) was corrected for blockage of the cowl by the method of reference 9. In no case did this correction exceed 1 percent.

The air-stream velocity (and, consequently, propeller advance ratio and efficiency) was corrected for the wind-tunnel-wall constraint on the propeller slipstream by the method of reference 10. Figure 5 presents a comparison of this correction with that determined experimentally by the method of reference 11 from measurements of wall pressures. The data included herein are for advance ratios at which the thrust-coefficient parameter $T_c/(1 - M^2)$ was greater than -0.5.

Analysis of the accuracy of the separate measurements of thrust, torque, and air-stream velocity, as in reference 8, indicates that errors in the propeller efficiencies reported herein are probably less than 2 percent.

<div align="center">CONFIDENTIAL</div>

RESULTS

The distribution of velocity across the propeller disc is listed in table I. These data are plotted in figure 6 for a few typical Mach numbers and inlet velocity ratios.

The characteristics of the propeller operating in the presence of the cowl are presented in figures 7 and 8 and the characteristics of the isolated propeller-spinner combination for conditions of positive thrust are presented in figure 9. The variation of maximum propeller efficiency with Mach number is summarized in figure 10 and the effect of inlet velocity ratio on the propeller characteristics is shown in figure 11.

The negative-thrust characteristics of the propeller-spinner combination are presented in figures 12 through 15 and the characteristics of the propeller-spinner combination at near static conditions are shown in figure 16 and are summarized in figure 17.

DISCUSSION

Propeller Characteristics at Positive Thrust

As in reference 2, the characteristics of the propeller operating in the presence of the cowl are presented as apparent values (figs. 7 and 8) since the determination of the propulsive thrust of the propeller was precluded by the fact that it was impractical, with the dynamometer arrangement used in the present investigation, to measure the increase in drag of the cowl and dynamometer parts within the influence of the propeller slipstream. The addition of the cowl behind the propeller resulted in reduced velocities throughout the propeller flow field, as evidenced by a comparison of figures 6(a) and 6(b) with figure 6(c). As a consequence of these reduced velocities (and in accord with the discussion of ref. 12), the thrust and power for the propeller operating ahead of the cowl were greater than that for the isolated propeller-spinner combination (at the same advance ratio), as can be seen from a comparison of figures 7 and 8 with figure 9.

Maximum efficiency.- As shown in figure 10, the efficiency of the propeller in the presence of the cowl was higher at all Mach numbers than that of the isolated propeller-spinner combination. At design cruise conditions (M = 0.60, β = 53°), the efficiency of the propeller with the l-series spinner and cowl was 80 percent, as compared with 72 percent for the isolated propeller-spinner combination. It may be noted here that the higher efficiencies for the propeller with the cowl were due not only to interference effects but partly to the fact that, in the presence of

the cowl, the propeller was operating more nearly in the flow field for
which it was designed.

The onset of marked compressibility losses was delayed (also as a
consequence of the interference effects) from a Mach number of 0.50 to a
Mach number of 0.60 by the addition of the cowl (fig. 10). The large
losses in efficiency at Mach numbers from 0.60 to 0.80 were due not only
to the effects of compressibility but also to the fact that at blade angles
of 58.5^O and 63° the inner portions of the blades were probably operating
at negative thrust, since the local blade angles for this portion of the
blade were greater than 90° (up to 98° for $\beta = 63^O$). Operation of the
propeller at lower blade angles at these Mach numbers (requiring higher
rotational speeds) might have resulted in higher efficiencies but was not
permissible because of structural limitations of the model propeller.

Effect of inlet velocity ratio.- Although the air-stream surveys
(tables I(a) and I(b), and figs. 6(a) and 6(b)) show that decreasing inlet
velocity ratio resulted in reduced local velocities at the propeller
plane, the changes were small in comparison with the reduction in veloc-
ity occasioned by the addition of the cowl to the spinner (fig. 6(a) com-
pared with fig. 6(c)). Consequently, as shown in figures 7, 8, and 11,
the effect of inlet velocity ratio on the propeller characteristics was
not large except at the higher Mach numbers (0.70 and 0.80), where small
changes in local velocity resulted in relatively large changes in the
propeller characteristics due to the effects of compressibility.

Effect of spinner shape.- Although the data of figures 6(a) and 6(b)
indicate only small differences in the local velocity distributions for
the two spinners with the propeller removed, figure 11 shows that higher
thrust and power coefficients were obtained with the propeller and modi-
fied conical spinner. However, as shown in figure 10, the differences in
maximum efficiency were generally of the order of the stated accuracy of
the results.

Propeller Characteristics at Negative Thrust

The data presented in figure 14(a) indicate that at any constant
value of advance ratio, relatively constant negative-thrust coefficients
were attained at blade angles from -5° to -20°. However, as shown in
figure 15(a), the power coefficients corresponding to this range of blade
angles increased rapidly, indicating that use of a more negative blade
angle resulted in additional power absorption rather than an increase in
negative thrust. For the range of blade angles and Mach numbers covered
in the present investigation, there was practically no effect of compres-
sibility on the negative-thrust and torque characteristics of the propel-
ler at Mach numbers up to 0.60 (see figs. 14 and 15).

Propeller Characteristics at Near Static Conditions

The thrust and torque characteristics presented in figures 16(a) and 16(b) were obtained at near static conditions, as shown by the variation of velocity with nD in figure 16(c). The abrupt decrease in thrust coefficient and increase in power coefficient at values of nD below 60 are believed to be due to the effects of Reynolds number. At these low values of nD, the blade sections were operating at Reynolds numbers less than about 500,000.

The experimental data shown in figure 16 were used to compute the static thrust per horsepower and were then plotted as a function of power disc loading for constant values of nD. The envelope of these curves is presented in figure 17. The theoretical curve shown in figure 17 was computed by the method of reference 13. The variation of static thrust per horsepower with disc loading was adequately predicted by the theory, but the experimental values were only approximately 67 percent of the theoretical ideal values. However, the theory neglects rotational losses and blade drag which presumably accounts for the discrepancy between experiment and theory.

CONCLUDING REMARKS

The following remarks may be made regarding the results of the subject investigation.

The efficiency of the propeller with the two different spinners and the cowl was higher at all Mach numbers than that of the isolated propeller-spinner combination. At design cruise conditions (M = 0.60, $\beta = 53^{\circ}$), the efficiency of the propeller with the 1-series spinner and cowl was 80 percent, as compared with 72 percent for the isolated propeller-spinner combination.

The onset of marked compressibility losses was delayed from a Mach number of 0.50 to a Mach number of 0.60 by the addition of the cowl.

The effects of inlet velocity ratio and spinner shape on the propeller characteristics were not large except at the higher Mach numbers (0.70 and 0.80).

There was practically no effect of compressibility on the characteristics of the propeller-spinner combination operating at negative thrust at Mach numbers through 0.60.

The propeller static thrust varied with power disc loading as predicted by actuator disc theory, but the experimental static thrust was only 67 percent of the theoretical ideal thrust.

Ames Aeronautical Laboratory
    National Advisory Committee for Aeronautics
        Moffett Field, Calif., Feb. 18, 1954

REFERENCES

1. Sammonds, Robert I., and Molk, Ashley J.: Effects of Propeller-Spinner Juncture on the Pressure-Recovery Characteristics of an NACA 1-Series D-Type Cowl in Combination With a Four-Blade Single-Rotation Propeller at Mach Numbers up to 0.83 and at an Angle of Attack of 0°. NACA RM A52D01a, 1952.

2. Reynolds, Robert M., Sammonds, Robert I., and Kenyon, George C.: An Investigation of a Four-Blade Single-Rotation Propeller in Combination With an NACA 1-Series D-Type Cowling at Mach Numbers up to 0.83. NACA RM A53B06, 1953.

3. Keith, Arvid L., Jr., Bingham, Gene J., and Rubin, Arnold J.: Effects of Propeller-Shank Geometry and Propeller-Spinner Juncture Configuration on Characteristics of an NACA 1-Series Cowling-Spinner Combination With an Eight-Blade Dual-Rotation Propeller. NACA RM L51F26, 1951.

4. Bingham, Gene J., and Keith, Arvid L., Jr.: Effects of Compressibility at Mach Numbers up to 0.8 on Internal-Flow Characteristics of a Cowling-Spinner Combination Equipped With an Eight-Blade Dual-Rotation Propeller. NACA RM L53E12, 1953.

5. Reynolds, Robert M., and Sammonds, Robert I.: Subsonic Mach and Reynolds Number Effects on the Surface Pressures, Gap Flow, Pressure Recovery, and Drag of a Nonrotating NACA 1-Series E-Type Cowling at an Angle of Attack of 0°. NACA RM A51E03, 1951.

6. Molk, Ashley J., and Reynolds, Robert M.: Effects of Two Spinner Shapes on the Pressure Recovery in an NACA 1-Series D-Type Cowl Behind a Three-Blade Propeller at Mach Numbers Up to 0.80. NACA RM A53L29a, 1953.

7. Reynolds, Robert M.: Preliminary Results of an Investigation of the Effects of Spinner Shape on the Characteristics of an NACA D-Type Cowl Behind a Three-Blade Propeller, Including the Characteristics of the Propeller at Negative Thrust. NACA RM A53J02, 1953.

8. Reynolds, Robert M., Buell, Donald A., and Walker, John H.: Investi-
    gation of an NACA 4-(5)(05)-041 Four-Blade Propeller With Several
    Spinners at Mach Numbers up to 0.90. NACA RM A52I19a, 1952.

9. Herriot, John G.: Blockage Corrections for Three-Dimensional-Flow
    Closed-Throat Wind Tunnels, With Consideration of the Effect of
    Compressibility. NACA Rep. 995, 1950. (Supersedes NACA RM A7B28)

10. Young, A. D.: Note on the Application of the Linear Perturbation
    Theory to Determine the Effect of Compressibility on the Wind
    Tunnel Constraint on a Propeller. R.A.E. TN No. Aero. 1539,
    British, 1944.

11. Delano, James Benjamin, and Carmel, Melvin M.: Investigation of the
    NACA 4-(5)(08)-03 Two-Blade Propeller at Forward Mach Numbers to
    0.925. NACA RM L9G06a, 1949.

12. Glauert, H.: Airplane Propellers Body and Wing Interference. Vol. IV
    of Aerodynamic Theory, div. L, ch. VIII, W. F. Durand, ed.
    Julius Springer (Berlin), 1935. (CIT reprint 1943)

13. Gilman, Jean, Jr.: Analytical Study of Static and Low-Speed Per-
    formance of Thin Propellers Using Two-Speed Gear Ratios to Obtain
    Optimum Rotational Speeds. NACA RM L52I09, 1952.

TABLE I.- LOCAL VELOCITY RATIO, U/V

(a) The 1-series spinner with cowl

M = 0.20 — Inlet velocity ratio, V_1/V

Radial station, in.	0.52	0.56	0.58	0.67	0.85	1.02	1.36
3.44	0.912	0.922	0.917	0.942	0.957	0.963	0.983
3.69	.916	.916	.916	.941	.951	.962	.982
3.94	.912	.912	.911	.936	.946	.962	.977
4.19	.901	.906	.911	.926	.936	.952	.962
4.44	.905	.905	.910	.925	.935	.951	.961
4.94	.900	.905	.905	.920	.930	.936	.956
5.44	.914	.909	.914	.928	.934	.935	.945
5.94	.923	.923	.918	.918	.938	.939	.944
6.44	.923	.909	.923	.928	.938	.939	.944
7.44	.947	.947	.942	.942	.947	.953	.948
8.44	.956	.956	.956	.956	.956	.962	.962
9.44	.966	.966	.966	.966	.976	.971	.971
10.44	.975	.975	.975	.975	.980	.975	.975
12.44	.984	.984	.987	.984	.984	.979	.979
14.44	.987	.987	.991	.986	.982	.982	.977
16.44	.991	.991	.990	.986	.986	.986	.981
18.44	.990	.990	.990	.990	.985	.990	.990
20.44	.990	.990	.989	.990	.990	.990	.995
22.44	.989	.989	.989	.984	.994	.989	.999
24.44	.999	.999	.999	.983	.988	.993	.988
26.44	.993	.993	.988	.993	.993	.998	.993
28.44	.993	.993	.998	.998	.993	.998	.998
30.44	.993	.993	.998	.997	.999	.999	.993
32.44	.997	.997	.997	.997	.996	.999	.995

M = 0.40 — Inlet velocity ratio, V_1/V

Radial station, in.	0.32	0.40	0.52	0.61	0.80	1.00	1.33
3.44	0.908	0.913	0.923	0.948	0.963	0.963	0.981
3.69	.901	.912	.919	.942	.952	.962	.952
3.94	.899	.909	.912	.939	.945	.957	.962
4.19	.892	.902	.907	.924	.937	.947	.954
4.44	.899	.902	.909	.927	.937	.947	.952
4.94	.893	.901	.906	.918	.926	.936	.940
5.44	.898	.908	.911	.923	.934	.939	.942
5.94	.903	.916	.923	.931	.934	.939	.942
6.44	.919	.918	.923	.931	.941	.939	.948
7.44	.935	.935	.933	.940	.943	.959	.962
8.44	.954	.957	.957	.959	.959	.967	.972
9.44	.967	.967	.967	.969	.970	.970	.965
10.44	.972	.978	.970	.969	.972	.978	.967
12.44	.978	.978	.978	.980	.988	.984	.982
14.44	.989	.984	.984	.987	.987	.981	.985
16.44	.986	.981	.981	.983	.984	.986	.984
18.44	.988	.988	.988	.988	.988	.981	.990
20.44	.993	.992	.993	.995	.993	.986	.996
22.44	.994	.989	.980	.991	.989	.992	.992
24.44	.998	.995	.993	.996	.998	.995	.995
26.44	.997	.996	.993	.997	.995	.994	.996
28.44	.996	.993	.995	.996	.996	.993	.996
30.44	.995	.993	.995	.995	.995	.991	.991
32.44	.999	.999	.999	.996	.997	.997	.999

M = 0.50 — Inlet velocity ratio, V_1/V

Radial station, in.	0.29	0.39	0.50	0.60	0.80	1.00	1.31
3.44	0.892	0.906	0.916	0.936	0.953	0.965	0.973
3.69	.889	.905	.913	.935	.948	.958	.972
3.94	.883	.900	.907	.927	.942	.954	.962
4.19	.875	.892	.896	.919	.932	.944	.954
4.44	.881	.894	.900	.919	.929	.942	.950
4.94	.879	.888	.896	.909	.923	.927	.962
5.44	.889	.909	.913	.915	.927	.929	.964
5.94	.901	.909	.902	.921	.923	.933	.942
6.44	.903	.911	.913	.921	.925	.931	.935
7.44	.904	.926	.928	.932	.939	.941	.945
8.44	.939	.943	.947	.951	.953	.953	.957
9.44	.953	.963	.965	.959	.963	.961	.965
10.44	.965	.963	.973	.963	.965	.967	.967
12.44	.971	.981	.983	.973	.976	.978	.978
14.44	.975	.981	.983	.983	.983	.985	.985
16.44	.981	.981	.983	.981	.981	.984	.984
18.44	.980	.989	.990	.984	.984	.986	.992
20.44	.986	.989	.990	.989	.990	.992	.992
22.44	.991	.991	.991	.990	.987	.987	.987
24.44	.990	.990	.998	.994	.992	.992	.996
26.44	.991	.991	.990	.993	.993	.994	.995
28.44	.987	.987	.991	.991	.989	.995	.996
30.44	.991	.992	.990	.991	.991	.991	.991
32.44	.994	.993	.995	.995	.993	.998	.998

M = 0.60 — Inlet velocity ratio, V_1/V

Radial station, in.	0.32	0.41	0.52	0.62	0.84	1.03	1.26
3.44	0.898	0.914	0.936	0.937	0.953	0.964	0.971
3.69	.898	.908	.926	.933	.950	.959	.966
3.94	.891	.905	.925	.928	.943	.950	.954
4.19	.883	.895	.914	.916	.931	.938	.947
4.44	.886	.897	.917	.911	.926	.940	.945
4.94	.883	.893	.910	.911	.924	.931	.935
5.44	.891	.898	.919	.916	.929	.928	.933
5.94	.903	.907	.921	.916	.931	.931	.930
6.44	.905	.912	.940	.930	.938	.938	.935
7.44	.926	.926	.950	.945	.950	.952	.952
8.44	.945	.947	.950	.959	.962	.964	.964
9.44	.961	.961	.966	.964	.964	.966	.964
10.44	.962	.962	.967	.967	.975	.973	.973
12.44	.958	.973	.973	.968	.982	.982	.979
14.44	.982	.980	.985	.980	.981	.981	.985
16.44	.983	.981	.984	.979	.984	.988	.988
18.44	.988	.984	.990	.981	.990	.990	.990
20.44	.992	.992	.996	.988	.989	.989	.989
22.44	.989	.989	.993	.990	.996	.992	.992
24.44	.994	.992	.997	.996	.993	.994	.993
26.44	.996	.996	.997	.991	.993	.996	.992
28.44	.994	.998	.999	.990	.996	.993	.993
30.44	.993	.993	.997	.990	.990	.995	.991
32.44	.999	.999	.999	.996	.996	.996	.996

M = 0.70 — Inlet velocity ratio, V_1/V

Radial station, in.	0.32	0.41	0.51	0.67	0.80	0.82	1.07
3.44	0.897	0.915	0.926	0.936	0.946	0.946	0.957
3.69	.892	.912	.925	.933	.946	.946	.957
3.94	.885	.906	.916	.924	.935	.935	.945
4.19	.874	.894	.905	.911	.923	.923	.933
4.44	.879	.895	.905	.911	.922	.923	.931
4.94	.874	.886	.895	.905	.913	.914	.922
5.44	.882	.891	.899	.904	.916	.913	.919
5.94	.891	.897	.905	.908	.908	.916	.924
6.44	.892	.898	.905	.907	.922	.914	.930
7.44	.912	.916	.919	.939	.925	.940	.942
8.44	.933	.936	.937	.954	.953	.953	.957
9.44	.951	.952	.950	.954	.950	.961	.952
10.44	.952	.964	.964	.961	.962	.975	.960
12.44	.964	.976	.973	.975	.974	.974	.973
14.44	.976	.979	.977	.978	.977	.980	.976
16.44	.979	.984	.983	.982	.982	.983	.979
18.44	.985	.988	.984	.985	.988	.986	.985
20.44	.990	.989	.988	.985	.986	.988	.986
22.44	.988	.987	.989	.986	.985	.987	.992
24.44	.989	.989	.993	.988	.988	.988	.992
26.44	.993	.993	.994	.991	.994	.990	.992
28.44	.987	.992	.992	.988	.992	.990	.989
30.44	.992	.993	.990	.988	.992	.992	.992
32.44	.995	.995	.994	.992	.996	.993	.991

M = 0.80 — Inlet velocity ratio, V_1/V

Radial station, in.	0.32	0.41	0.51	0.62	0.82	0.96
3.44	0.905	0.916	0.916	0.927	0.942	0.946
3.69	.896	.915	.915	.936	.936	.944
3.94	.886	.905	.905	.915	.928	.932
4.19	.885	.894	.895	.905	.914	.920
4.44	.877	.886	.886	.904	.911	.922
4.94	.878	.878	.886	.896	.904	.910
5.44	.868	.885	.891	.893	.904	.910
5.94	.873	.886	.891	.897	.906	.910
6.44	.896	.891	.891	.897	.902	.916
7.44	.921	.900	.891	.907	.912	.935
8.44	.937	.939	.923	.928	.928	.948
9.44	.946	.933	.938	.940	.944	.942
10.44	.952	.953	.938	.939	.942	.954
12.44	.965	.967	.964	.968	.955	.967
14.44	.970	.979	.970	.977	.966	.972
16.44	.978	.981	.976	.964	.970	.978
18.44	.981	.984	.983	.979	.971	.982
20.44	.984	.986	.986	.983	.982	.986
22.44	.987	.989	.987	.983	.985	.985
24.44	.985	.987	.990	.984	.982	.986
26.44	.991	.992	.987	.991	.989	.989
28.44	.992	.996	.990	.987	.984	.989
30.44	.993	.993	.990	.991	.991	.992
32.44	.994	.995	.995	.995	.993	.994

NACA

TABLE I.- LOCAL VELOCITY RATIO, U/V - Continued.

(b) Modified conical spinner with cowl

Radial station, in.	M = 0.20 Inlet velocity ratio, V₁/V						M = 0.40 Inlet velocity ratio, V₁/V						M = 0.50 Inlet velocity ratio, V₁/V					
	0.48	0.55	0.65	0.84	1.02	1.36	0.43	0.53	0.63	0.82	0.96	1.35	0.42	0.53	0.63	0.83	1.04	1.31
3.34	0.881	0.897	0.912	0.927	0.937	0.954	0.871	0.900	0.905	0.920	0.928	0.945	0.866	0.897	0.903	0.920	0.928	0.936
3.59	.885	.901	.911	.926	.941	.956	.870	.899	.924	.919	.929	.944	.863	.896	.904	.917	.929	.937
3.84	.880	.901	.911	.926	.936	.956	.870	.896	.922	.917	.926	.942	.861	.892	.900	.915	.925	.931
4.09	.880	.896	.906	.916	.931	.946	.868	.894	.899	.909	.919	.932	.859	.888	.894	.907	.917	.927
4.34	.884	.900	.910	.915	.930	.945	.875	.896	.904	.914	.919	.932	.863	.890	.898	.911	.915	.929
4.84	.884	.895	.910	.929	.925	.940	.877	.893	.900	.908	.915	.928	.868	.888	.896	.907	.913	.919
5.34	.898	.909	.919	.929	.934	.939	.890	.903	.905	.916	.920	.933	.882	.896	.902	.911	.917	.923
5.84	.908	.913	.923	.933	.938	.943	.905	.910	.912	.921	.925	.936	.894	.907	.913	.913	.923	.927
6.34	.918	.913	.923	.938	.938	.943	.908	.916	.918	.922	.928	.940	.898	.909	.913	.915	.923	.936
7.34	.932	.937	.947	.947	.961	.951	.928	.930	.930	.935	.937	.957	.920	.926	.928	.934	.936	.949
8.34	.946	.952	.956	.956	.961	.961	.949	.949	.949	.956	.957	.967	.940	.945	.947	.952	.949	.961
9.34	.966	.964	.971	.971	.971	.976	.964	.962	.962	.965	.964	.975	.957	.959	.961	.959	.961	.961
10.34	.975	.975	.980	.980	.980	.985	.967	.967	.967	.968	.975	.984	.963	.965	.965	.963	.973	.965
12.34	.984	.984	.989	.989	.989	.989	.975	.973	.973	.975	.981	.981	.975	.973	.973	.982	.984	.973
14.34	.987	.982	.987	.987	.987	.987	.987	.984	.984	.984	.983	.983	.985	.985	.985	.978	.983	.985
16.34	.991	.986	.991	.991	.991	.991	.983	.981	.981	.981	.986	.986	.983	.983	.983	.985	.981	.981
18.34	.990	.990	.995	.995	.995	.990	.983	.983	.983	.983	.986	.986	.986	.986	.986	.988	.986	.986
20.34	.995	.995	1.000	.995	.995	1.000	.992	.982	.992	.989	.992	.991	.994	.990	.990	.986	.992	.990
22.34	.989	.989	.994	.994	.994	.994	.994	.981	.991	.991	.991	.993	.989	.991	.991	.997	.989	.992
24.34	.999	.999	1.004	1.004	1.004	1.004	.998	.990	.996	.996	.993	.993	.996	.996	.996	.998	.994	.994
26.34	.993	.988	.993	.993	.998	.998	.997	.997	.995	.995	.994	.994	.995	.995	.995	.996	.995	.994
28.34	.993	1.003	1.003	.993	1.003	1.003	.996	.988	.994	.990	.994	.994	.991	.991	.991	.997	.993	.991
30.34	.998	1.000	1.003	1.003	1.008	1.003	.993	.993	.990	.990	.993	.993	.991	1.000	.993	.991	.993	.991
32.34	.997	1.002	1.007	1.007	1.002	1.007	.997	.988	.994	.994	.997	.997	.998	1.000	.998	1.000	1.000	.998

Radial station, in.	M = 0.60 Inlet velocity ratio, V₁/V						M = 0.70 Inlet velocity ratio, V₁/V							M = 0.80 Inlet velocity ratio, V₁/V					
	0.34	0.43	0.54	0.65	0.85	1.05	0.32	0.42	0.50	0.62	0.82	0.96	1.11	0.30	0.41	0.52	0.62	0.82	0.98
3.34	0.867	0.885	0.893	0.898	0.912	0.917	0.856	0.880	0.883	0.894	0.907		0.916	0.838	0.865	0.874	0.884	0.894	0.902
3.59	.872	.888	.901	.902	.916	.921	.856	.882	.885	.895	.907		.919	.841	.867	.875	.884	.897	.903
3.84	.867	.883	.898	.898	.907	.917	.853	.877	.880	.888	.901		.911	.837	.861	.870	.880	.890	.896
4.09	.867	.878	.886	.891	.900	.910	.847	.870	.873	.882	.893		.904	.830	.855	.863	.872	.882	.890
4.34	.867	.879	.888	.895	.900	.912	.851	.873	.880	.885	.896		.907	.836	.857	.866	.874	.882	.891
4.84	.868	.879	.886	.893	.900	.907	.853	.870	.876	.883	.890		.899	.834	.855	.862	.872	.882	.887
5.34	.880	.886	.893	.896	.902	.909	.863	.880	.883	.888	.896		.904	.844	.862	.867	.875	.883	.890
5.84	.893	.897	.901	.905	.910	.917	.878	.889	.891	.895	.904		.910	.857	.870	.875	.883	.890	.896
6.34	.898	.898	.903	.909	.914	.917	.883	.892	.894	.897	.910		.910	.862	.874	.879	.884	.891	.895
7.34	.919	.917	.921	.921	.928	.928	.902	.909	.912	.913	.919		.922	.886	.894	.896	.900	.903	.908
8.34	.939	.936	.948	.941	.943	.943	.926	.933	.933	.933	.938		.938	.910	.916	.918	.923	.924	.927
9.34	.957	.954	.955	.955	.955	.959	.946	.946	.946	.948	.950		.946	.931	.934	.935	.937	.940	.943
10.34	.960	.955	.959	.959	.959	.970	.940	.940	.942	.942	.944		.938	.915	.918	.918	.910	.922	.927
12.34	.971	.966	.970	.972	.970	.970	.962	.964	.966	.964	.965		.965	.951	.952	.954	.955	.942	.957
14.34	.982	.977	.980	.979	.979	.980	.974	.976	.976	.976	.976		.980	.966	.964	.965	.967	.967	.968
16.34	.981	.976	.980	.978	.978	.979	.977	.979	.979	.978	.979		.979	.971	.972	.972	.973	.976	.973
18.34	.990	.984	.983	.983	.981	.979	.980	.982	.982	.982	.982		.981	.975	.977	.977	.979	.979	.979
20.34	.992	.989	.989	.989	.989	.988	.989	.988	.990	.989	.988		.989	.985	.984	.984	.985	.986	.987
22.34	.991	.988	.992	.992	.992	.994	.987	.989	.990	.987	.989		.994	.988	.986	.987	.987	.984	.979
24.34	.995	.990	.992	.994	.994	.994	.989	.992	.992	.994	.994		.994	.987	.986	.989	.989	.989	.987
26.34	.994	.993	.994	.994	.991	.991	.994	.994	.995	.994	.993		.993	.996	.992	.987	.988	.993	.989
28.34	.996	.994	.992	.992	.991	.991	.993	.995	.994	.990	.996		.994	.987	.986	.994	.994	.987	.987
30.34	.995	.991	.995	.993	.991	.996	.995	.999	.999	.994	.993		.993	.996	.992	.988	.988	.989	.998
32.34	1.001	.996	.996	1.000	.996	.996	.999	.999	.999	.999	.996		.999	.995	.992	.993	.993	.993	.995

TABLE I.- LOCAL VELOCITY RATIO, U/V - Concluded

(c) The 1-series spinner, no cowl

Radial station, in.	M=0.15	M=0.20	M=0.40	M=0.50	M=0.60	M=0.70	M=0.80
3.44	1.071	1.079	1.088	1.092	1.102	1.108	1.124
3.69	1.070	1.078	1.082	1.095	1.102	1.109	1.124
3.94	1.063	1.068	1.077	1.079	1.089	1.094	1.107
4.19	1.049	1.063	1.062	1.067	1.076	1.081	1.092
4.44	1.042	1.057	1.059	1.063	1.071	1.076	1.088
4.94	1.021	1.037	1.043	1.046	1.059	1.064	1.071
5.44	1.020	1.030	1.035	1.038	1.050	1.052	1.065
5.94	1.019	1.029	1.028	1.036	1.044	1.046	1.055
6.44	1.013	1.019	1.020	1.024	1.031	1.034	1.043
7.44	1.005	1.018	1.014	1.014	1.023	1.027	1.032
8.44	.997	1.012	1.015	1.014	1.023	1.027	1.033
9.44	1.003	1.011	1.008	1.014	1.021	1.025	1.035
10.44	1.002	1.005	1.005	1.006	1.011	1.013	1.013
12.44	1.001	1.004	1.001	1.004	1.004	1.005	1.005
14.44	.999	.997	1.005	1.003	1.006	1.007	1.004
16.44	.998	.996	.999	.997	1.002	1.003	1.001
18.44	.997	.995	.996	.996	1.002	1.002	1.000
20.44	.997	1.000	1.000	1.004	1.004	1.005	1.001
22.44	.899	.999	.997	1.001	1.001	1.002	1.000
24.44	1.003	1.009	1.001	1.004	1.002	1.003	.998
26.44	.995	1.003	1.000	1.002	1.005	1.003	.997
28.44	1.002	1.008	1.001	1.001	1.004	1.005	.999
30.44	1.002	1.008	1.003	1.001	1.003	1.003	1.001
32.44	1.001	1.007	1.004	1.006	1.008	1.004	1.001

NACA
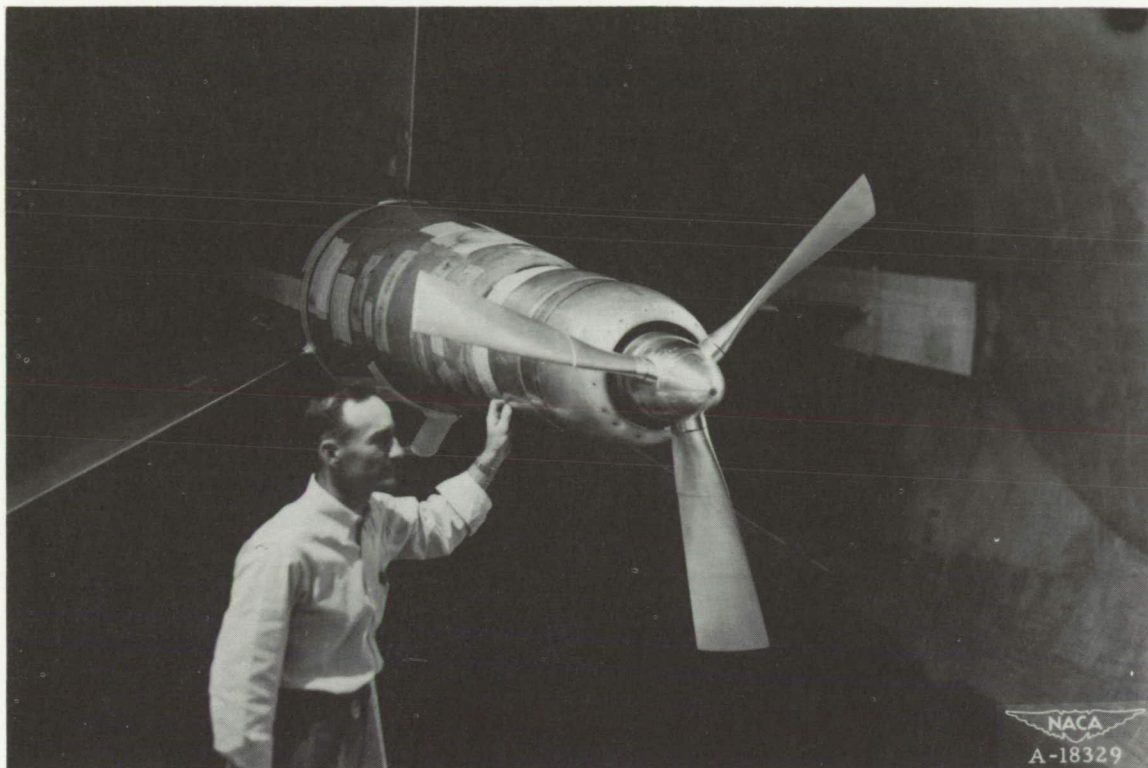
Figure 1.- The model mounted on the 1000-horsepower propeller dynamometer in the 12-foot pressure wind tunnel.
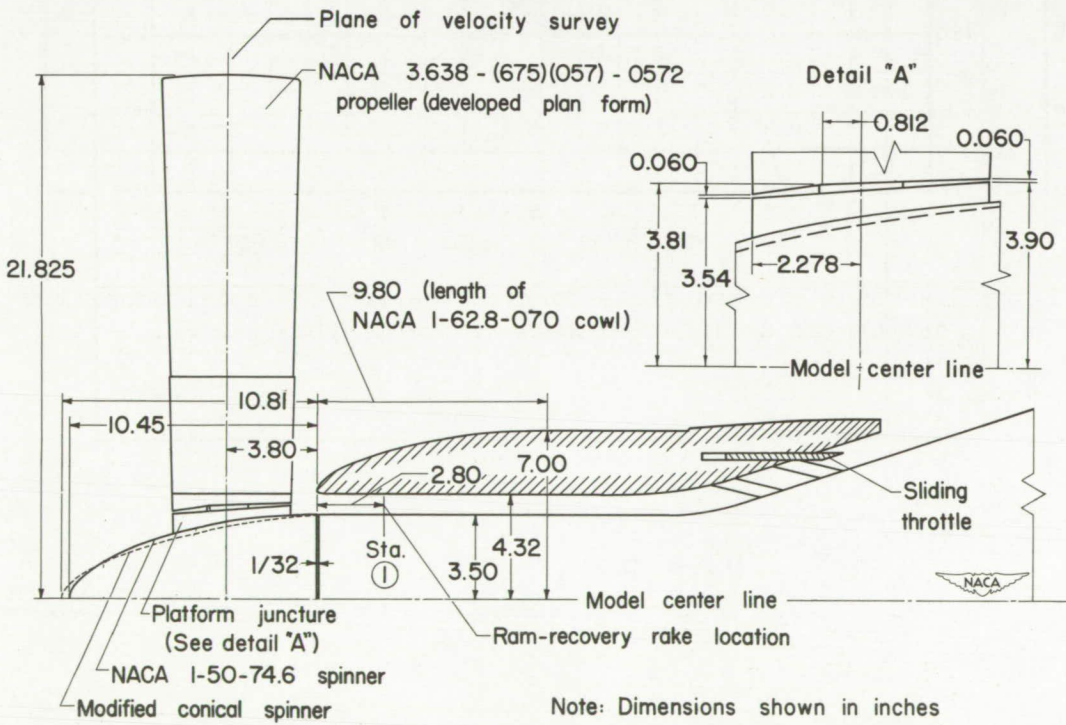
Figure 2.- Model arrangement.
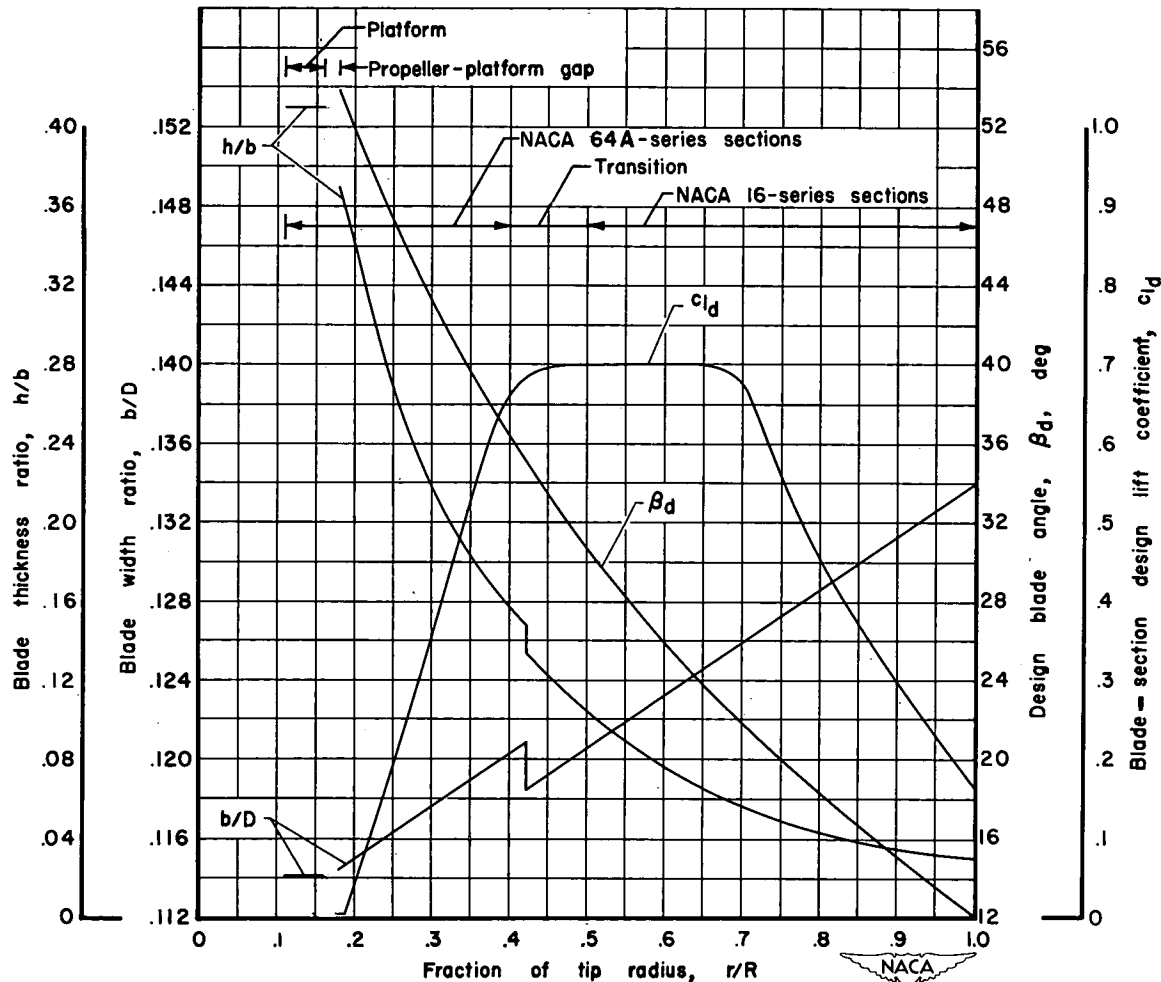
Figure 3.- Plan-form and blade-form curves for the model propeller
        having the designation NACA 3.638-(675)(057)-0572.
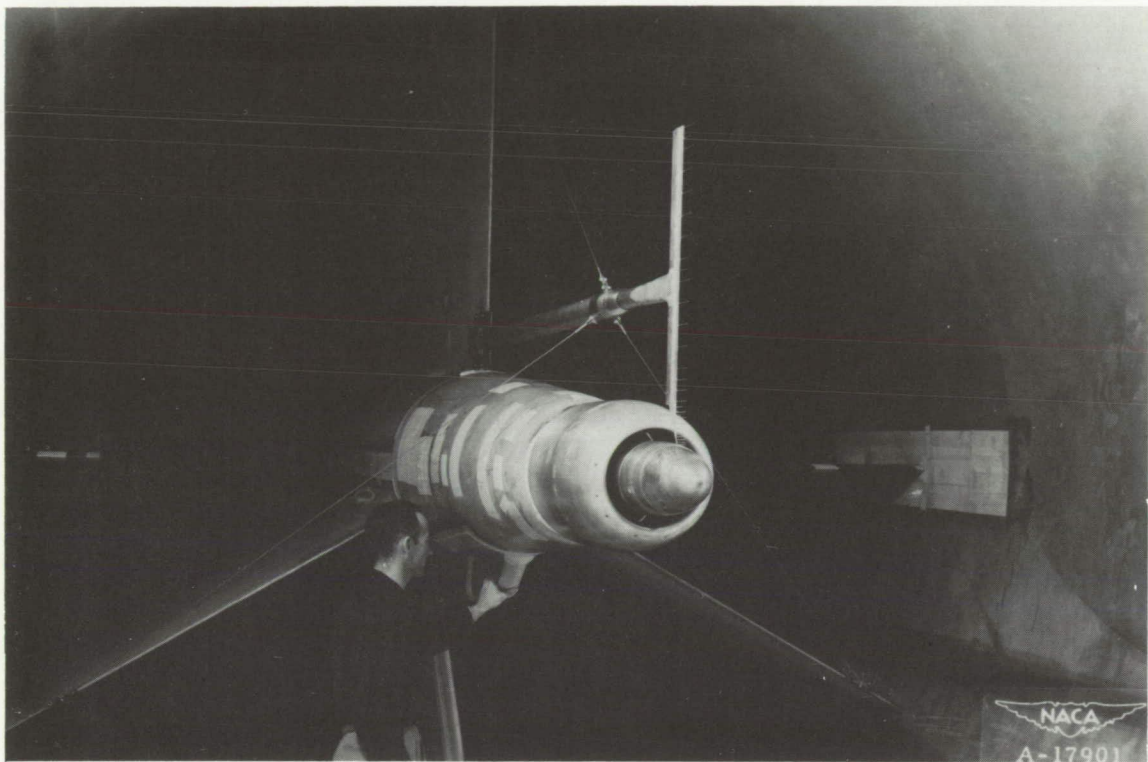
Figure 4.- Photograph of the survey rake.

CONFIDENTIAL

NACA RM A54B18a
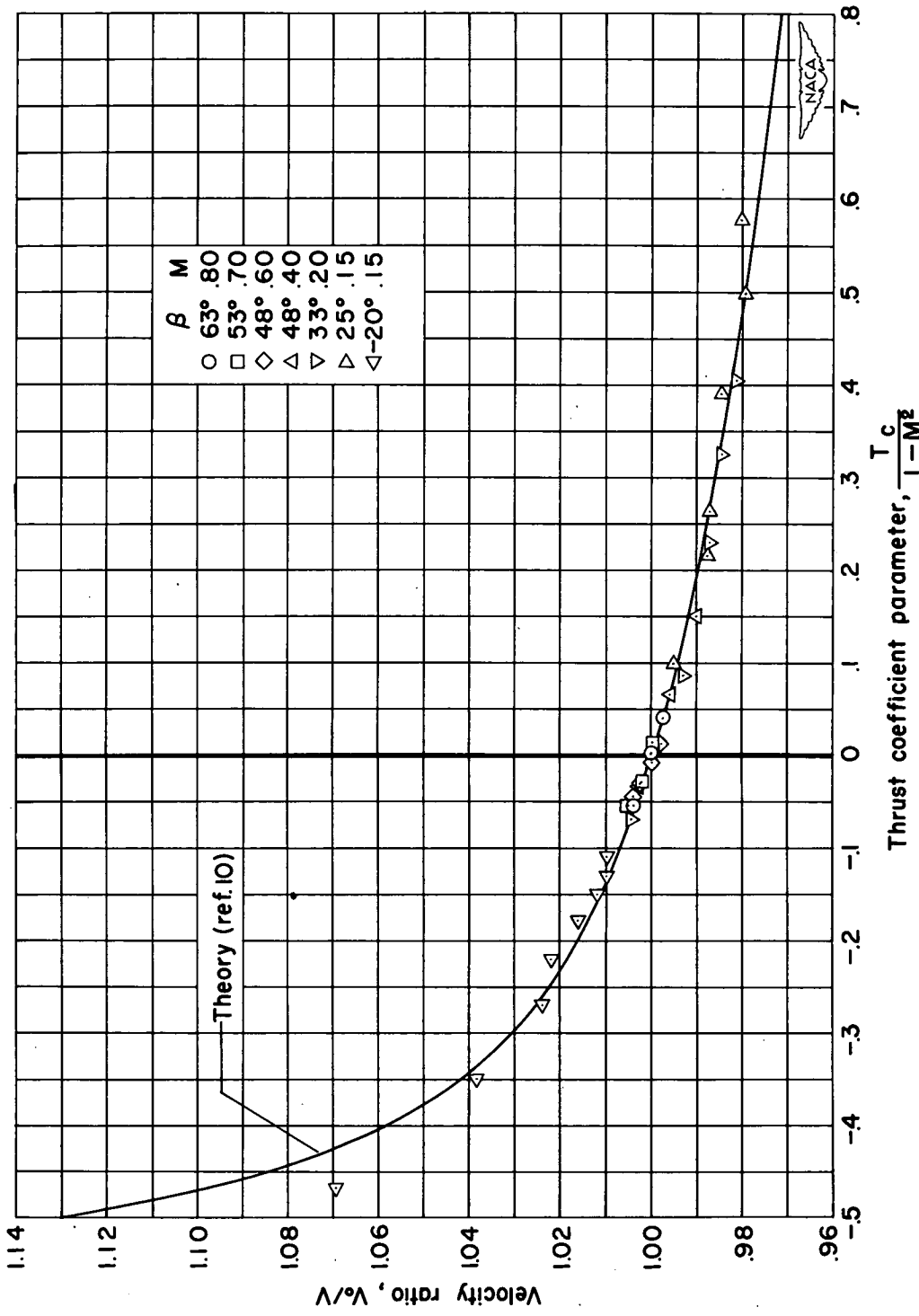
Figure 5.- Tunnel-wall-interference correction for a 3.6-foot-diameter propeller in the Ames 12-foot pressure wind tunnel.
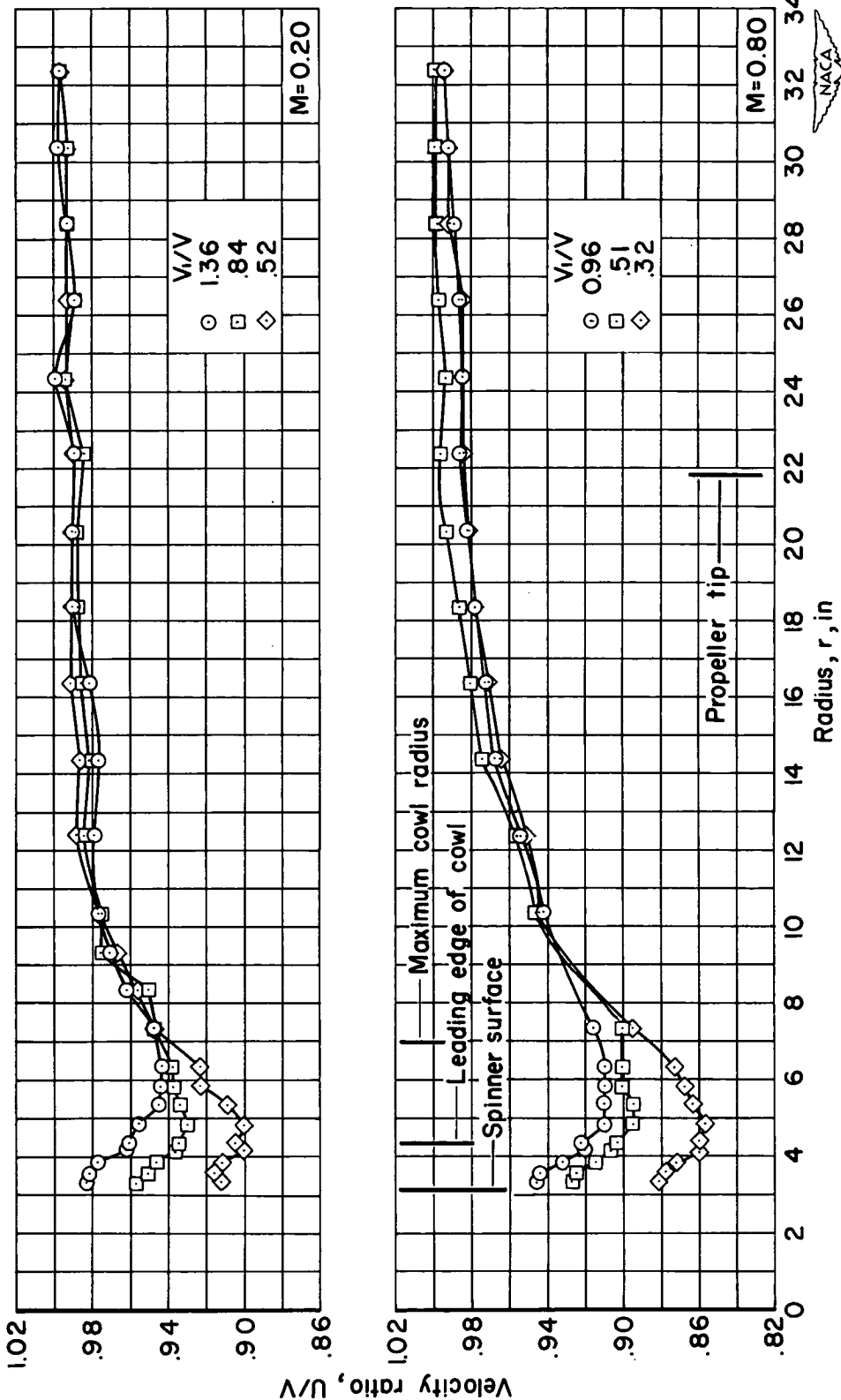
(a) The 1-series spinner with cowl.

Figure 6.- Typical radial distributions of the local velocity ratio in the plane of the propeller.
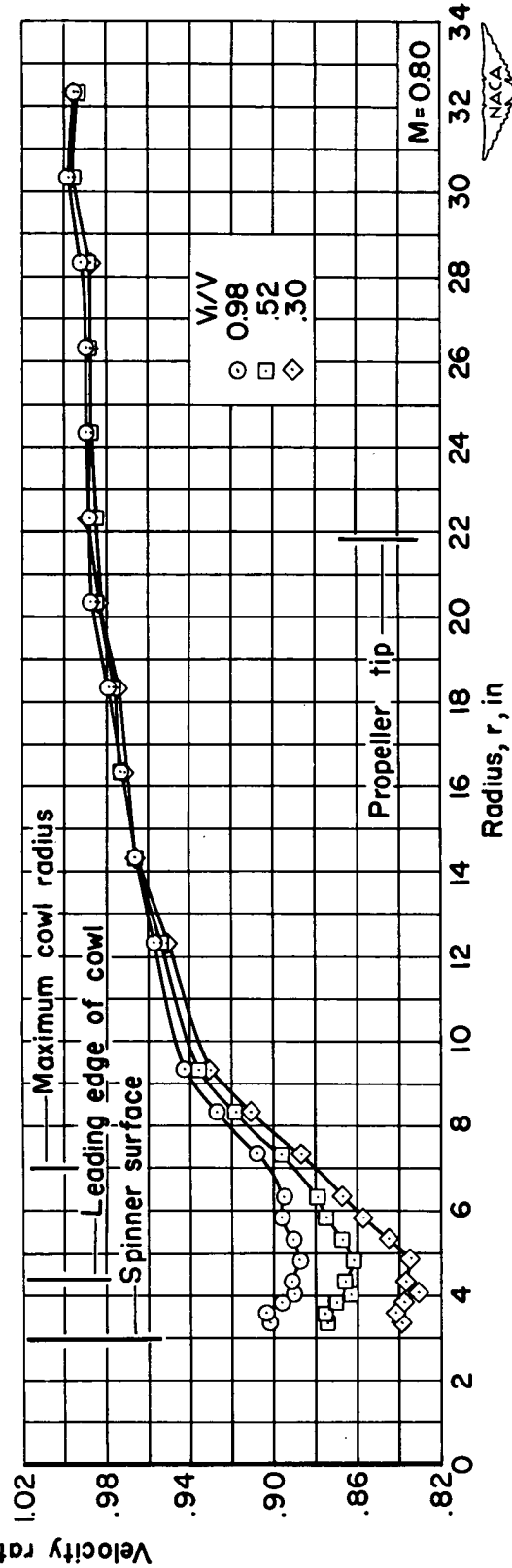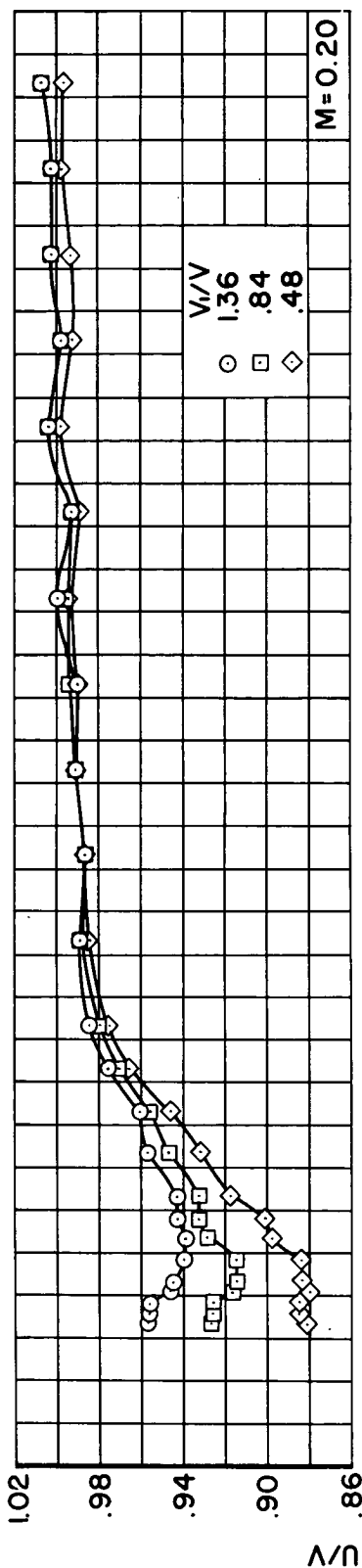
(b) Modified conical spinner with cowl.

Figure 6.- Continued.
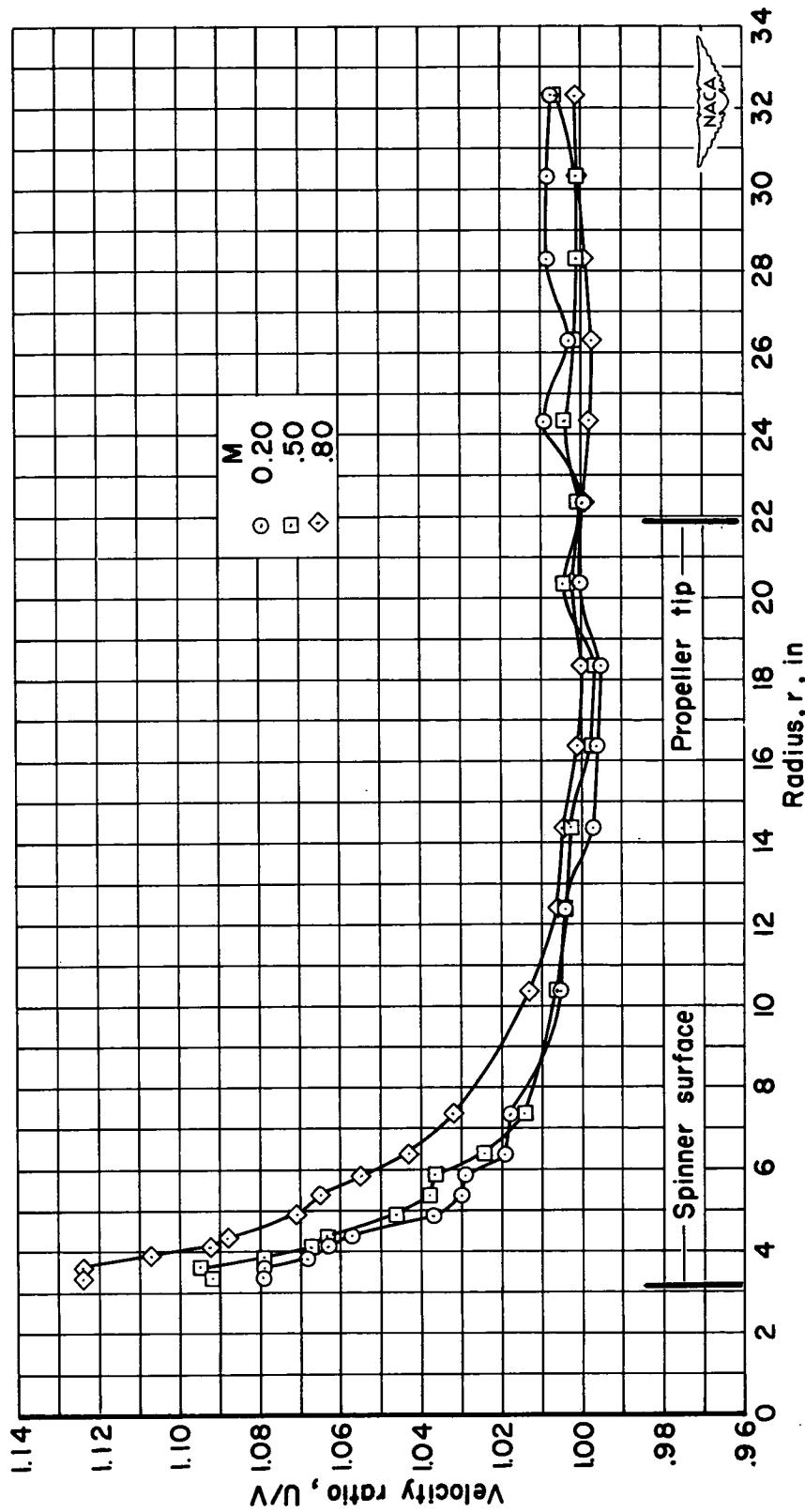
(c) The l-series spinner, no cowl.

Figure 6.- Concluded.

CONFIDENTIAL
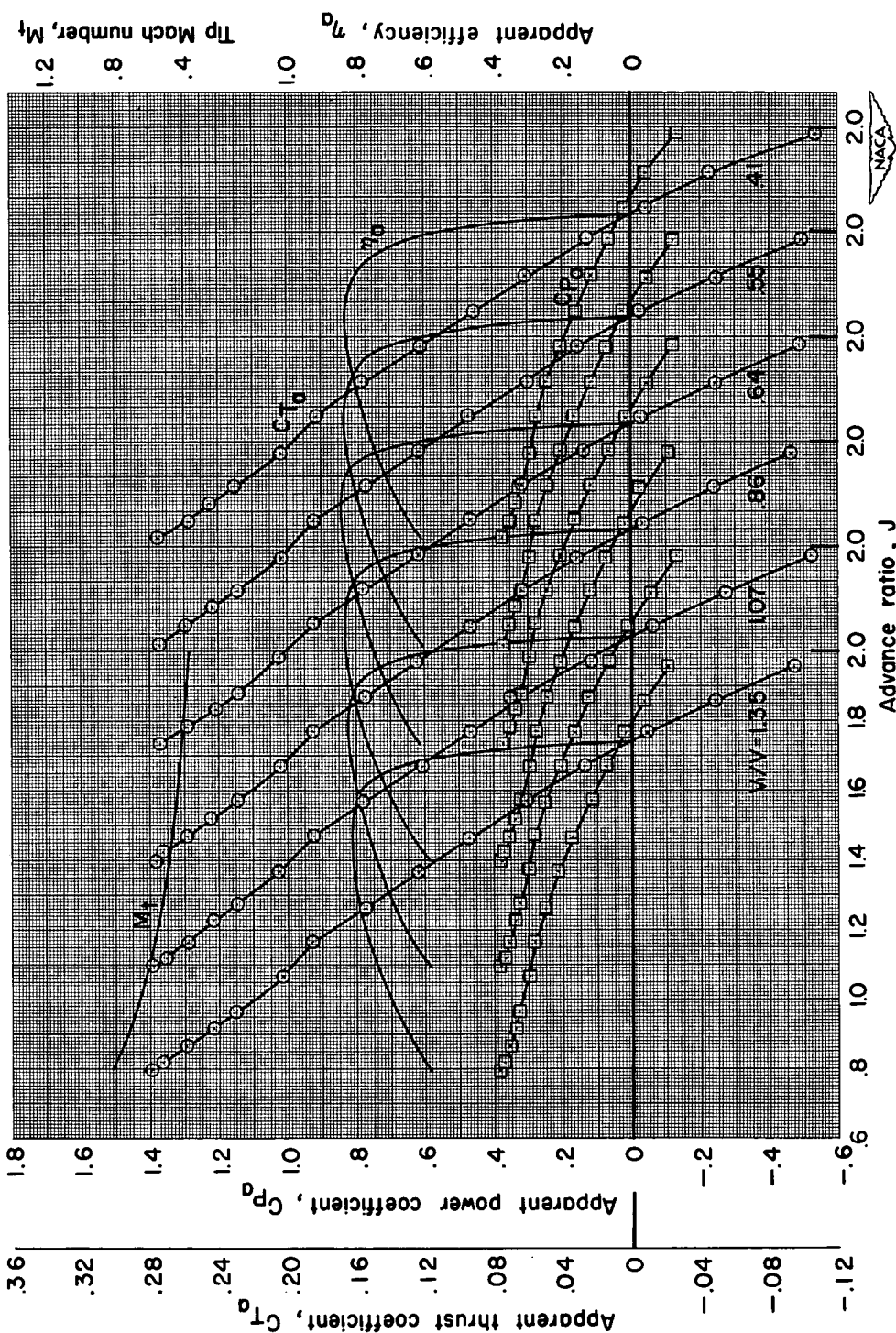
(a) M = 0.20, β = 33°

Figure 7.- Characteristics of the propeller with the 1-series spinner and cowl.
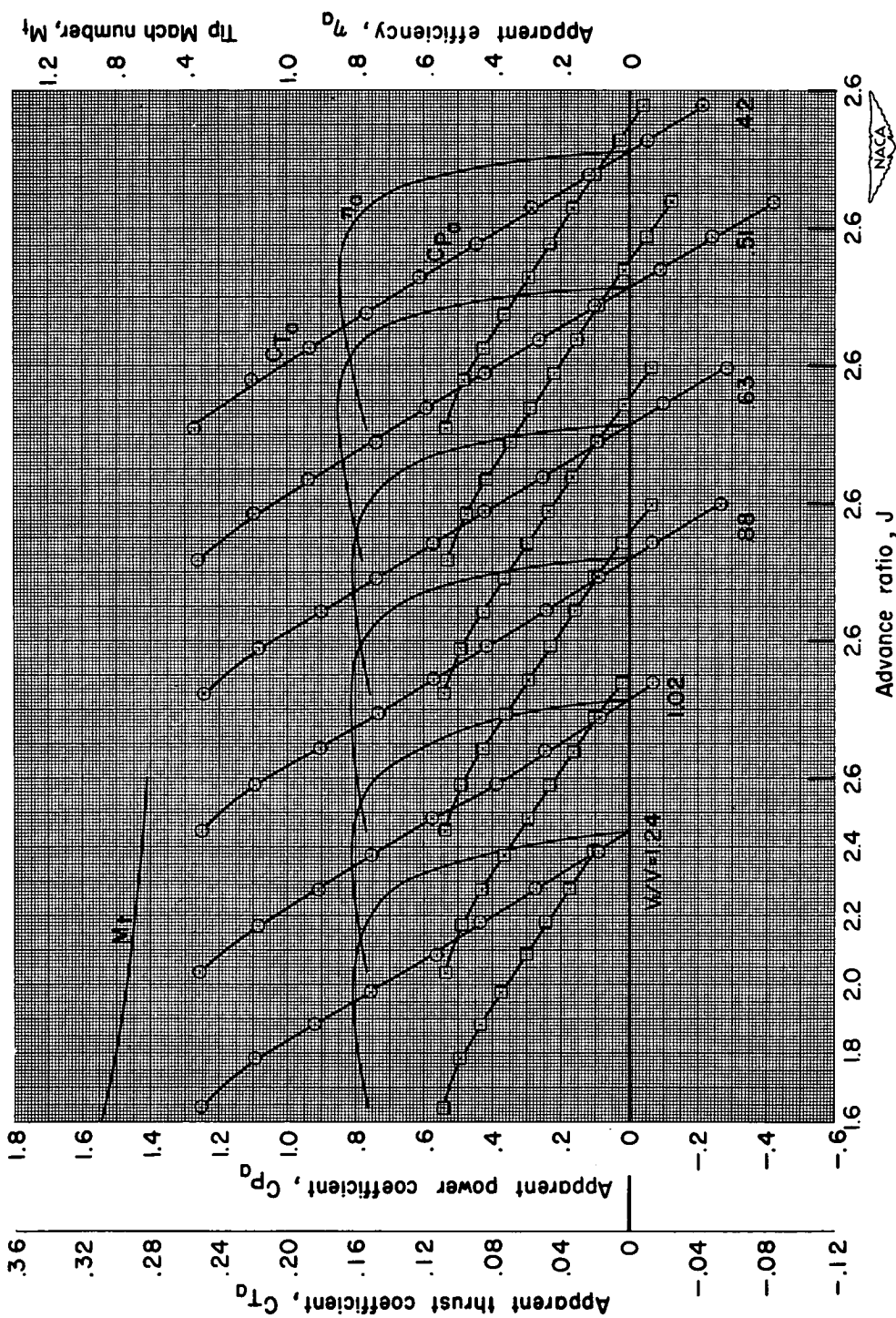
(b) M = 0.40, β = 43°

Figure 7.- Continued.
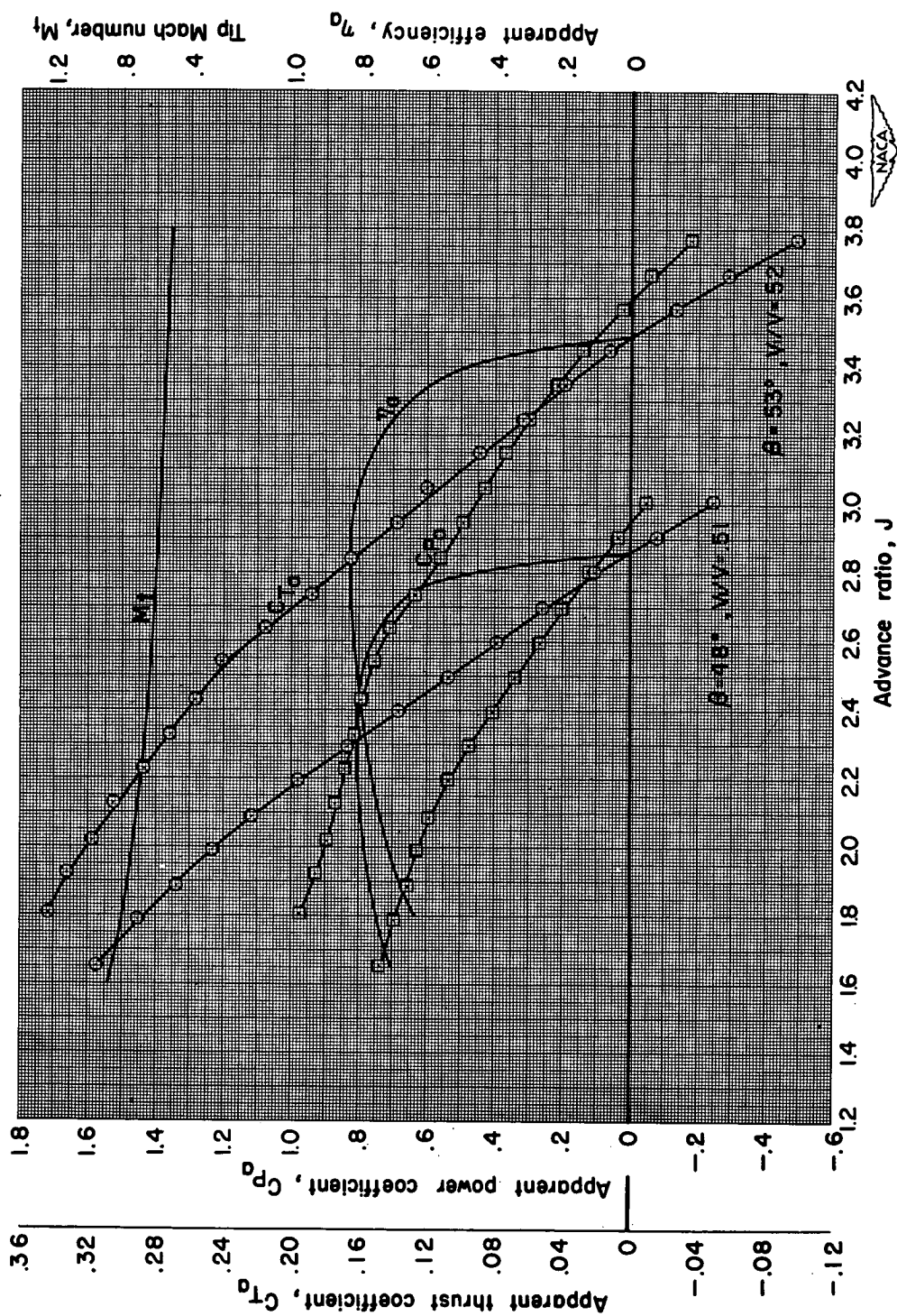
(c) $M = 0.40$, $\beta = 48^\circ$ and 53°

Figure 7.-- Continued.

(d) M = 0.50, β = 48°

Figure 7.- Continued.

(e) M = 0.50, β = 43° and 53°

(f) M = 0.60, β = 48°
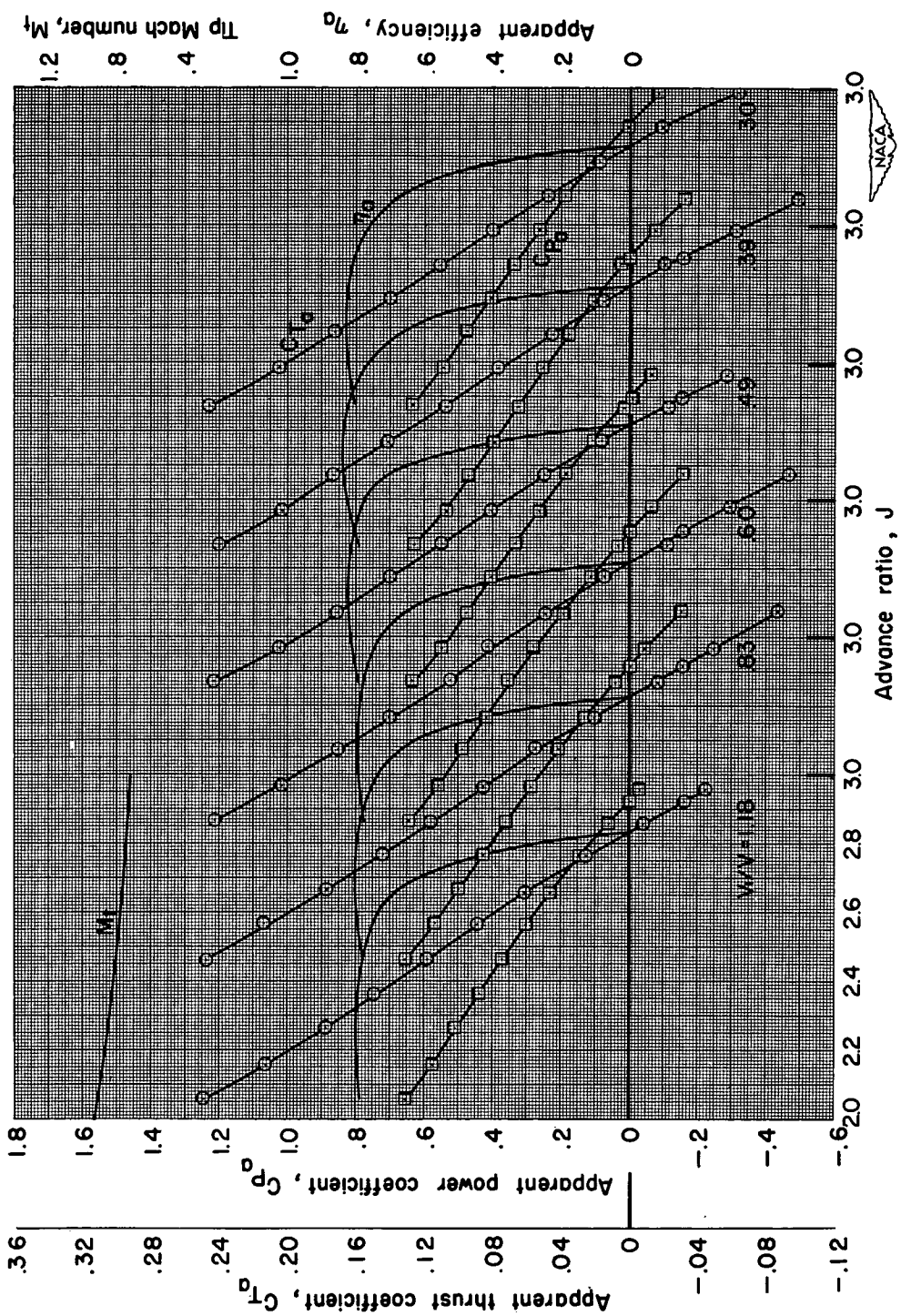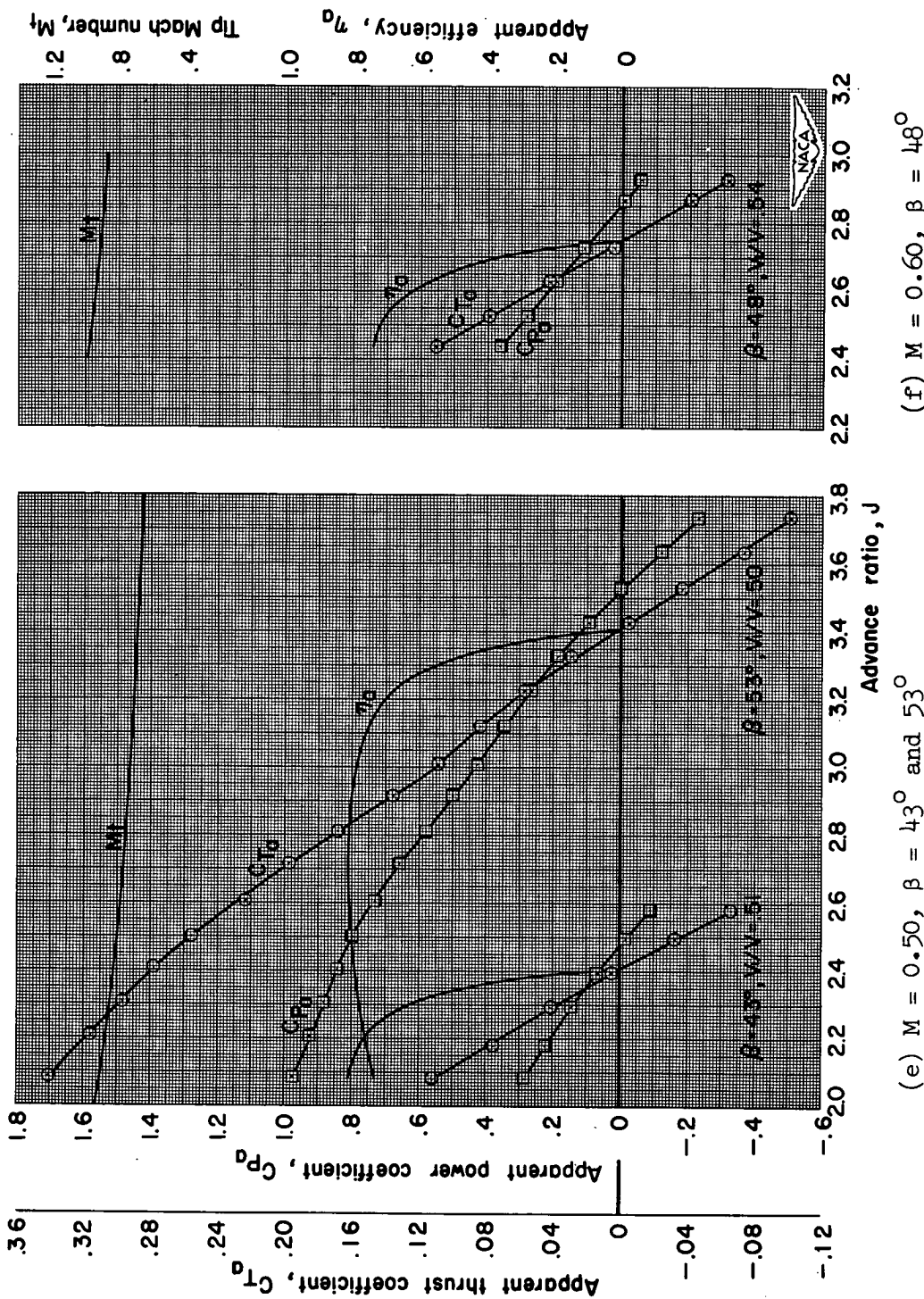
Figure 7.- Continued.

(g) M = 0.60, β = 53°

Figure 7.- Continued.

(h) M = 0.70, β = 58.5°
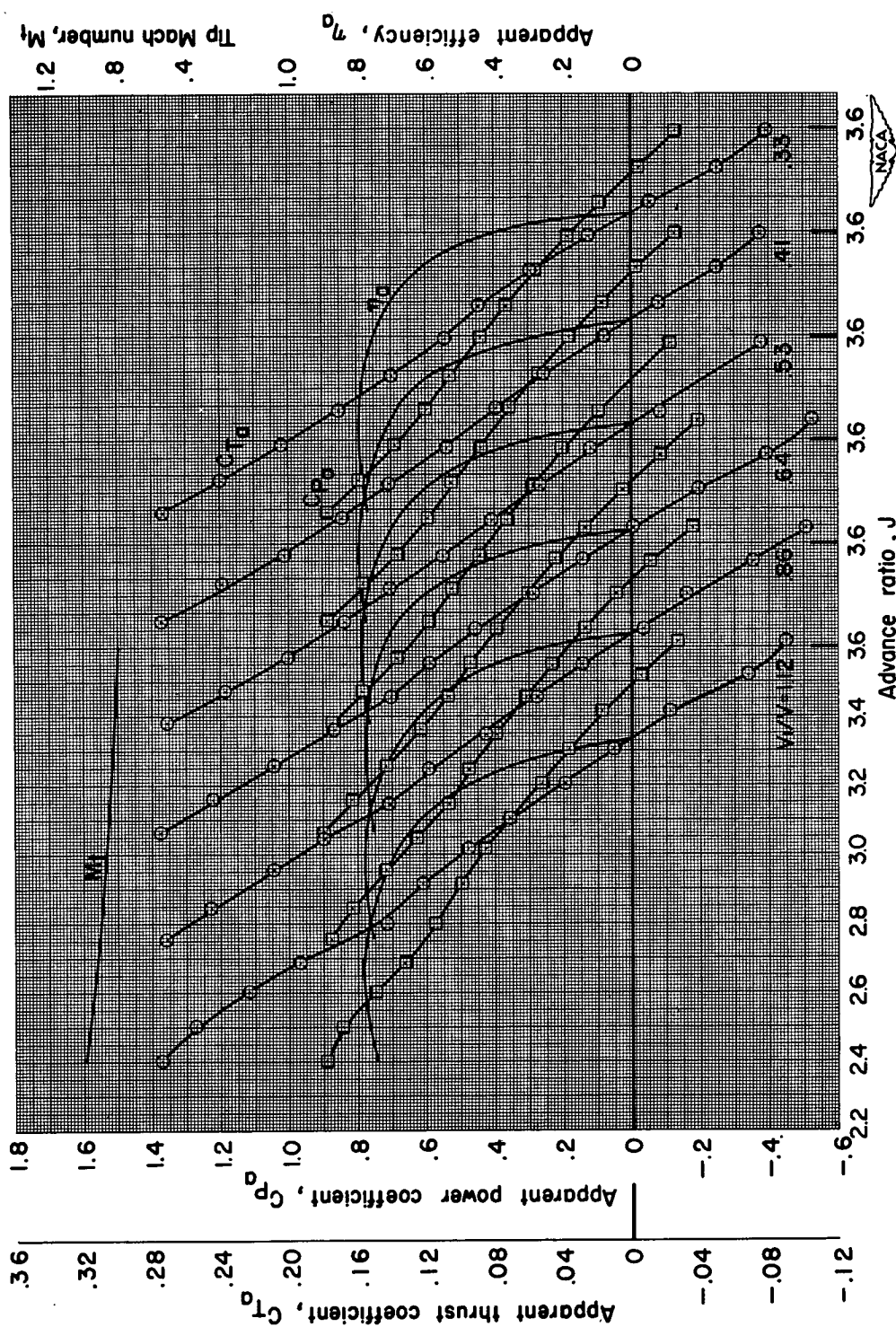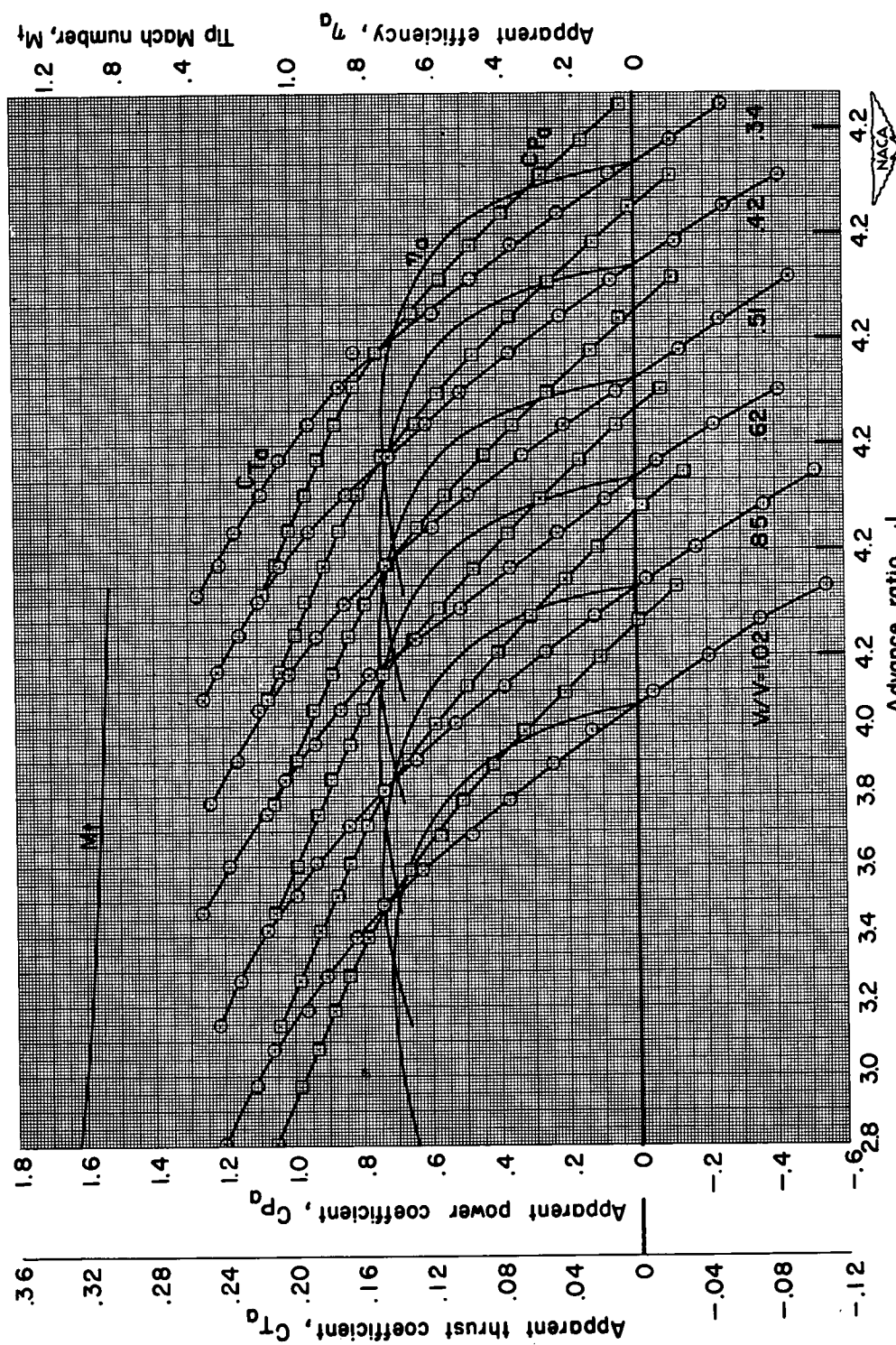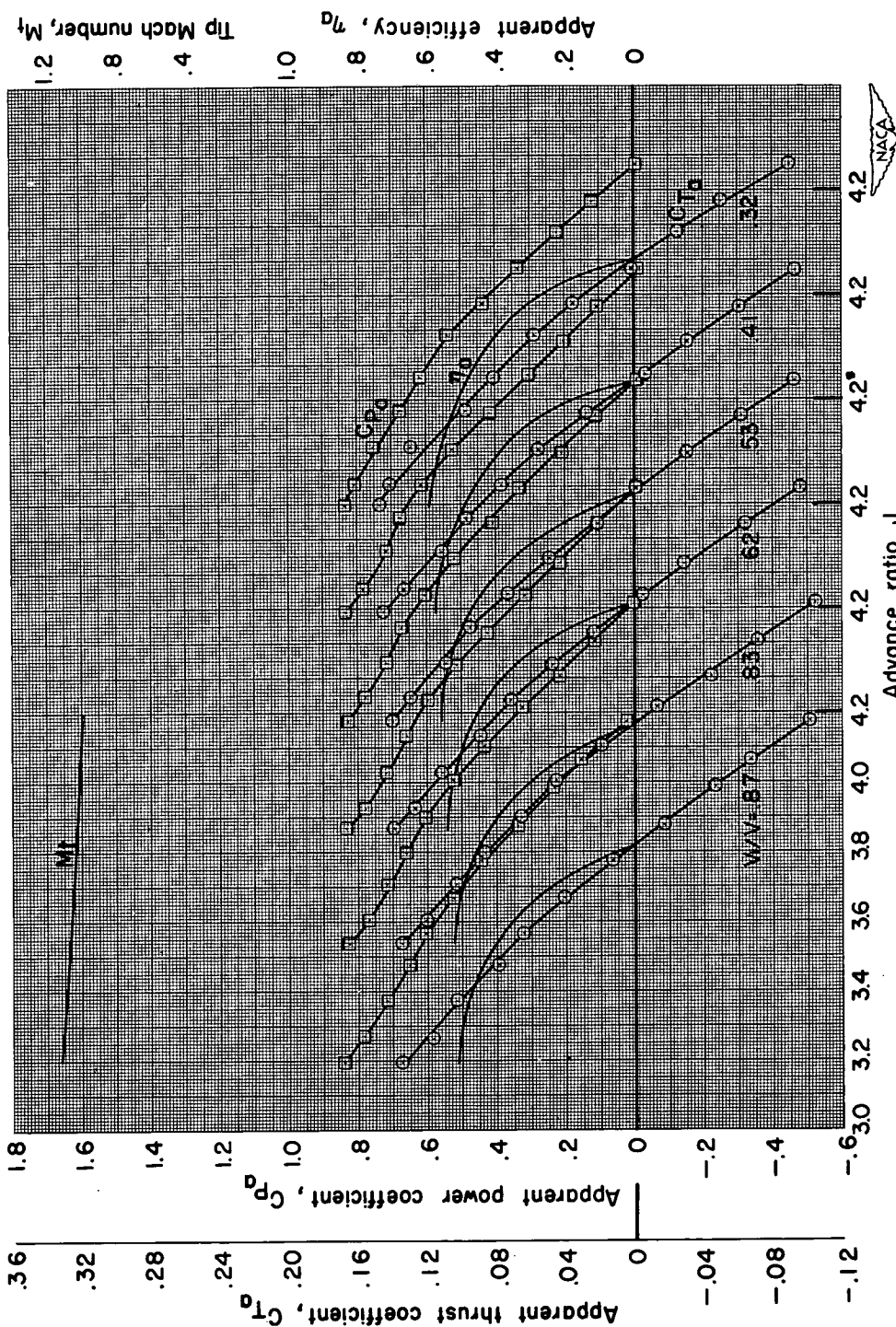
Figure 7.- Continued.

(i) $M = 0.80$, $\beta = 58.5°$

Figure 7.- Concluded.
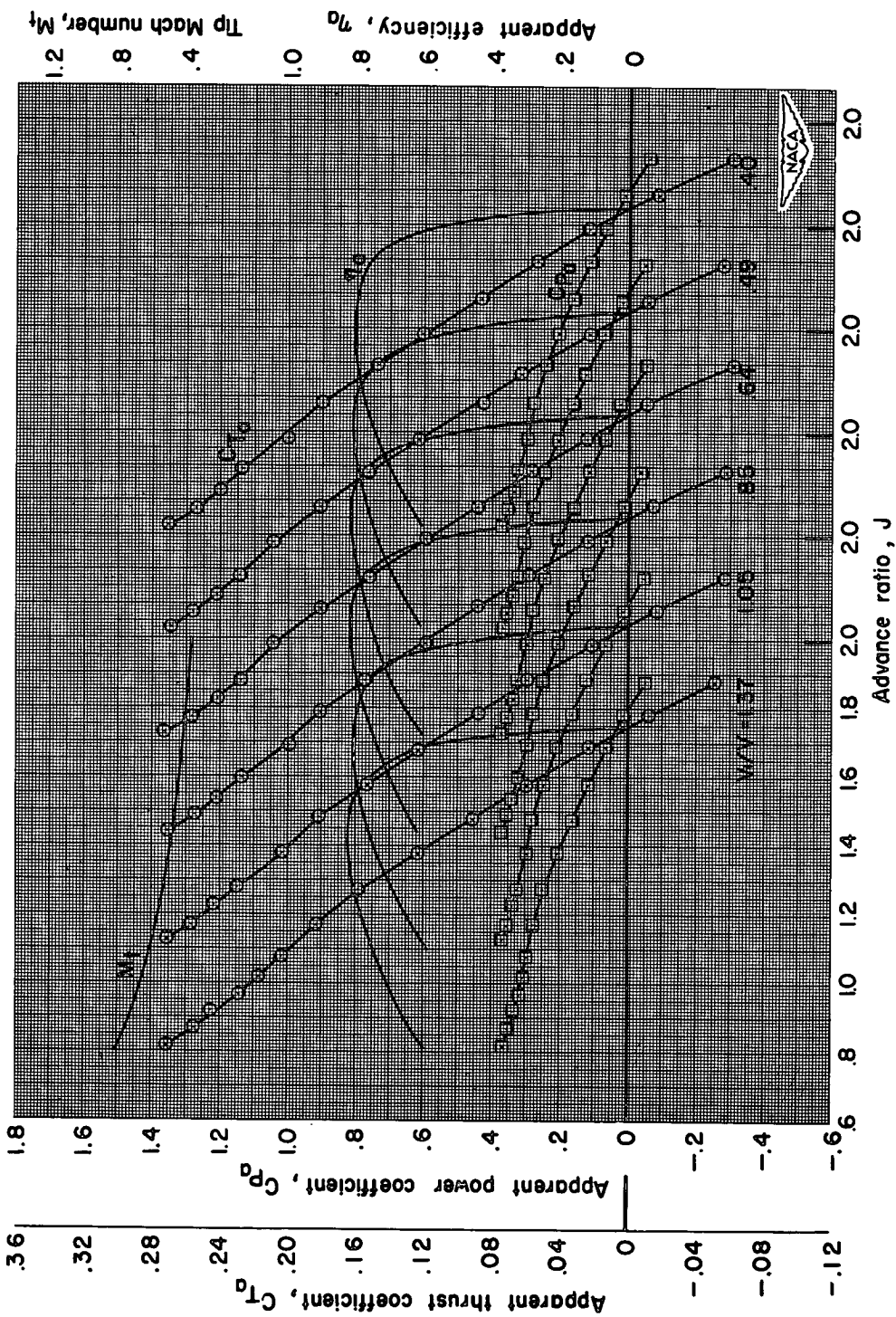
(a) $M = 0.20$, $\beta = 33°$

Figure 8.- Characteristics of the propeller with the modified conical spinner and cowl.
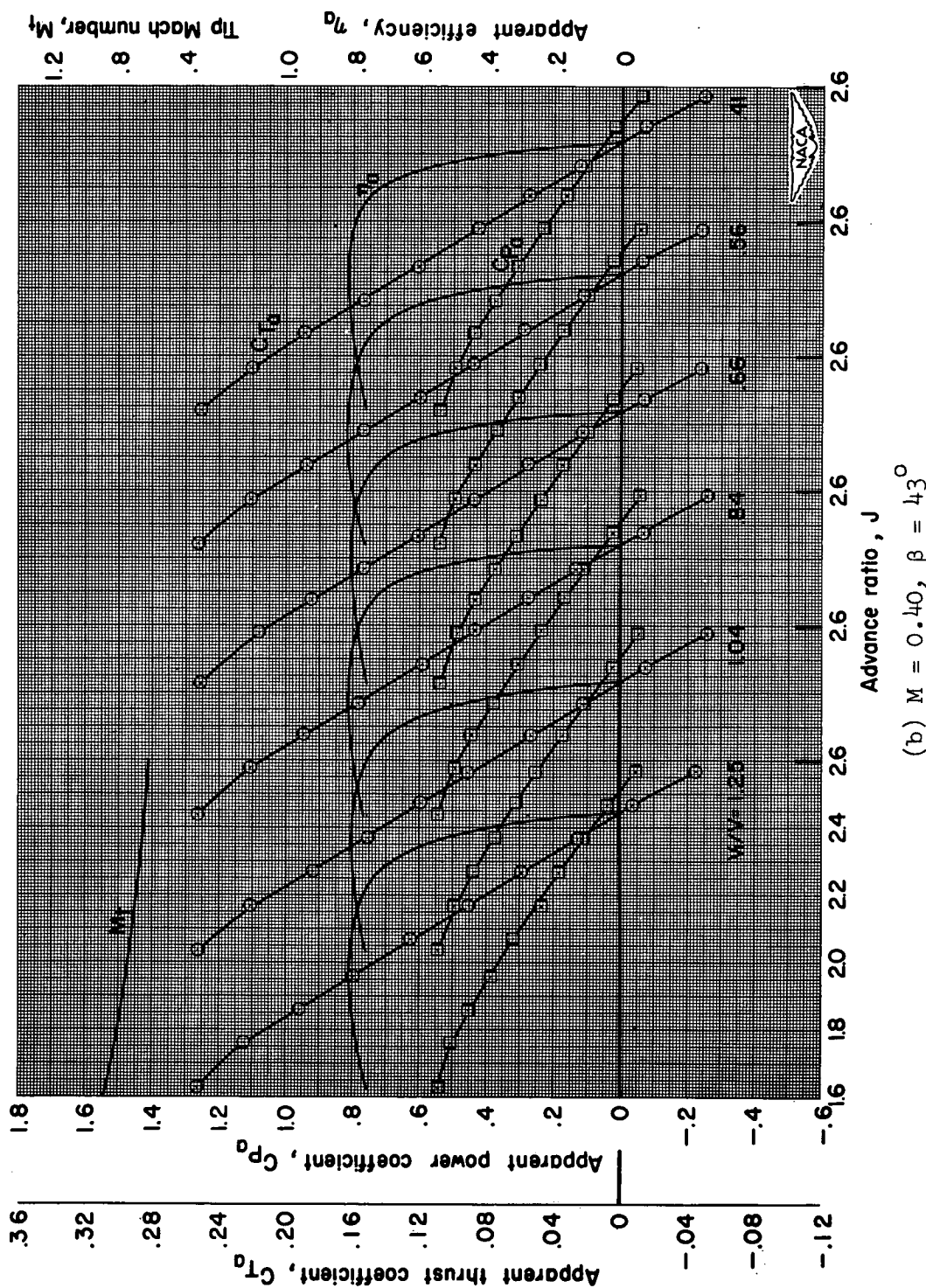
(b) $M = 0.40$, $\beta = 43^{\circ}$

Figure 8.- Continued.
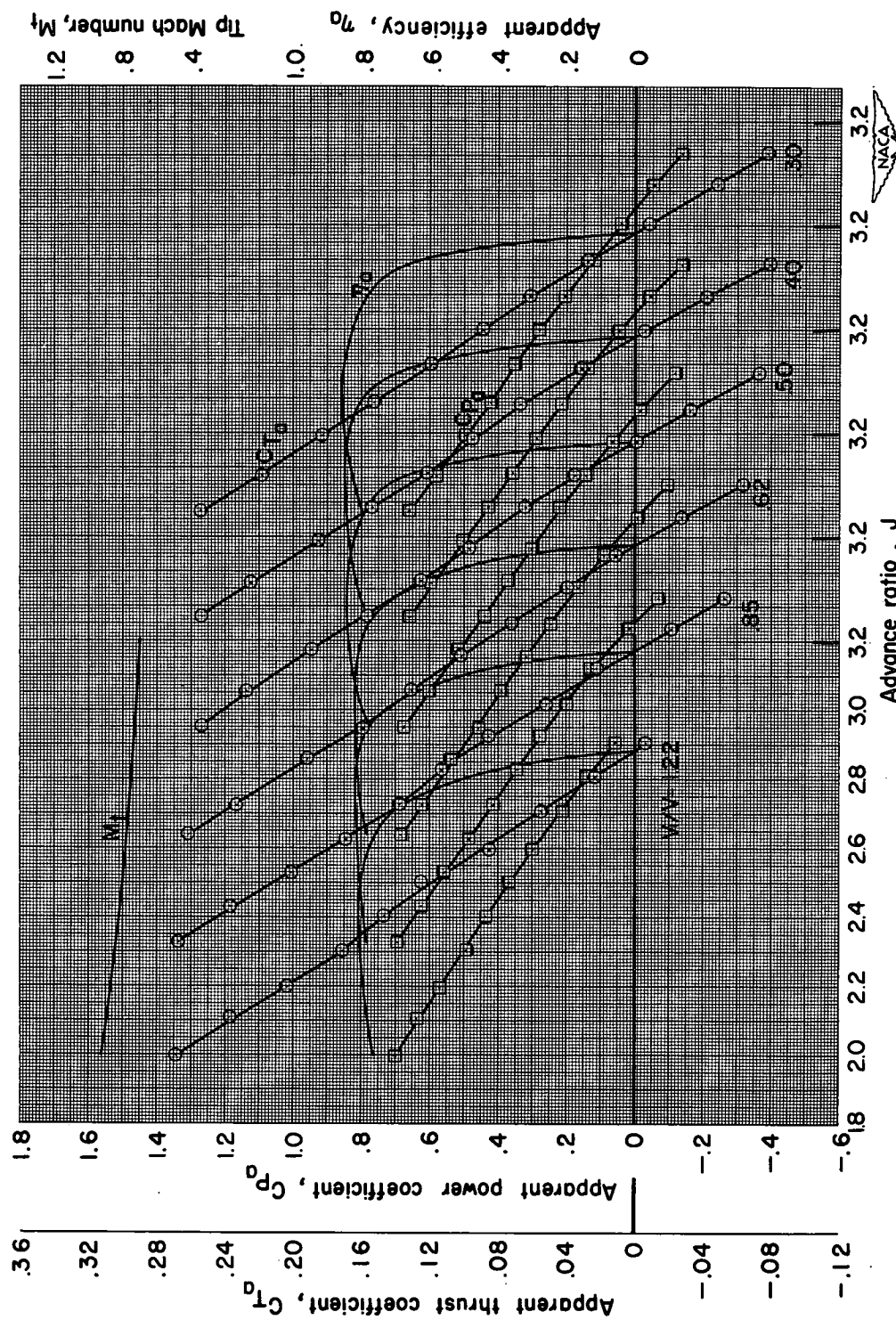
(c) $M = 0.50$, $\beta = 48°$

Figure 8.- Continued.
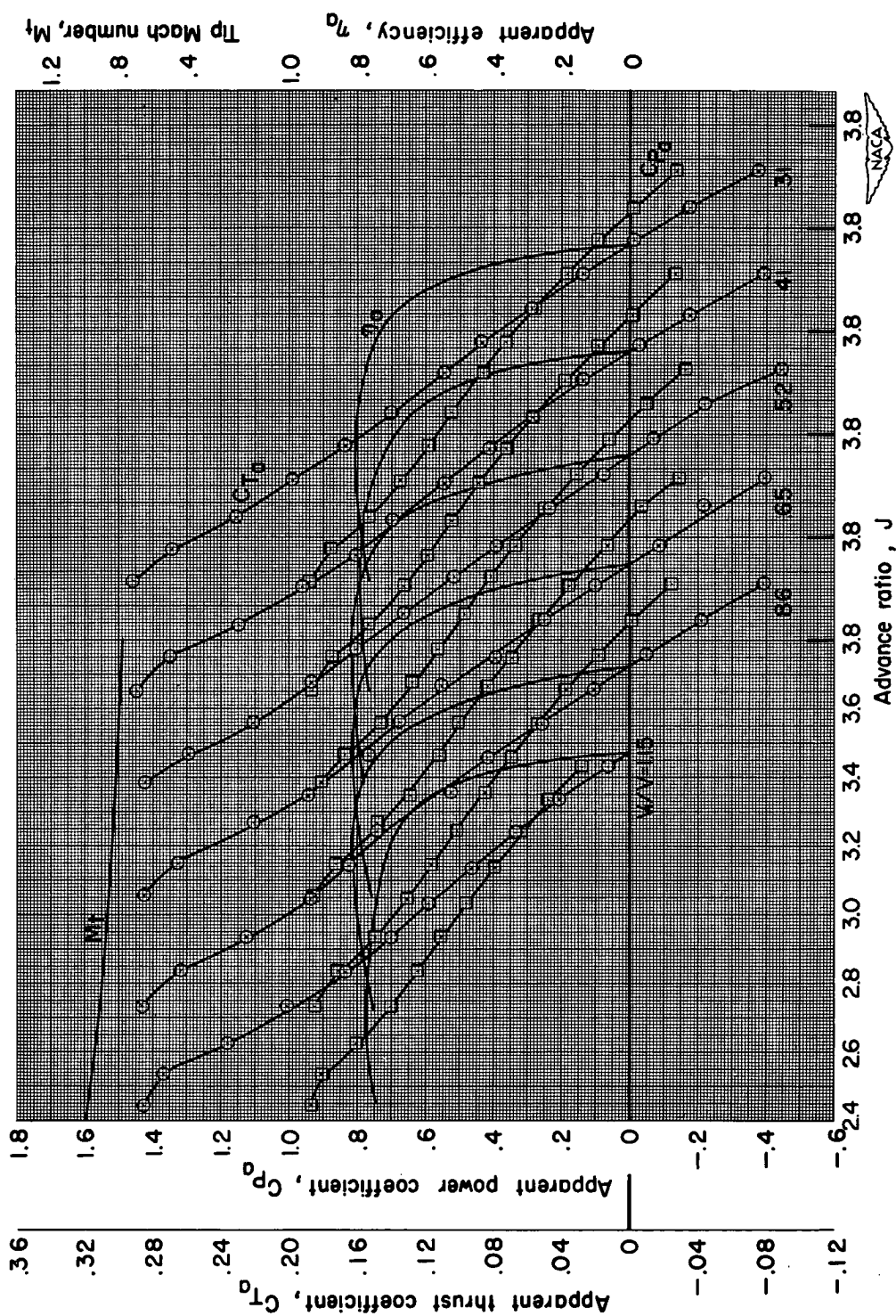
(d) M = 0.60, β = 53°

Figure 8.- Continued.
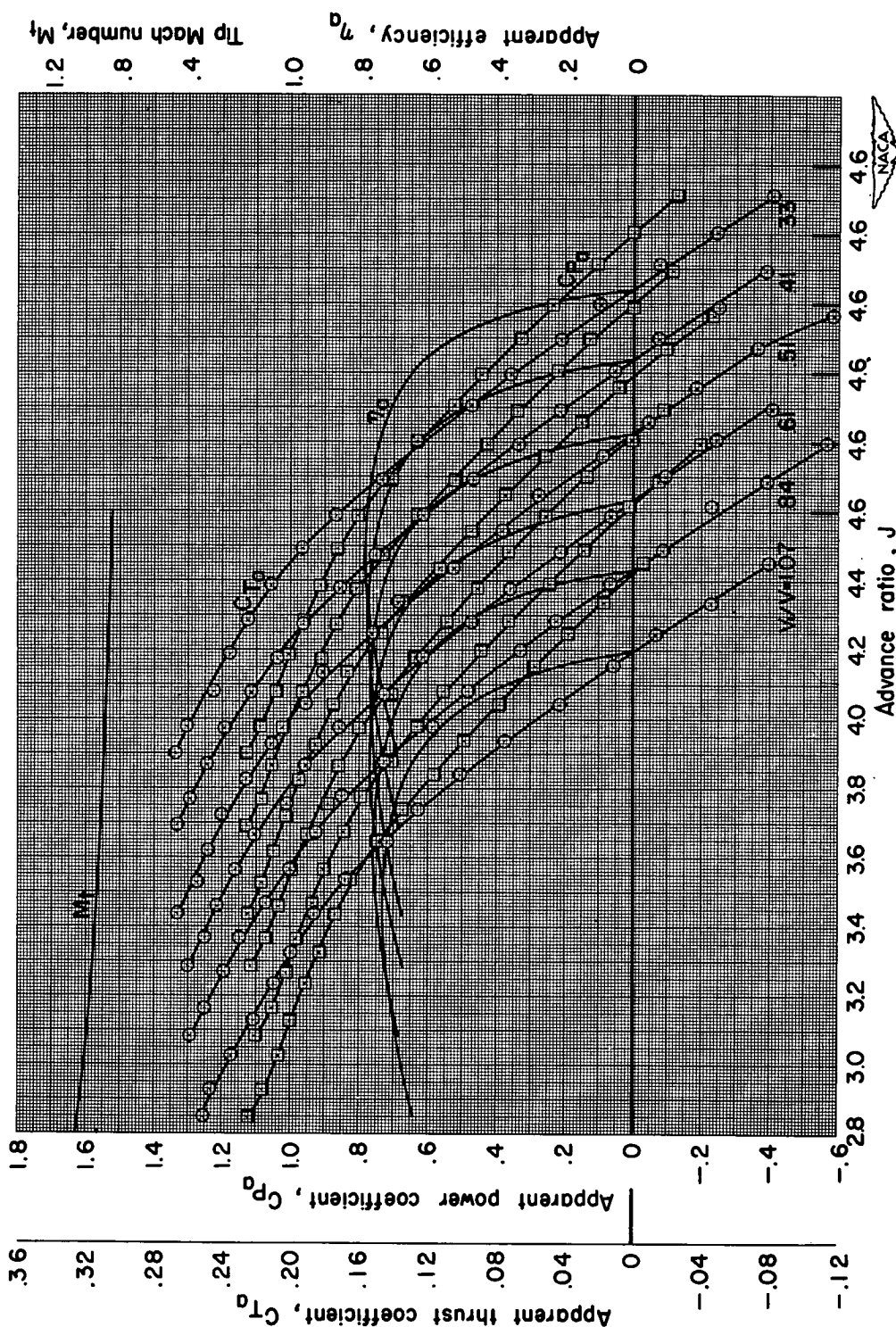
(e) $M = 0.70$, $\beta = 58.5°$

Figure 8.- Continued.
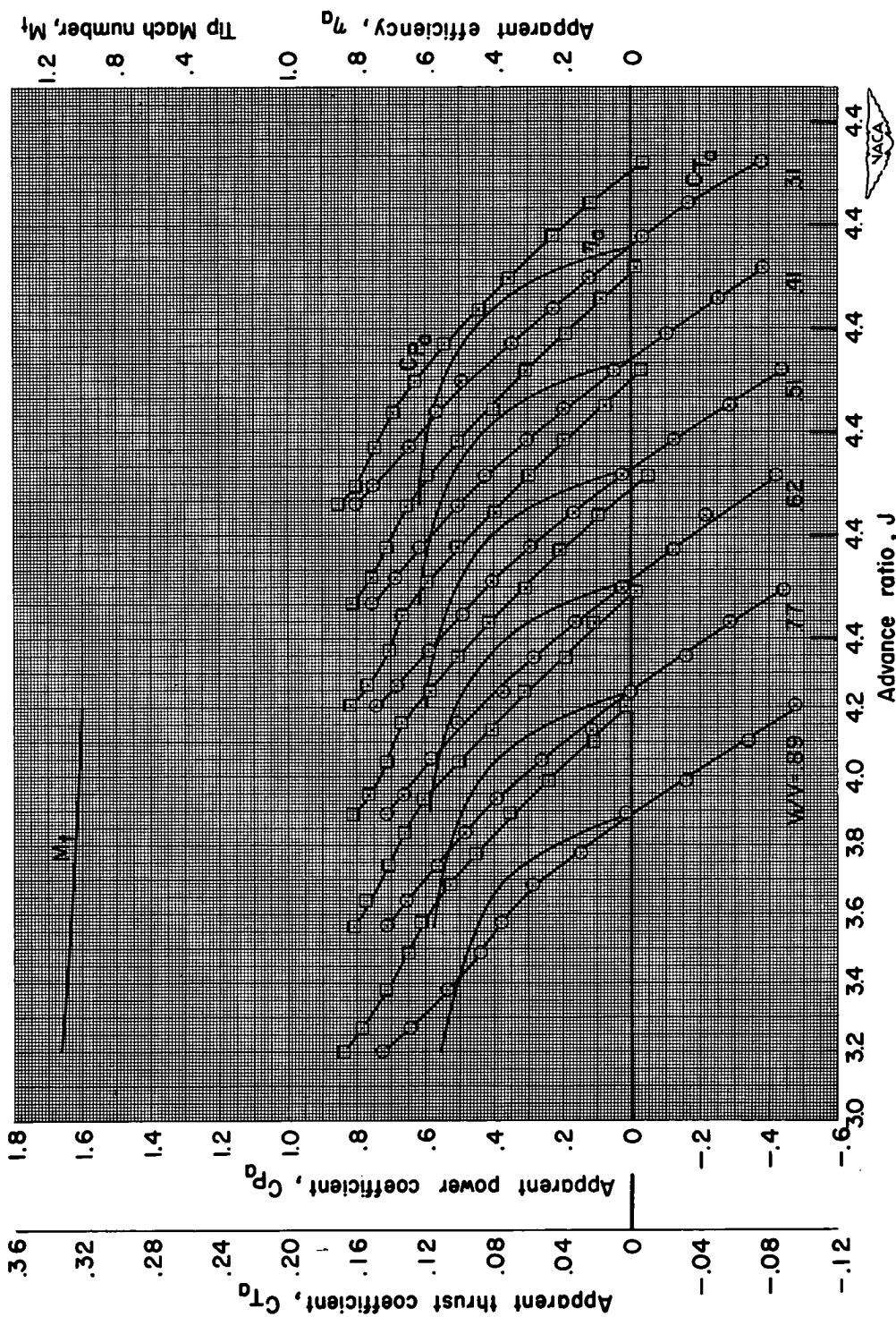
(f) $M = 0.80$, $\beta = 58.5°$

Figure 8.- Concluded.

(a) M = 0.15

(b) M = 0.20
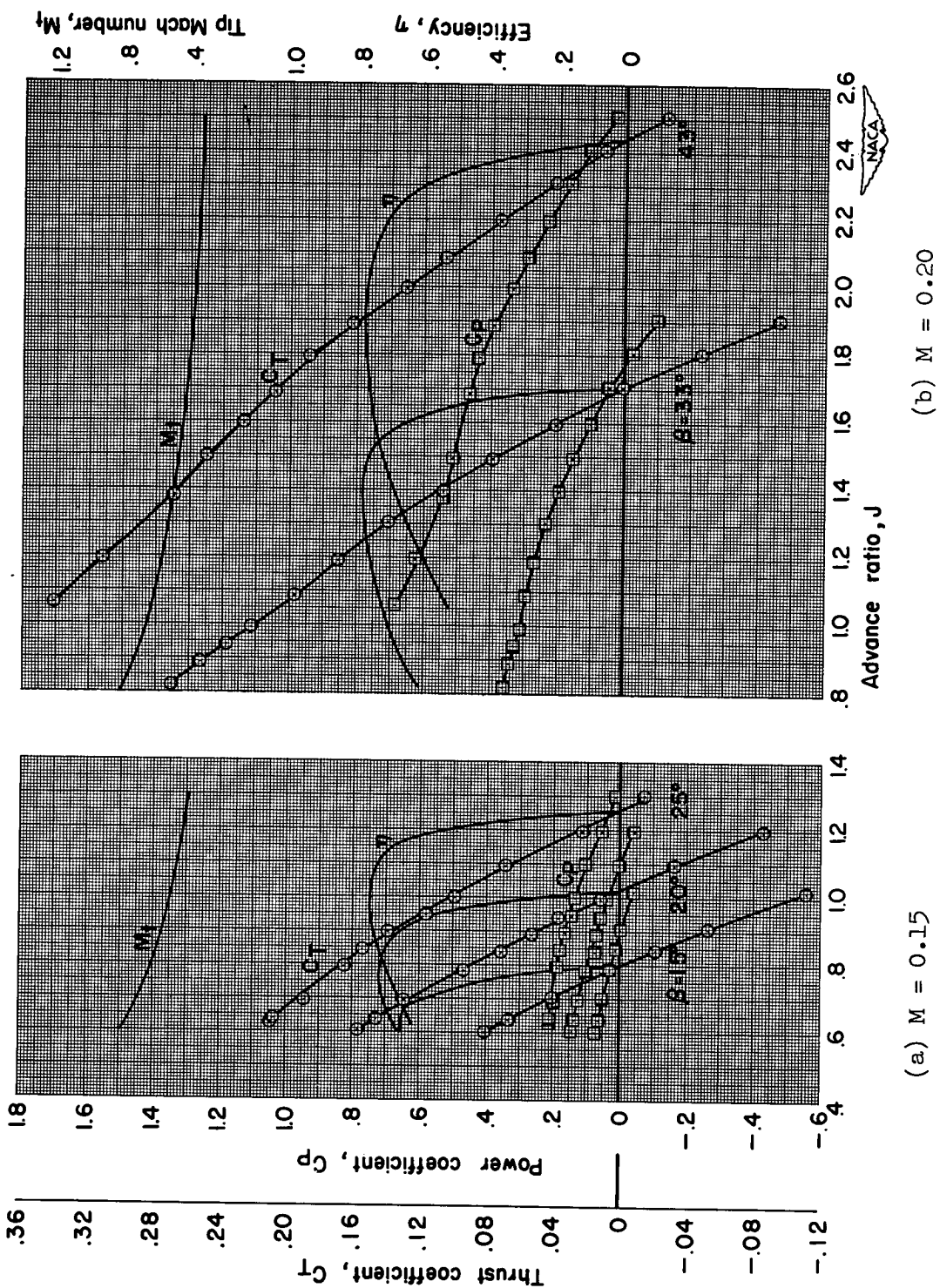
Figure 9.- Characteristics of the isolated propeller-spinner combination.
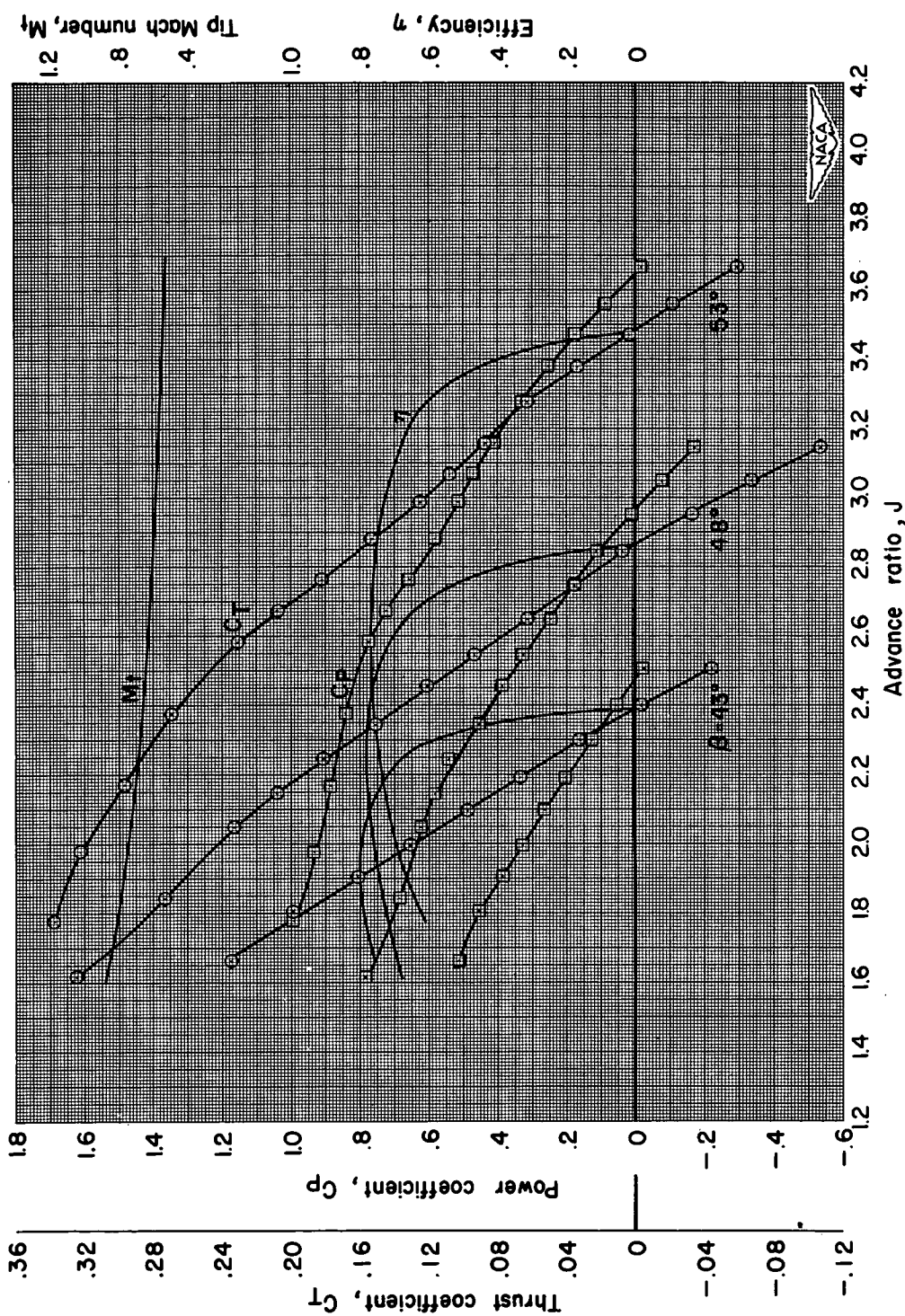
(c) M = 0.40

Figure 9.- Continued.
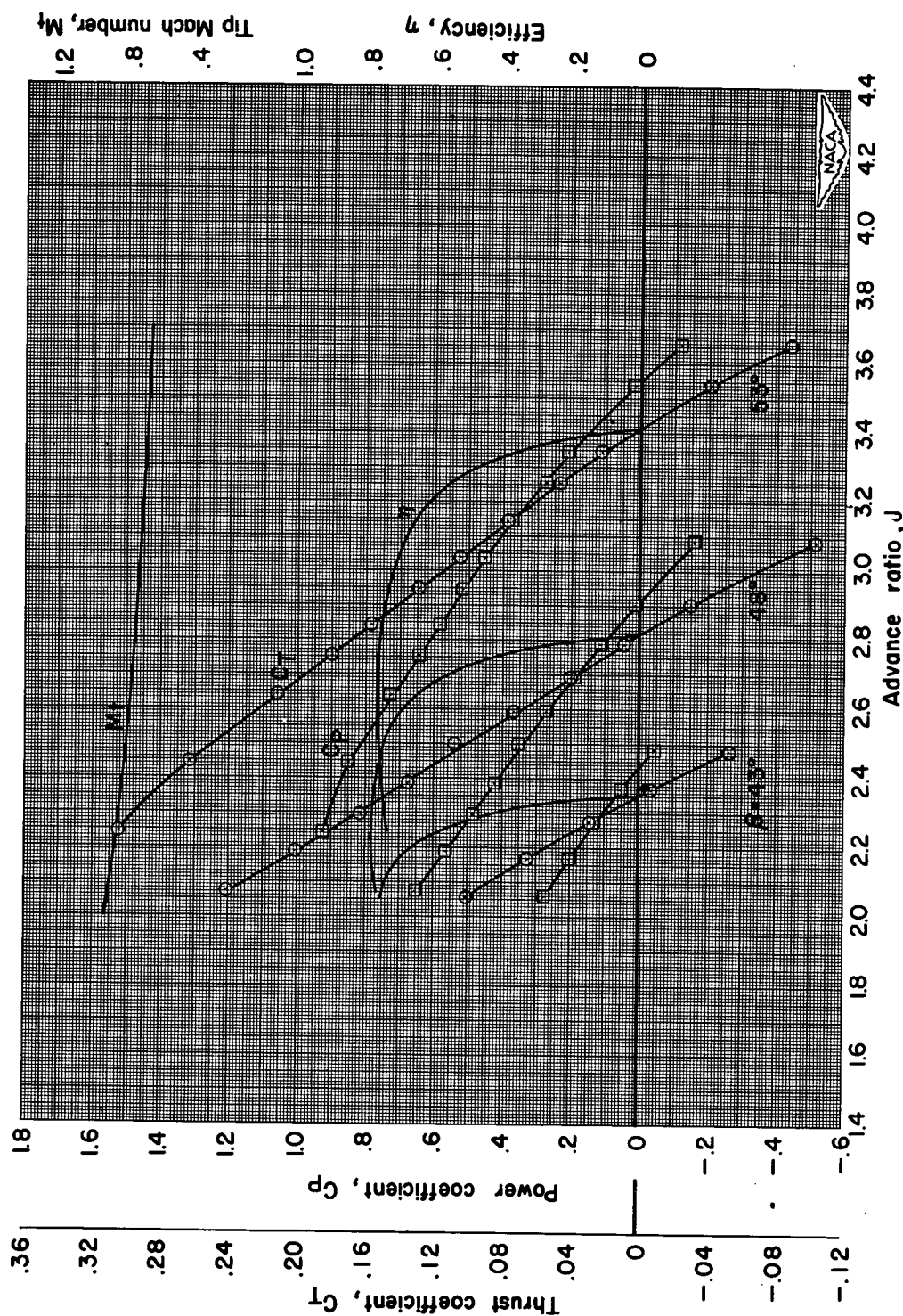
(d) M = 0.50

Figure 9.- Continued.
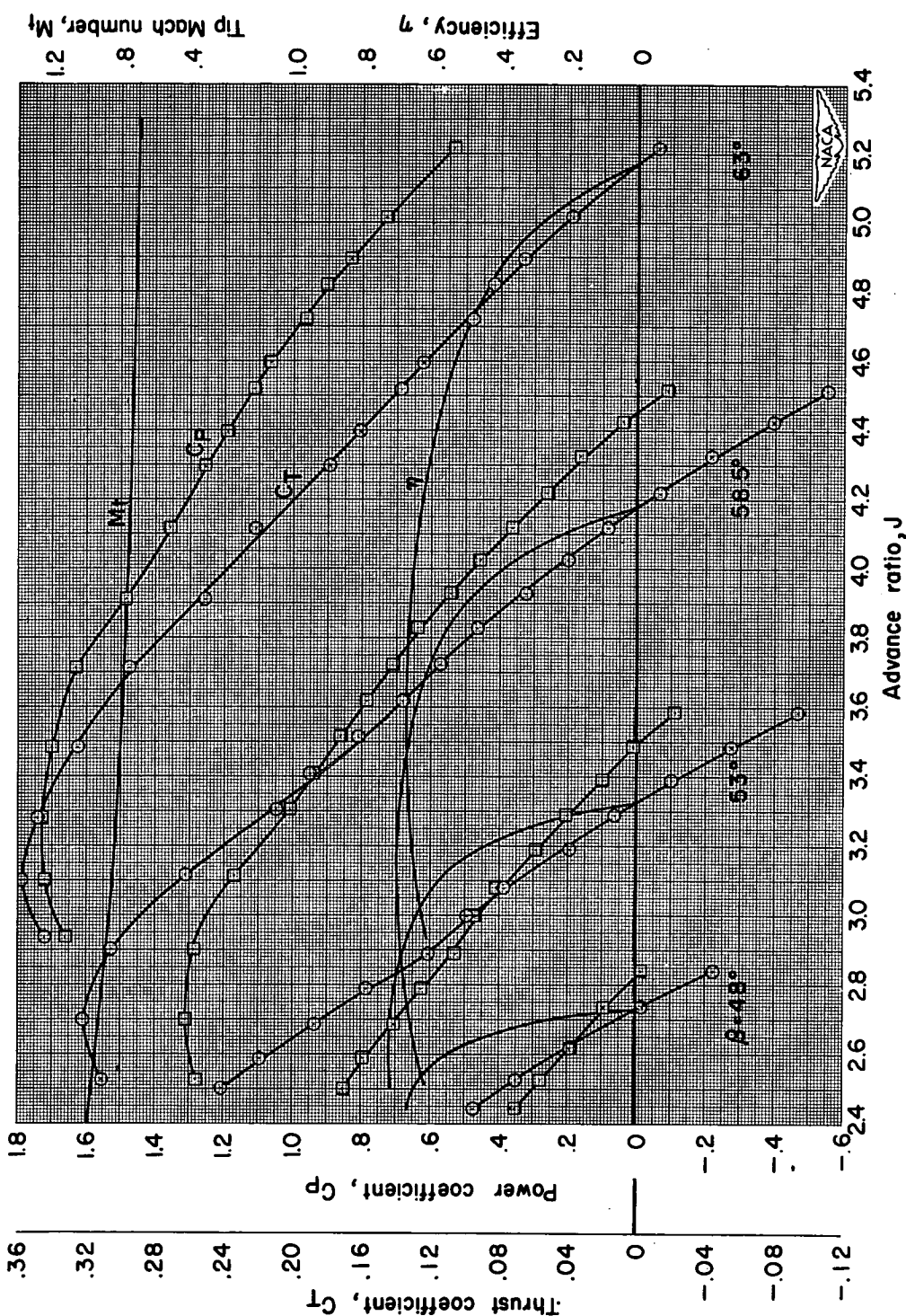
(e) M = 0.60

Figure 9.- Continued.
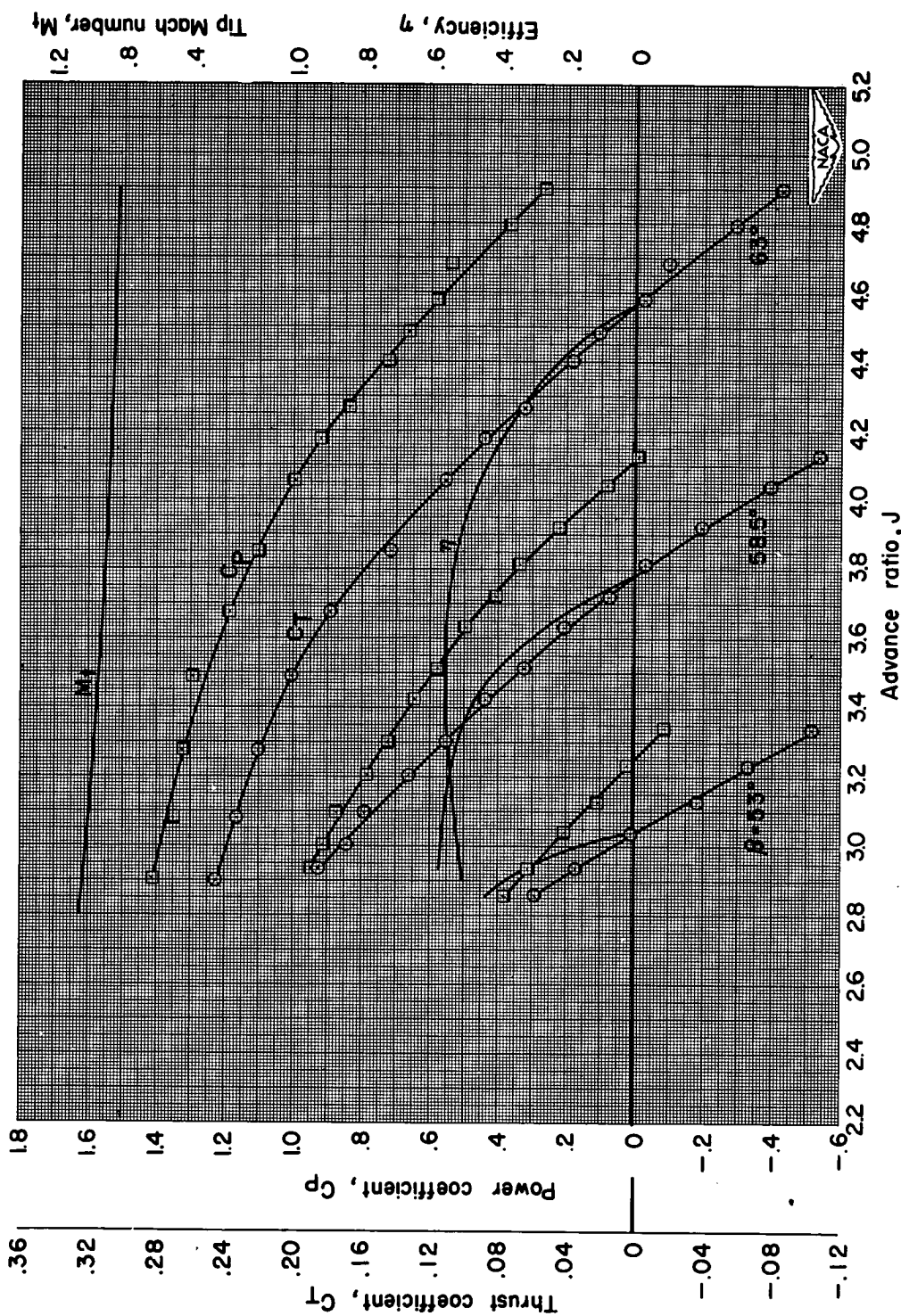
(f) M = 0.70

Figure 9.- Continued.
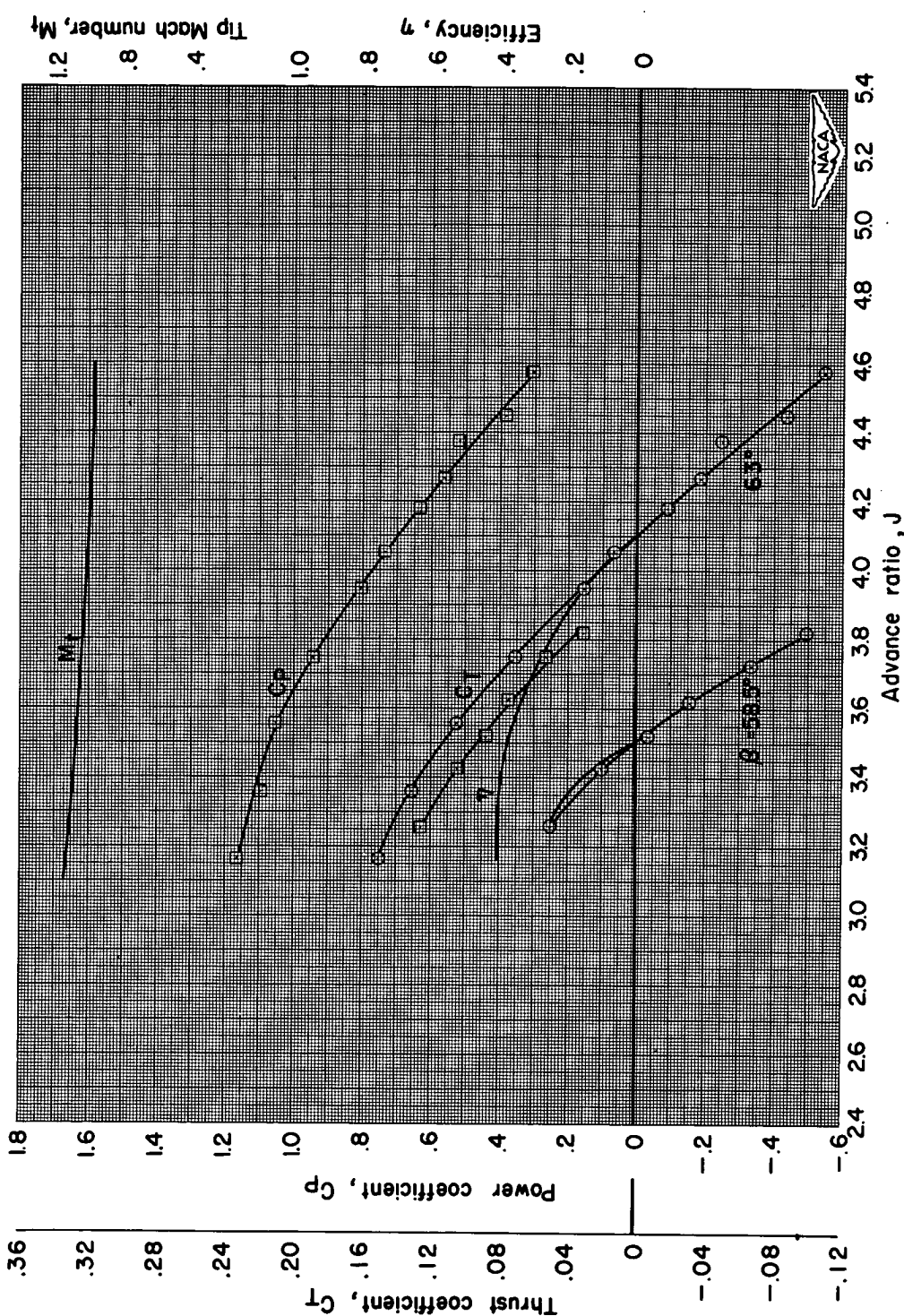
(g) M = 0.80

Figure 9.- Concluded.
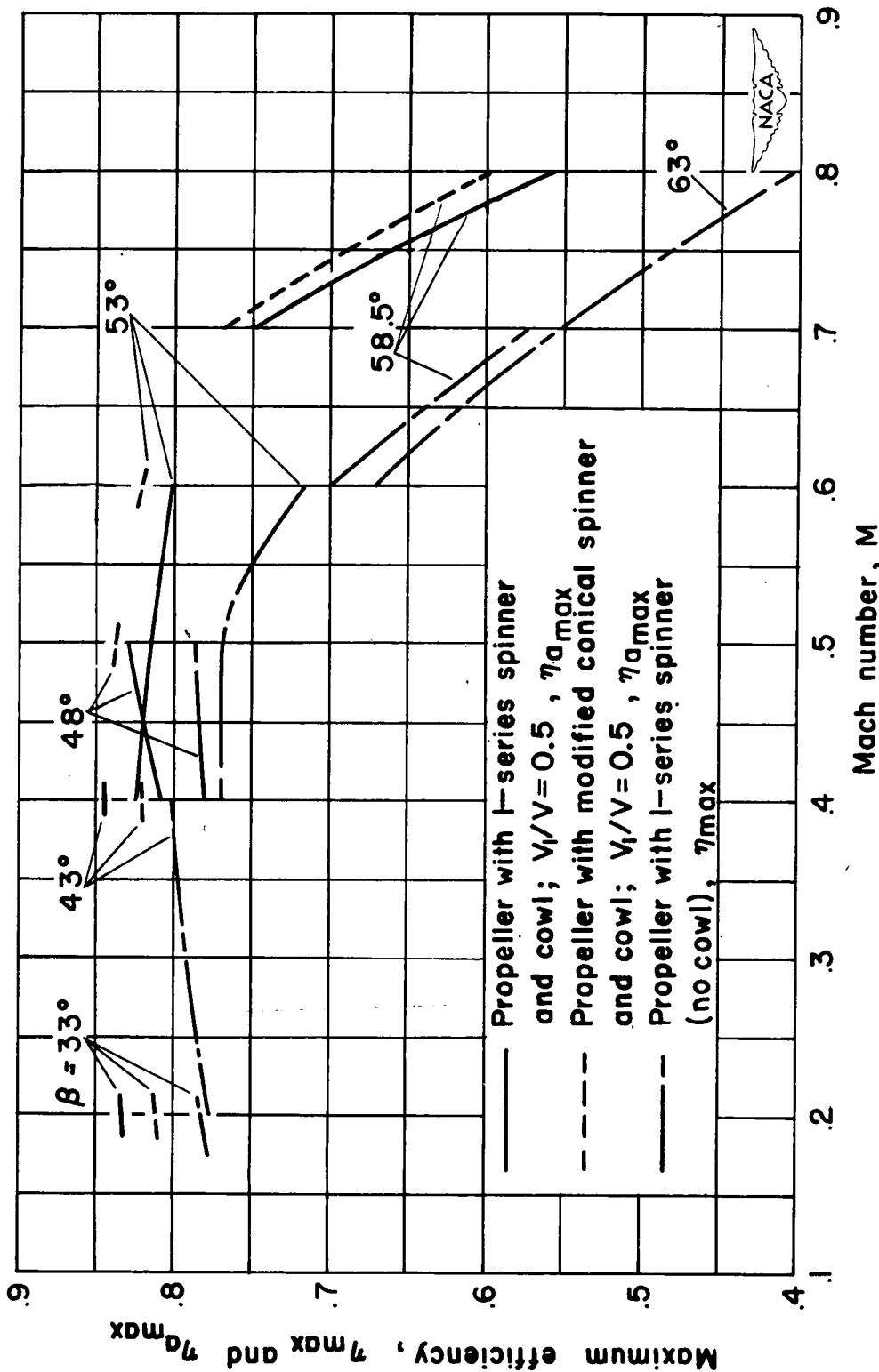
Figure 10.- Comparison of the maximum efficiency of the propeller with and without the cowl.

(a) C_{T_a} vs. V_1/V
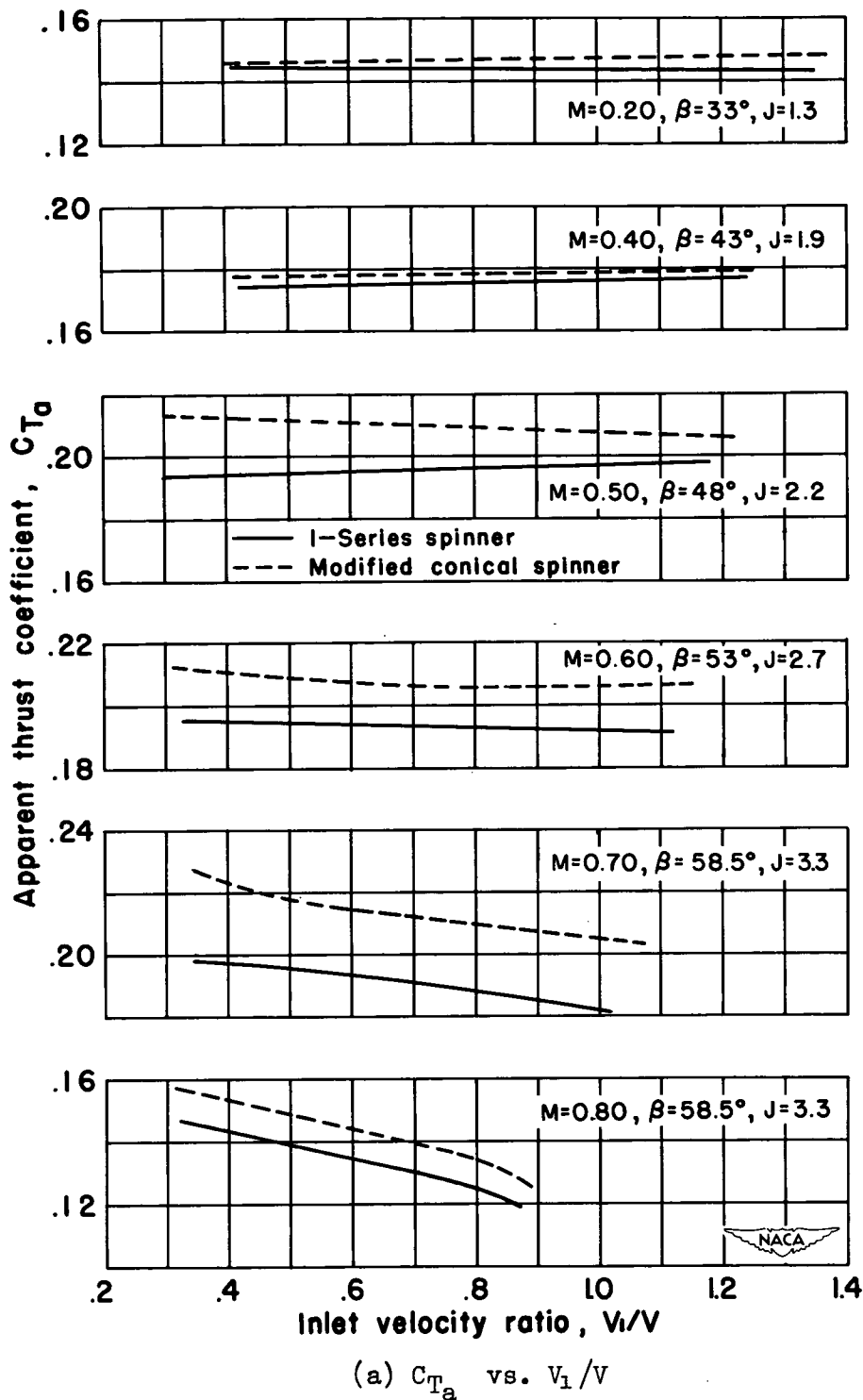
Figure 11.- Typical effect of inlet velocity ratio on the apparent thrust
and power coefficients of the propeller.
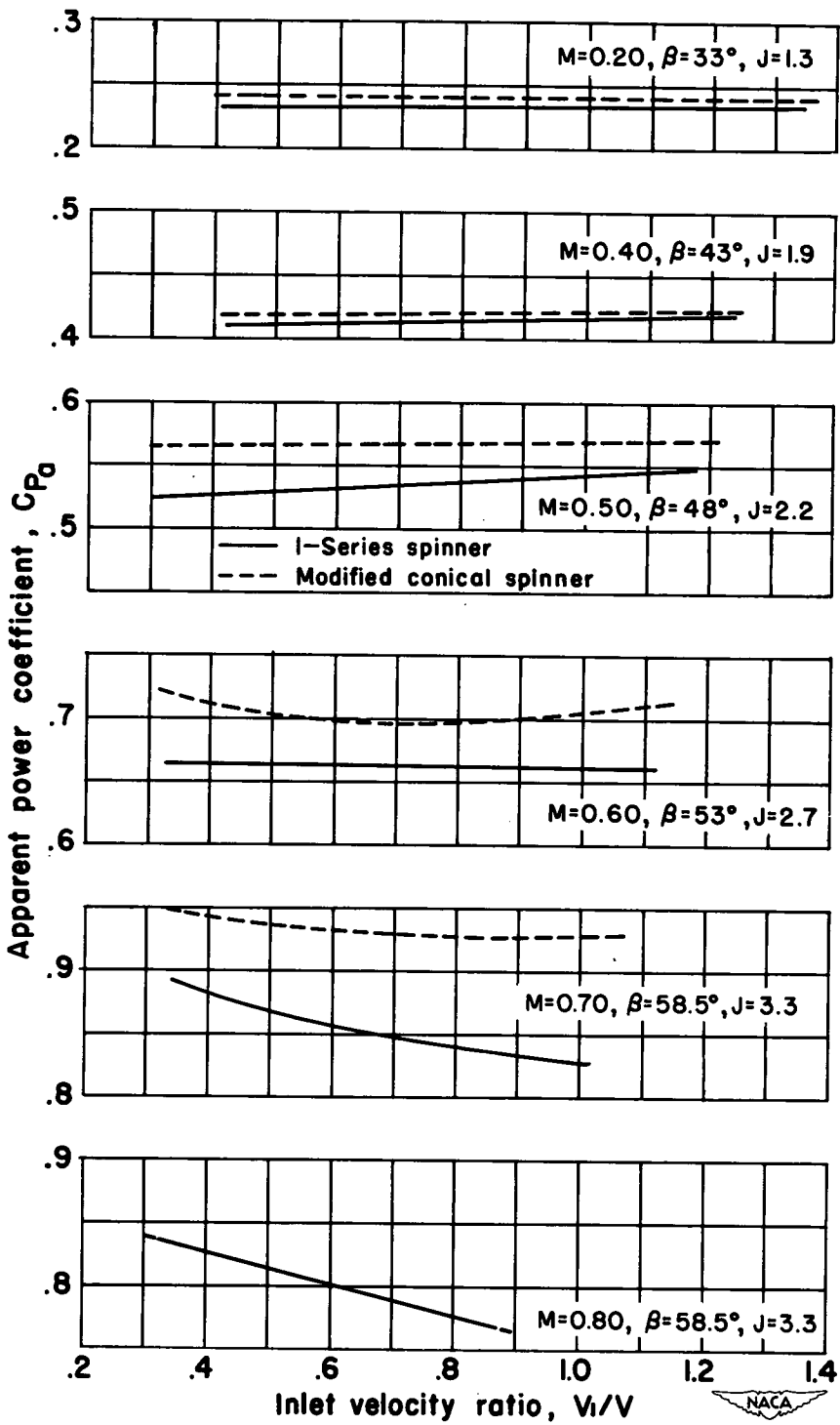
(b) C_{P_a} vs. V_1/V

Figure 11.- Concluded.
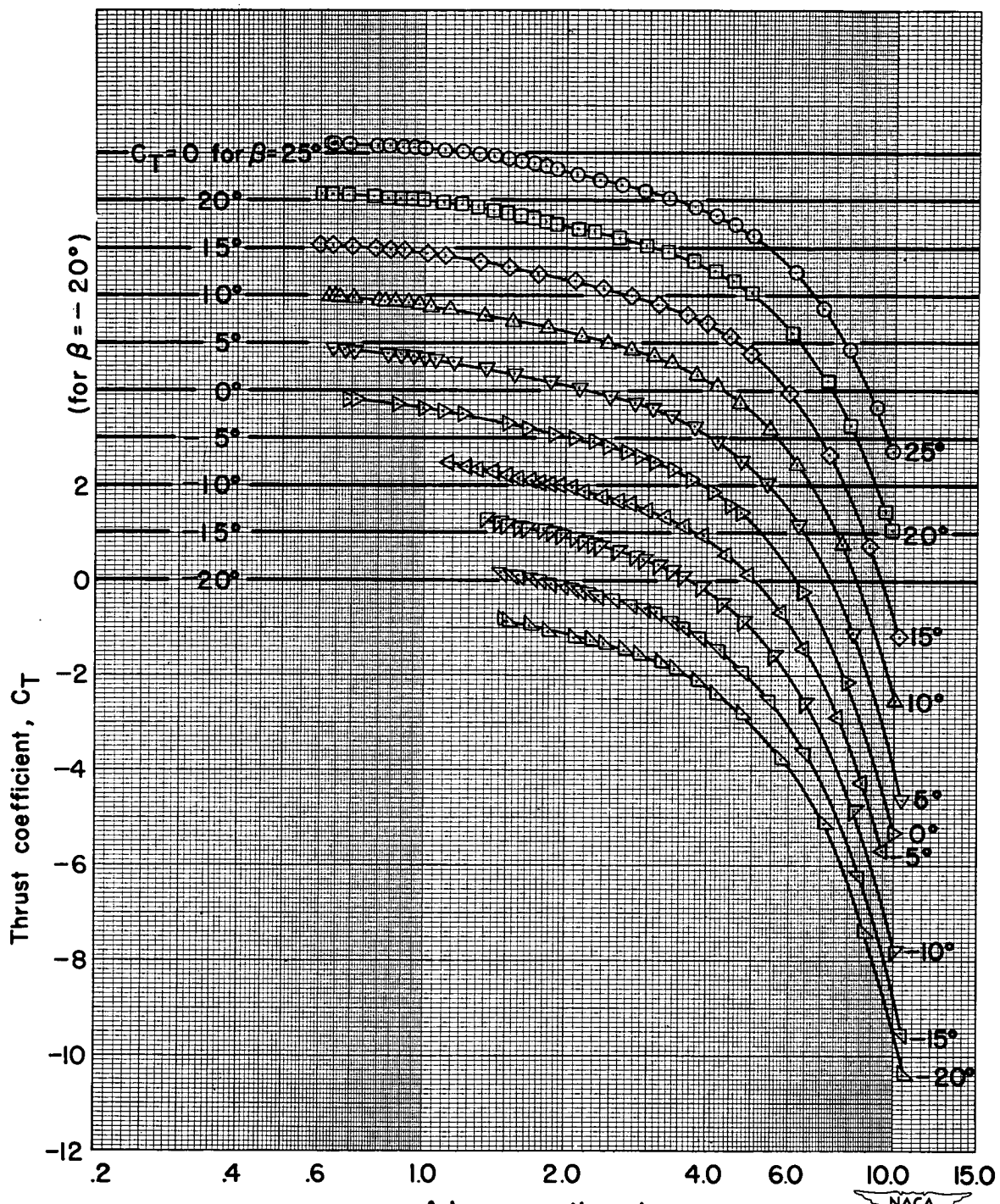
(a) M = 0.15

Figure 12.- Negative thrust coefficients for the isolated propeller-
spinner combination.
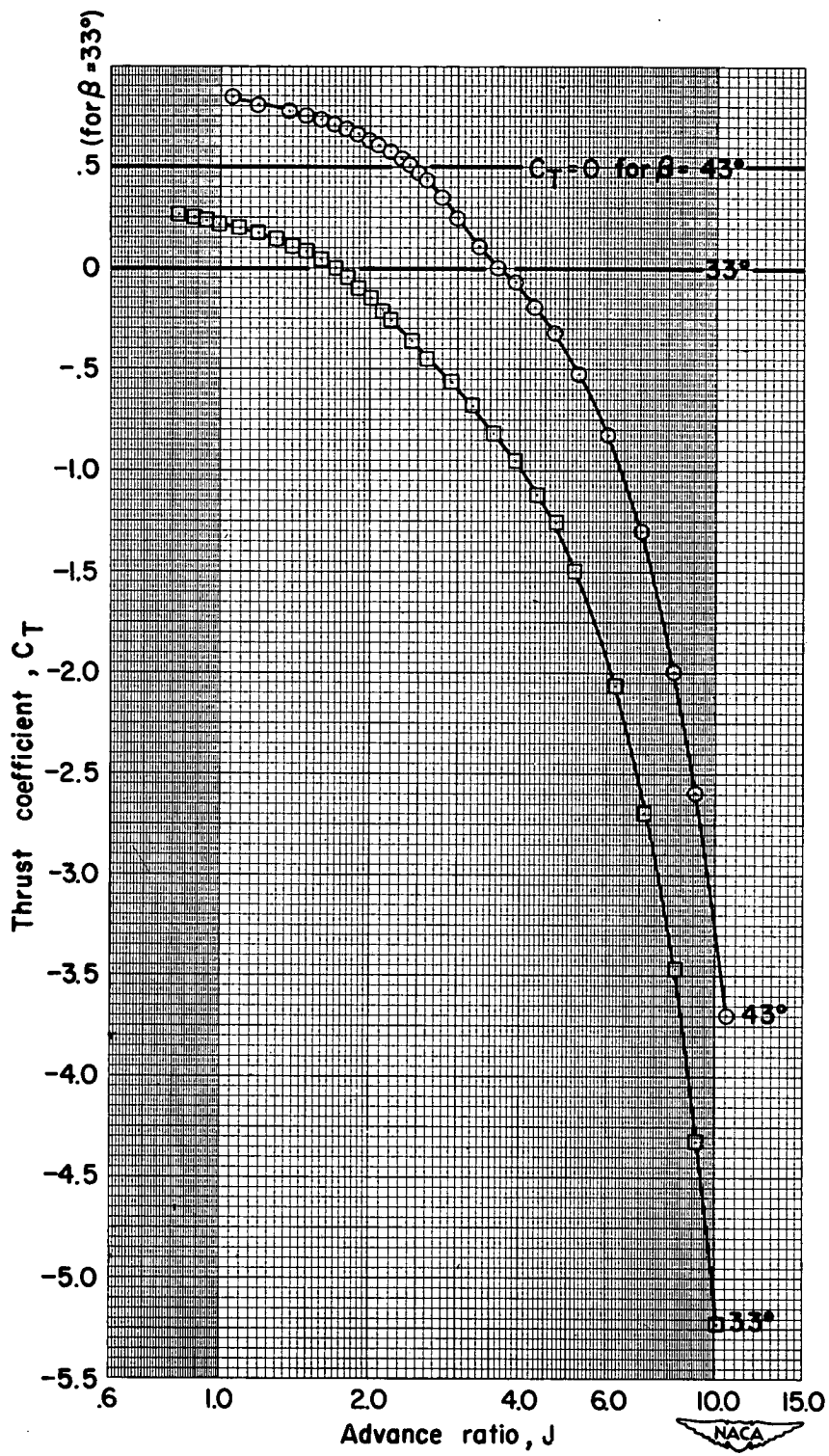
(b) M = 0.20

Figure 12.- Continued.

(c) M = 0.40
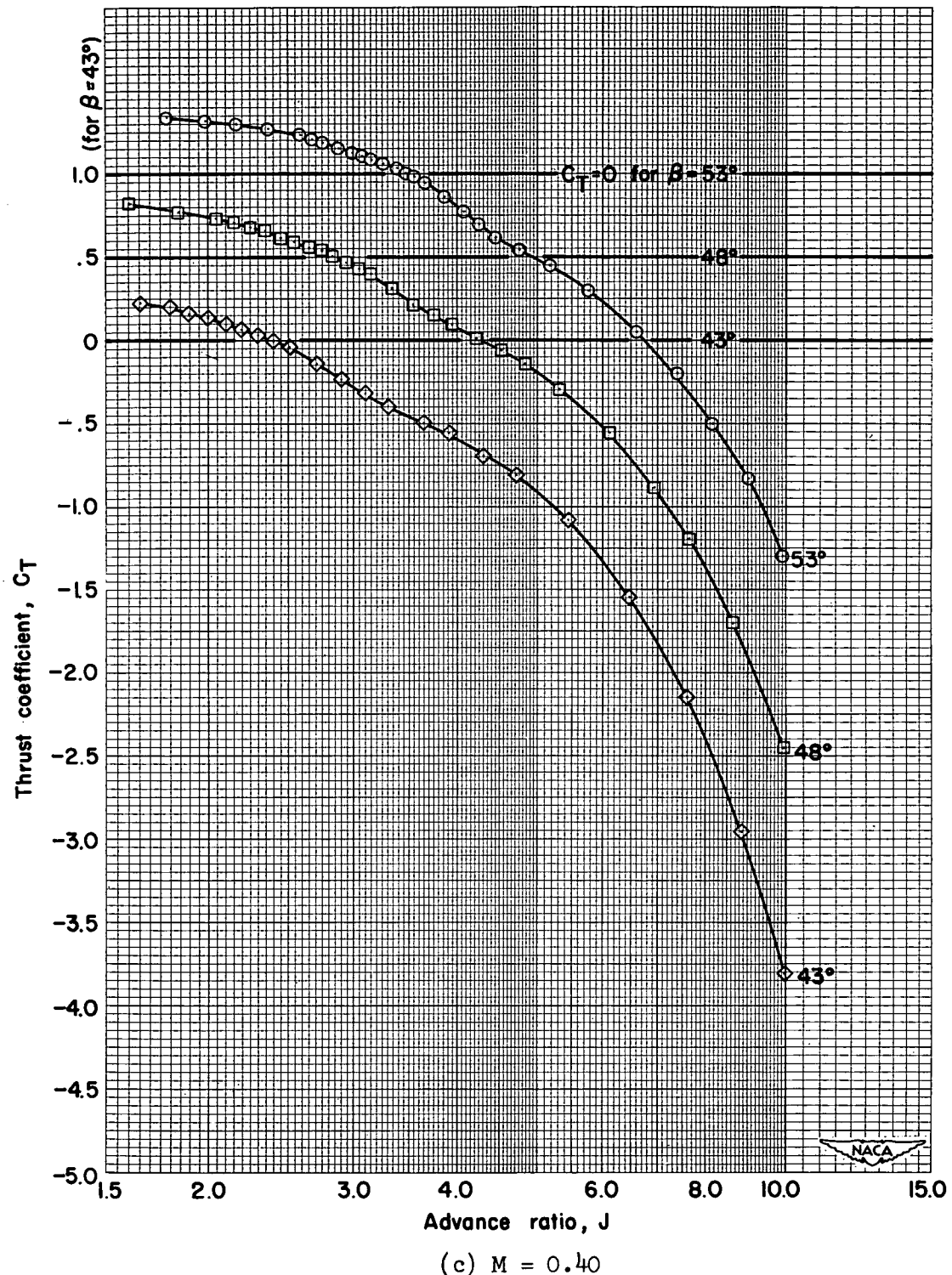
Figure 12.- Continued.
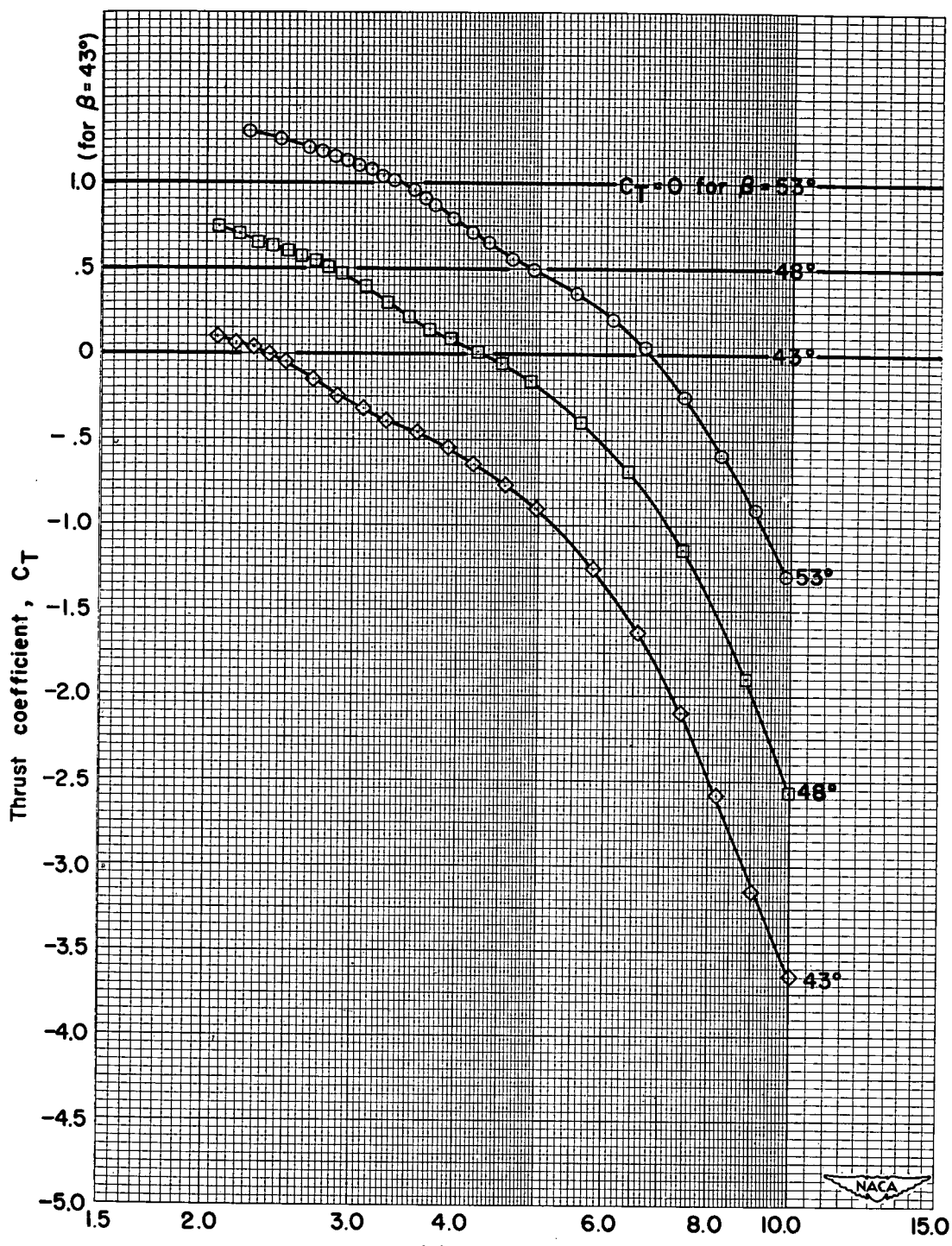
(d) M = 0.50

Figure 12.- Continued.
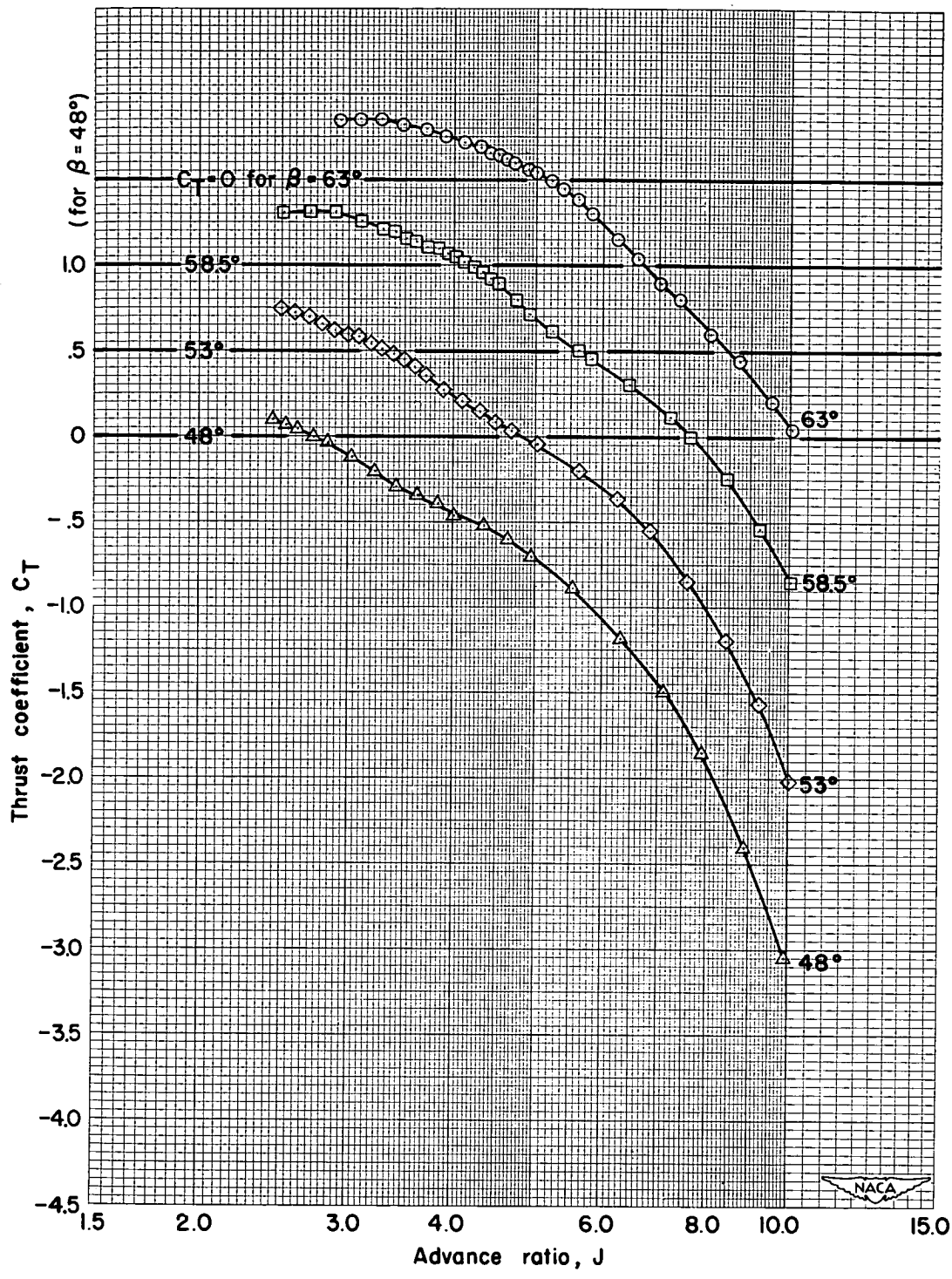
(e) M = 0.60

Figure 12.- Continued.
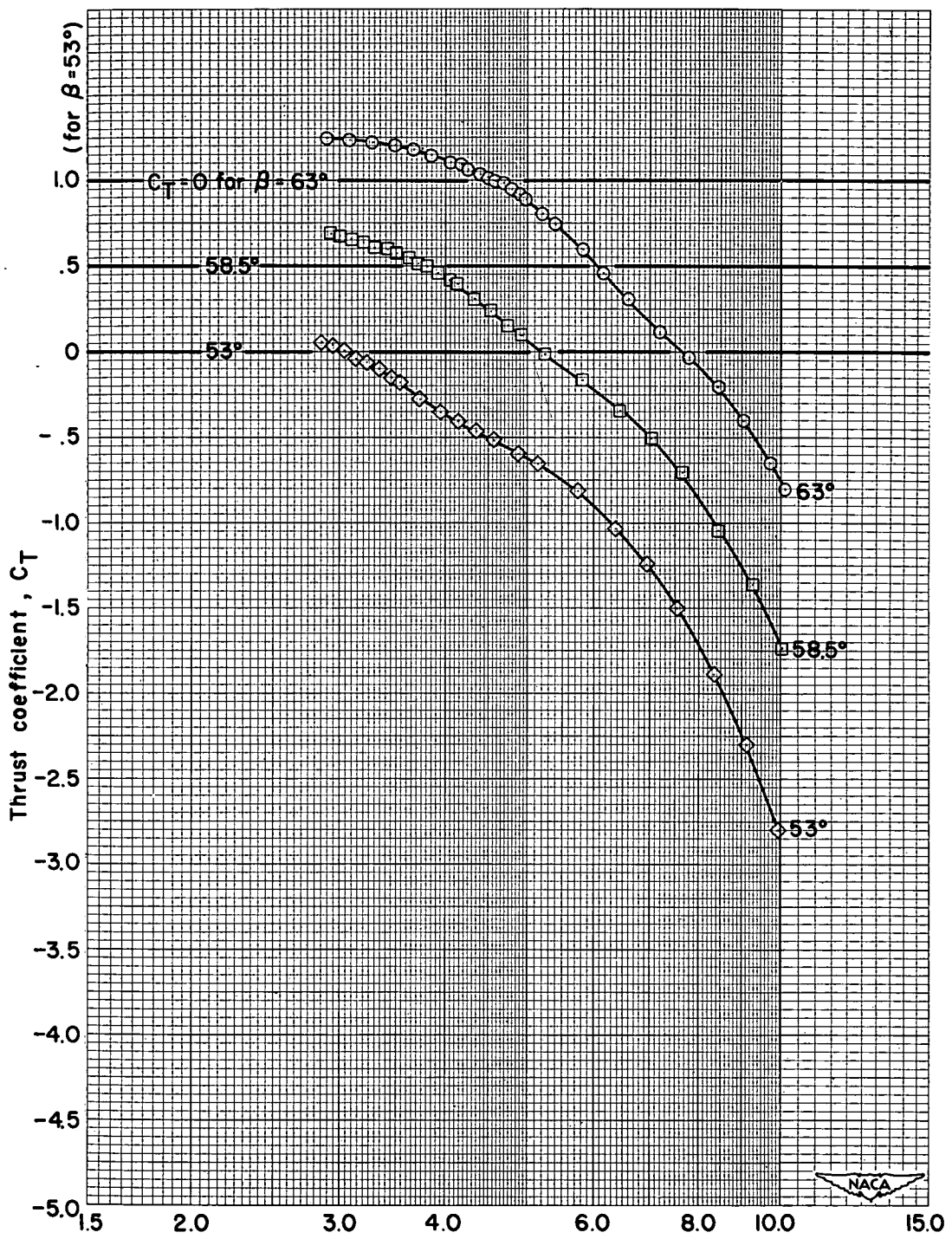
(f) M = 0.70

Figure 12.- Continued.
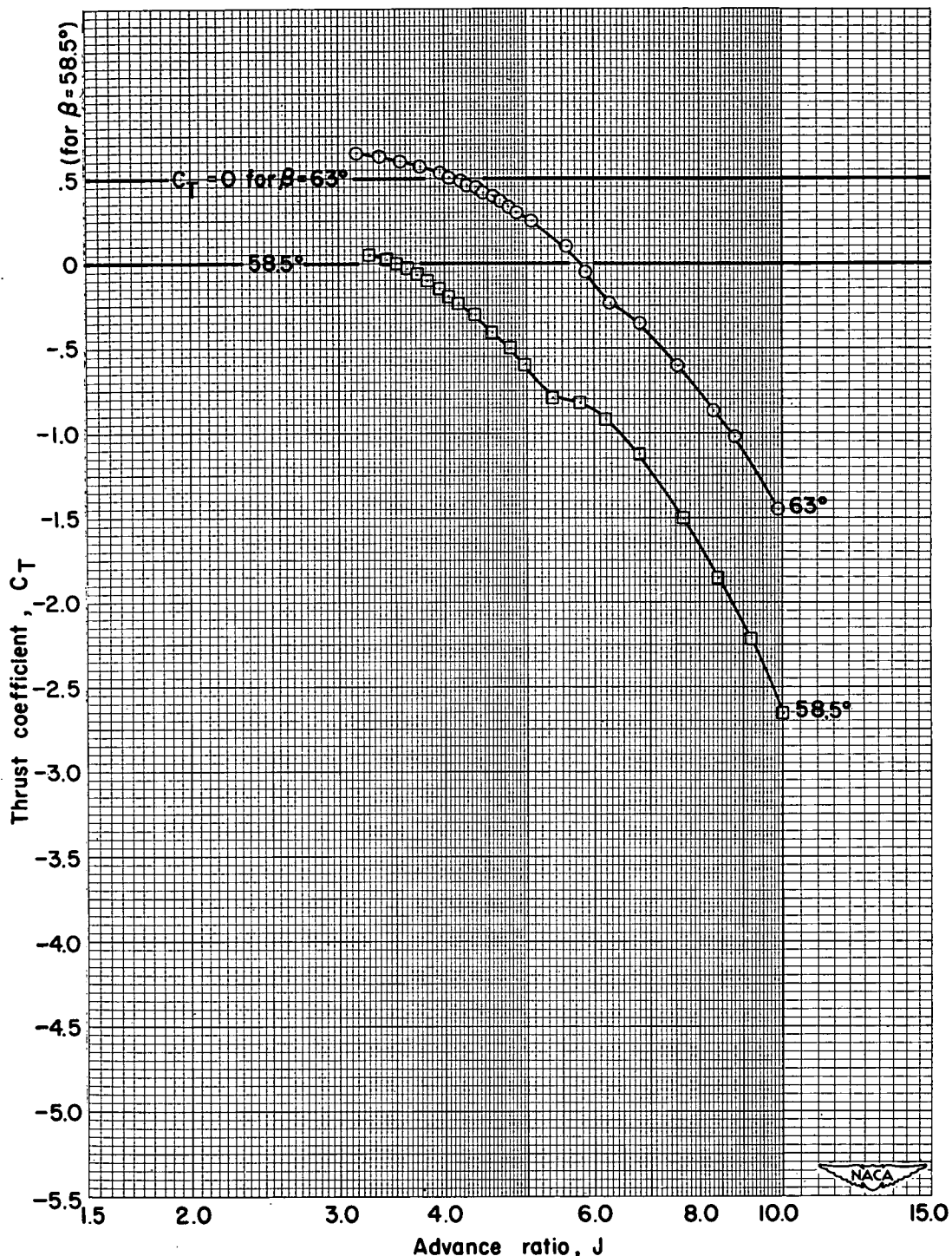
(g) M = 0.80

Figure 12.- Concluded.
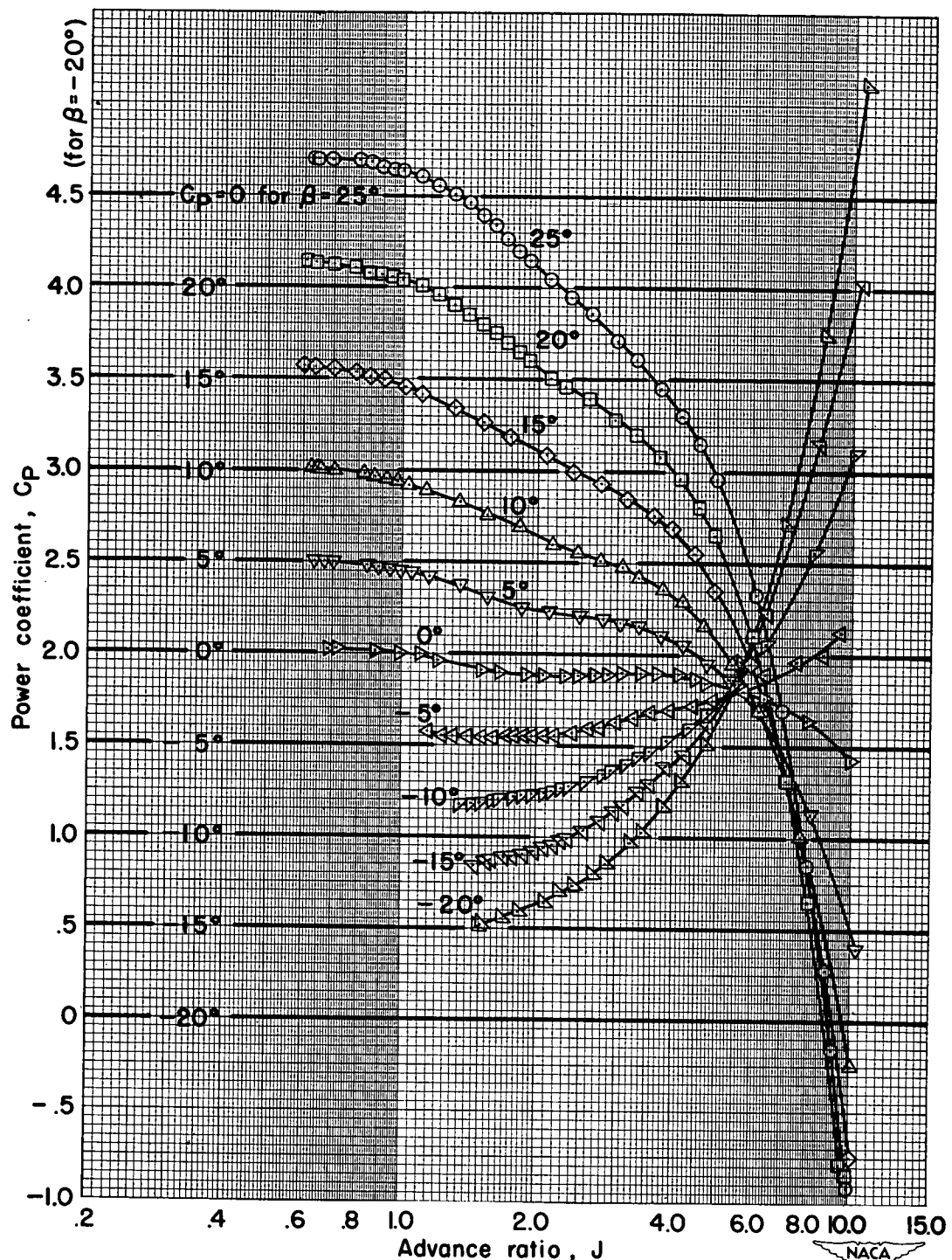
(a) M = 0.15

Figure 13.- Power coefficients for the isolated propeller-spinner combi-
nation in negative thrust.
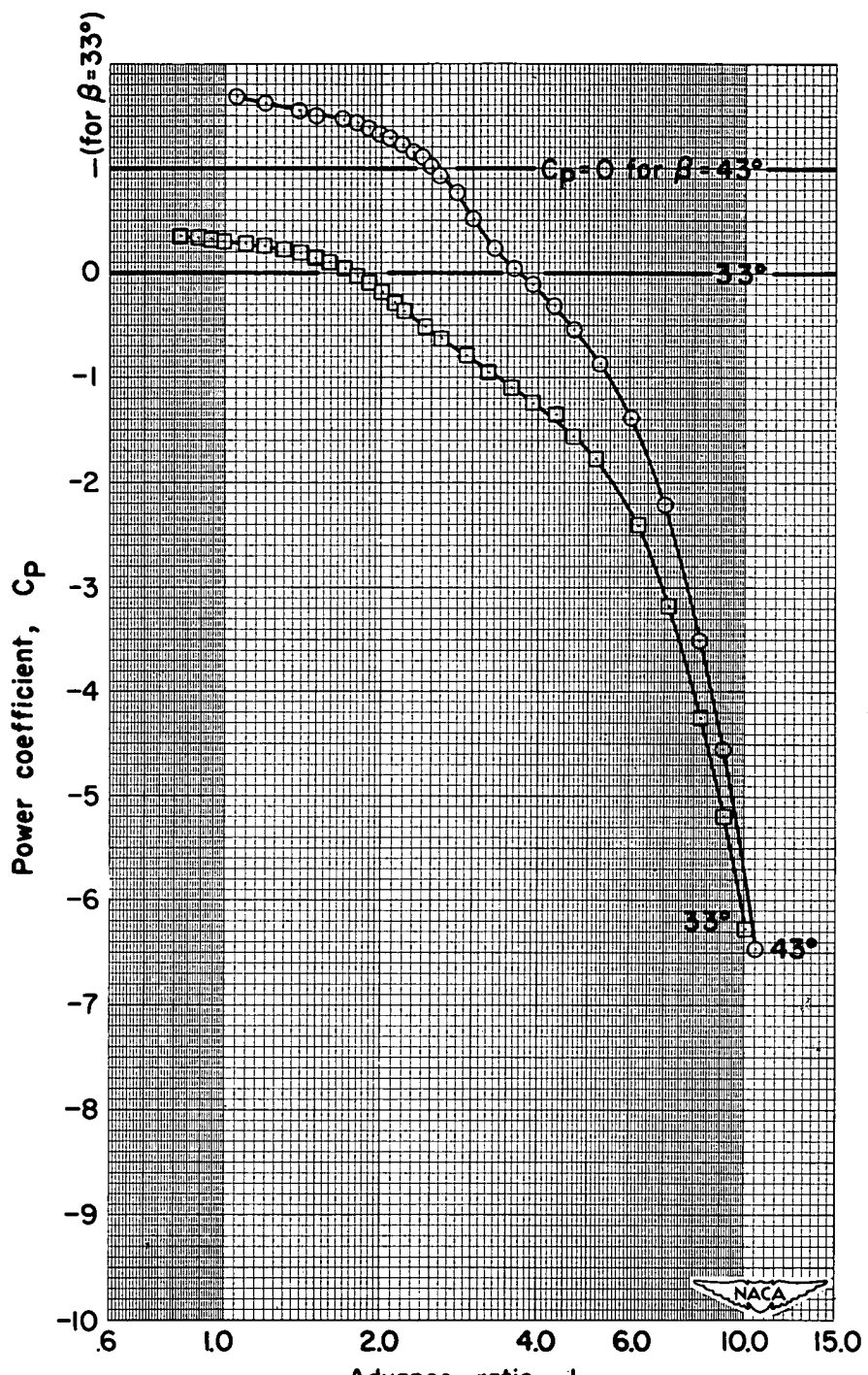
(b) M = 0.20

Figure 13.- Continued.
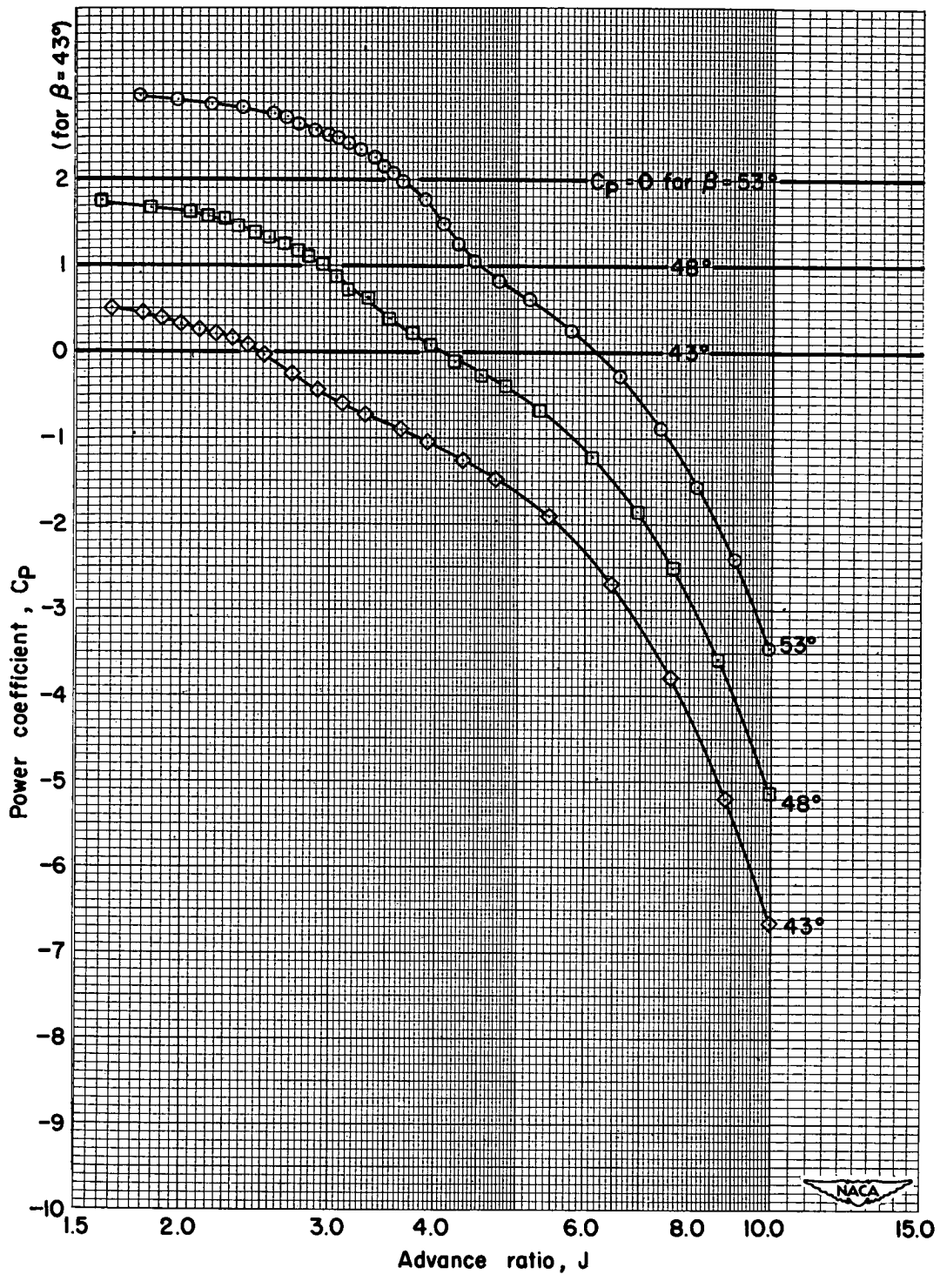
(c) M = 0.40

Figure 13.- Continued.

CONFIDENTIAL

(d) M = 0.50
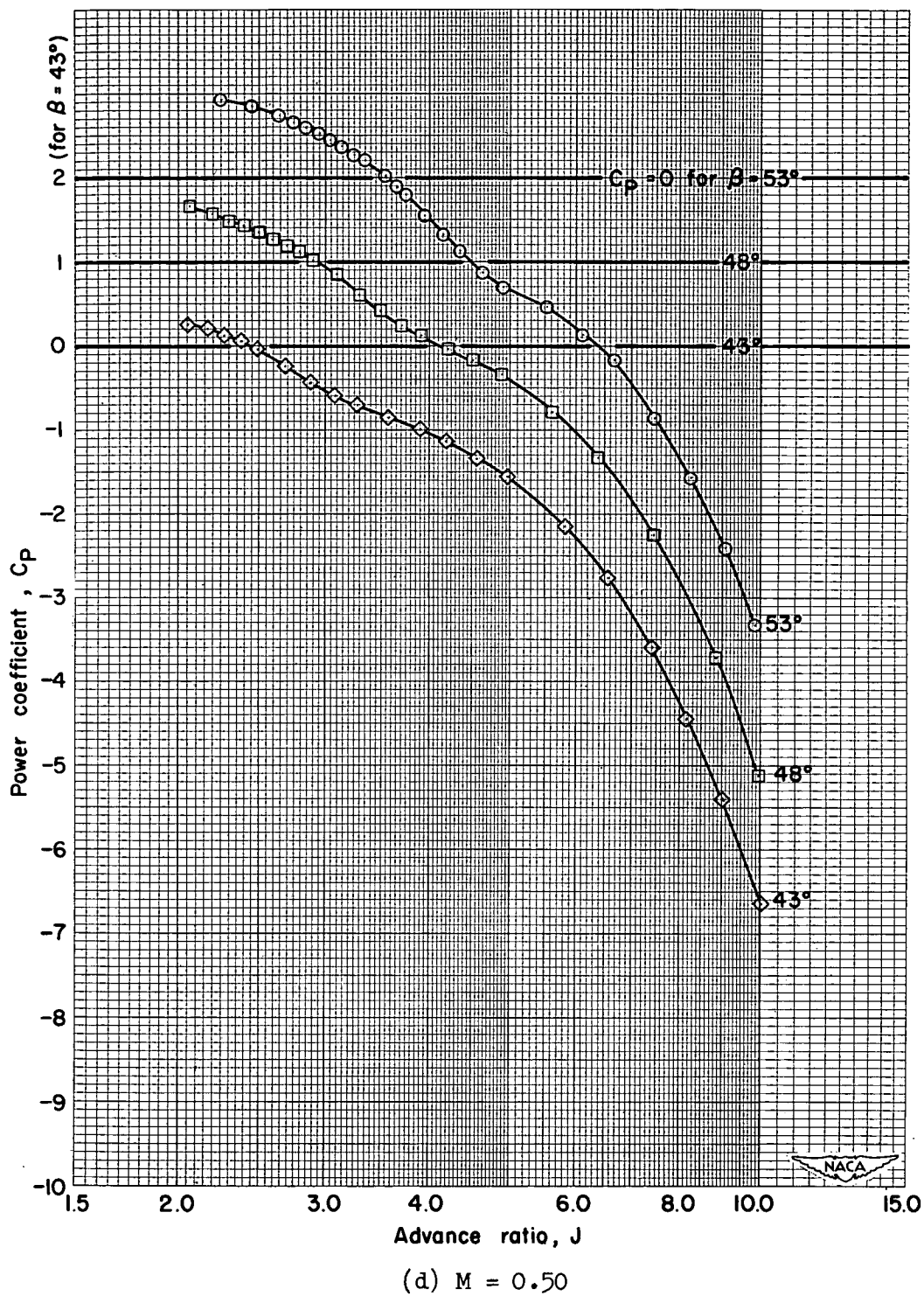
Figure 13.- Continued.
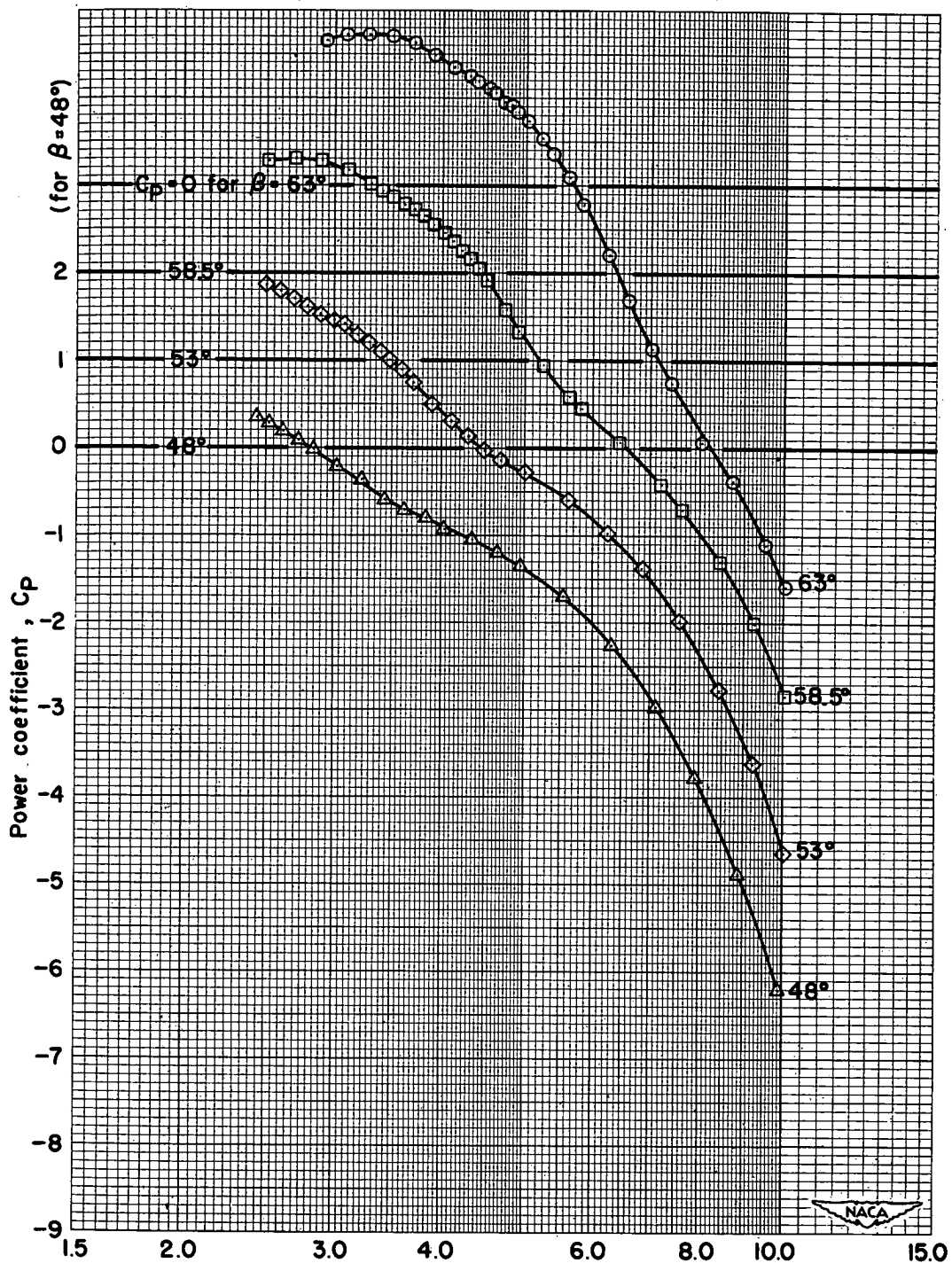
(e) M = 0.60

Figure 13.- Continued.
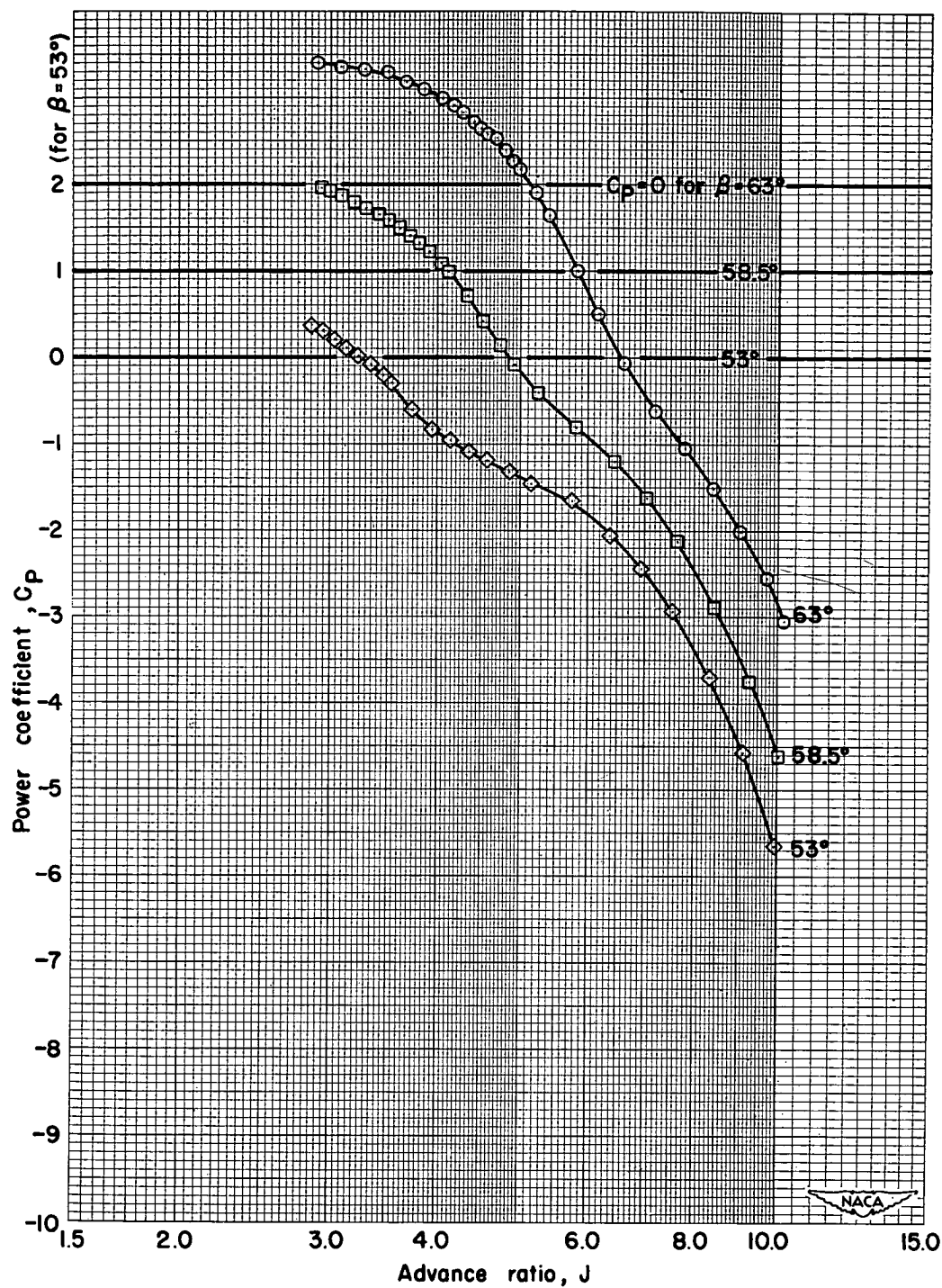
(f) M = 0.70

Figure 13.- Continued.

CONFIDENTIAL
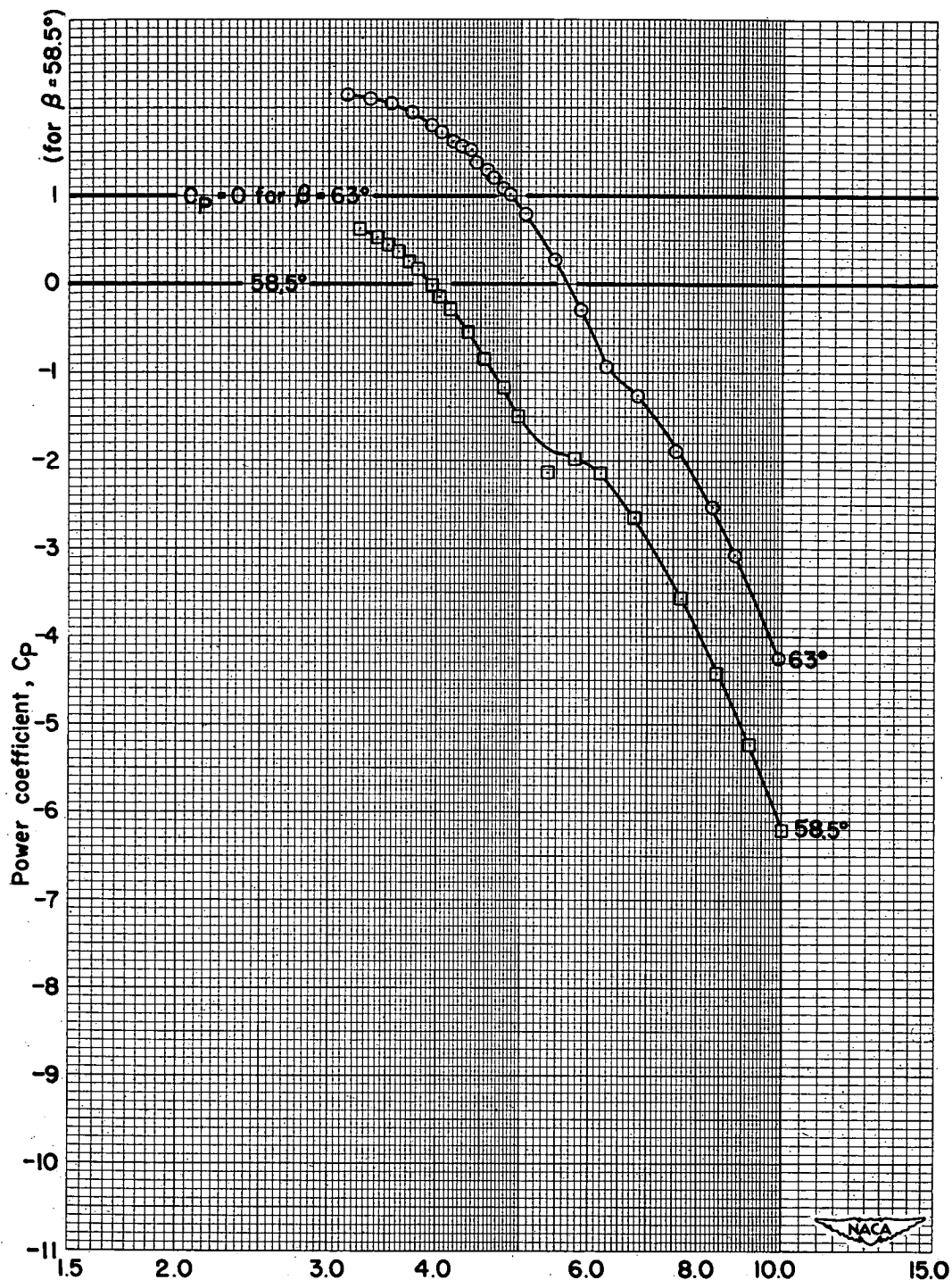
(g) M = 0.80

Figure 13.- Concluded.

CONFIDENTIAL
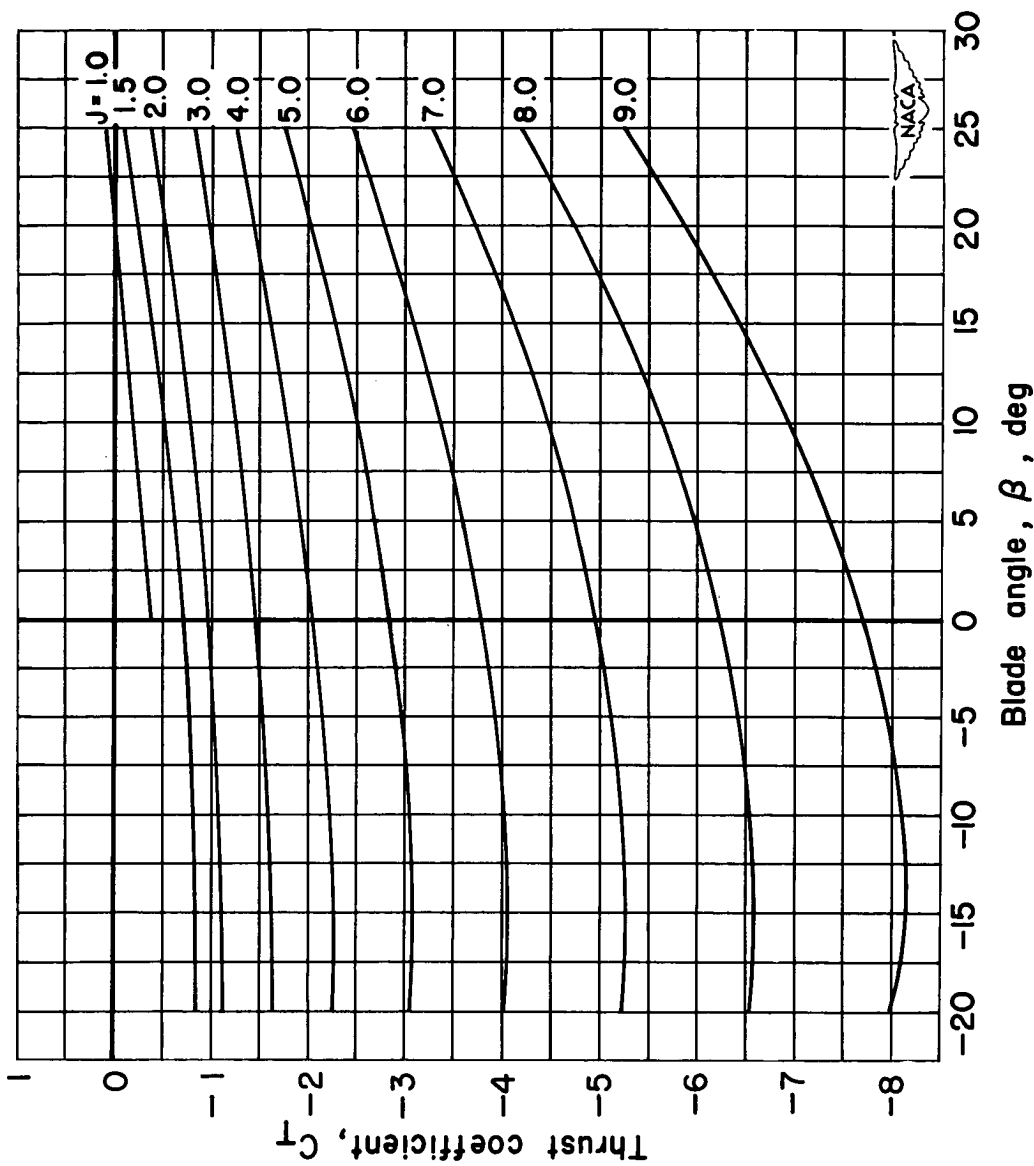
Figure 14.- The effect of blade angle on the negative-thrust characteristics of the propeller.

(a) M = 0.15
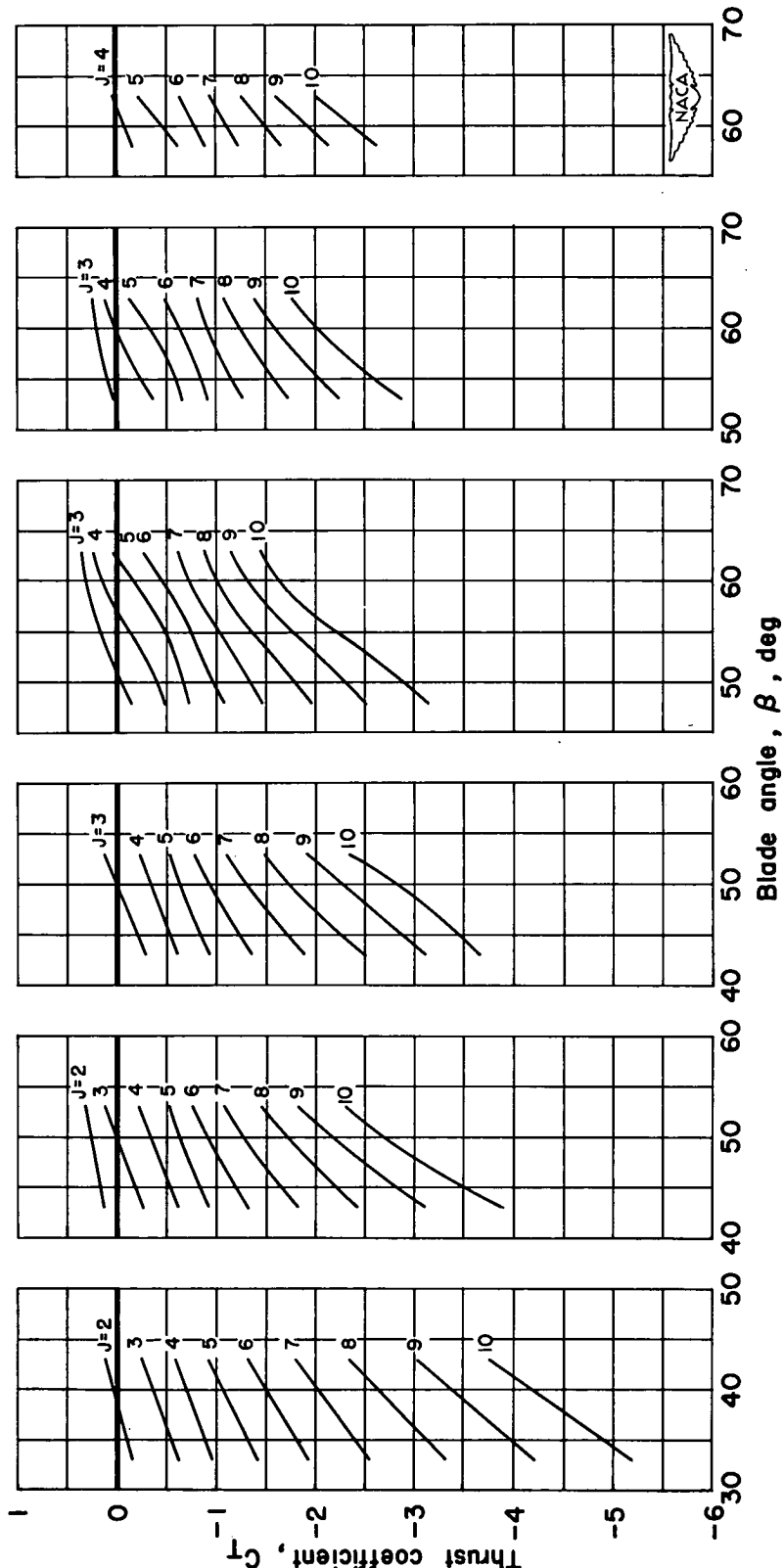
Figure 14.- Concluded.
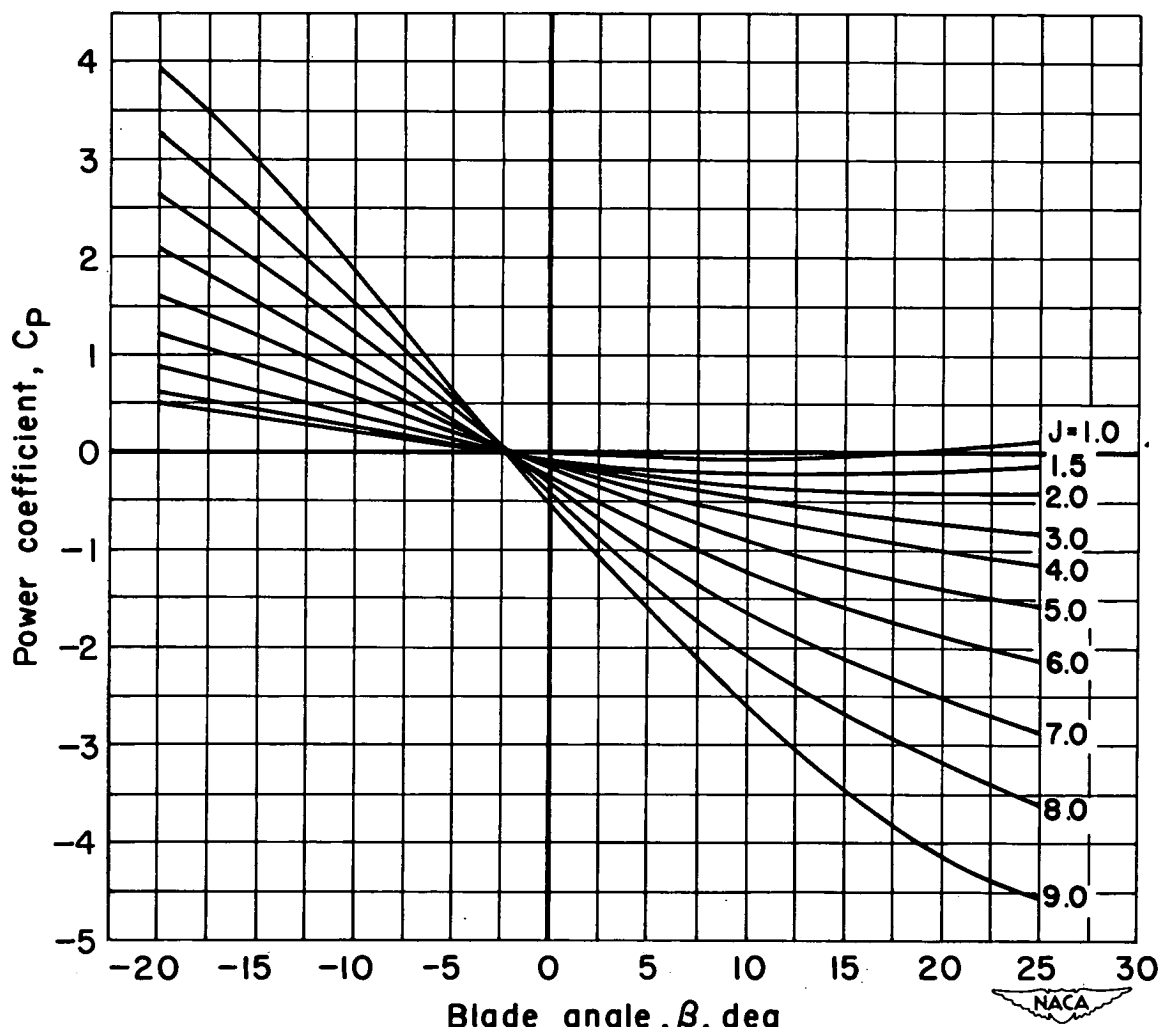
(a) M = 0.15

Figure 15.- The effect of blade angle on the power coefficients for the propeller in negative thrust.
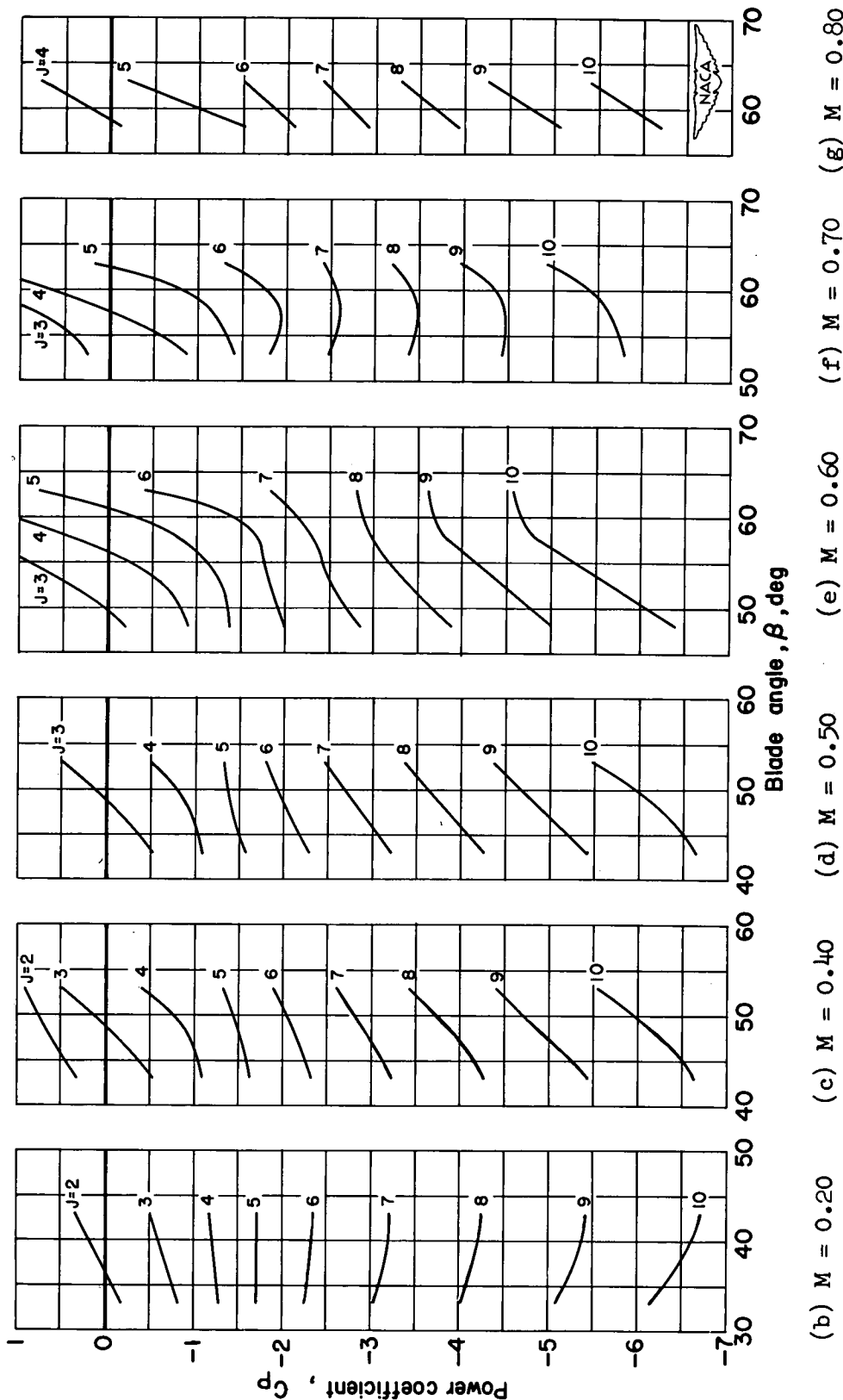
Figure 15.- Concluded.

(a) C_T vs. nD

(b) C_P vs. nD

(c) V vs. nD
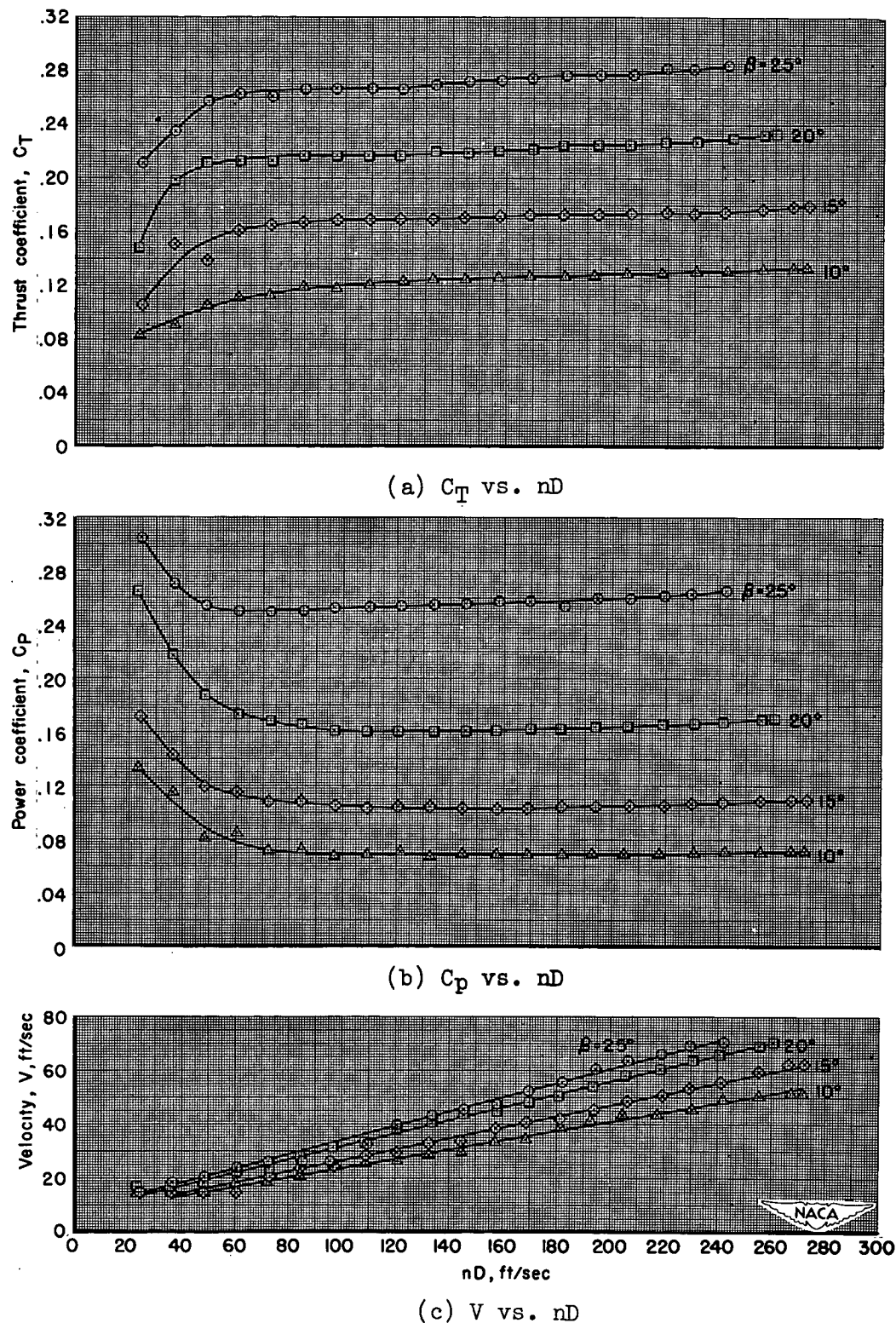
Figure 16.- Characteristics of the isolated propeller-spinner combination
at near static conditions.
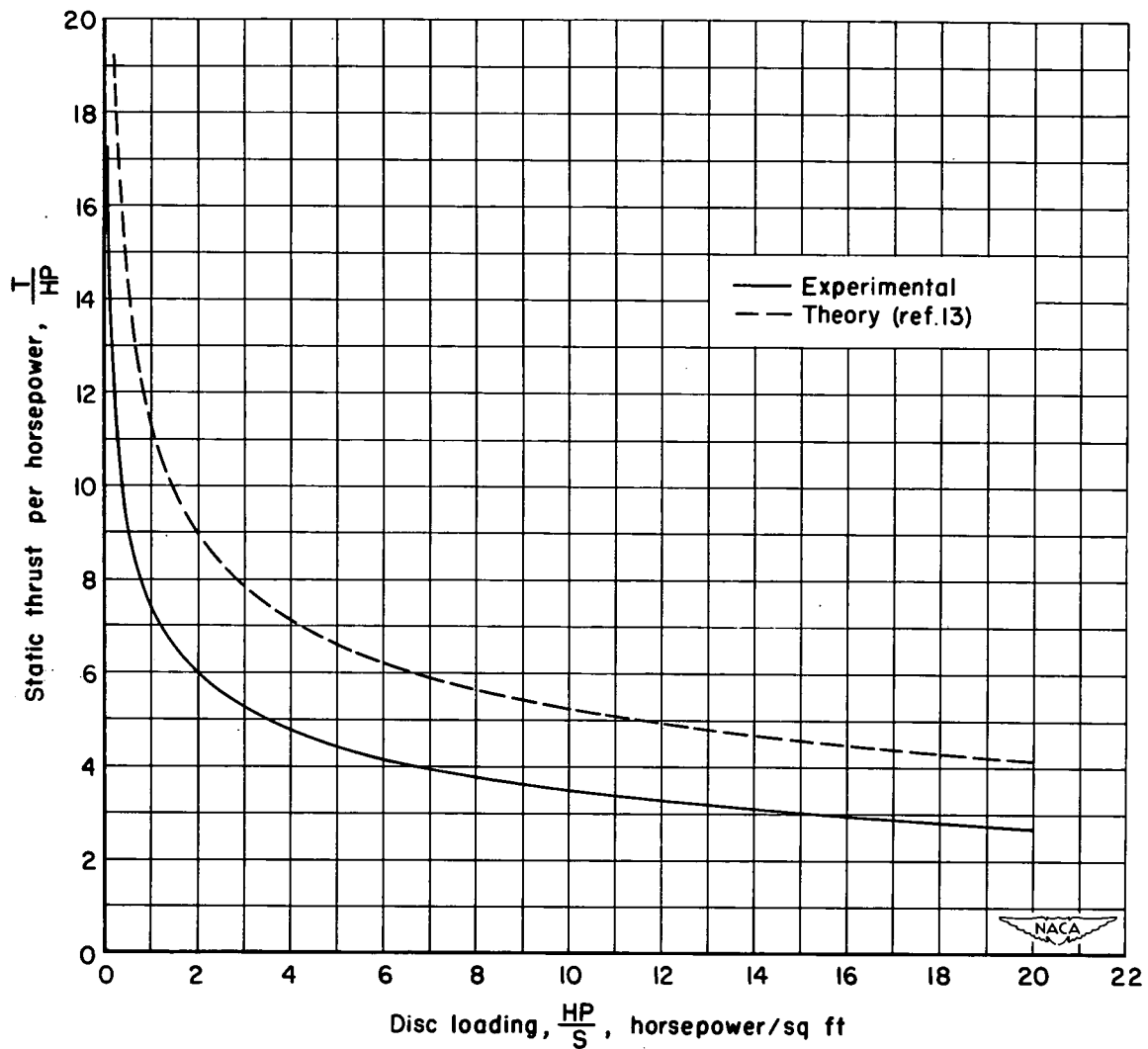
Figure 17.- Comparison with theory of the variation of sea-level static
   thrust per horsepower with power disc loading for the isolated
   propeller-spinner combination.